RRS Charles Darwin 81
Cruise Report

An Integrated Geophysical Investigation of the Axial Volcanic Region of the Reykjanes Ridge at 57° 45'N

3rd October - 1st November 1993

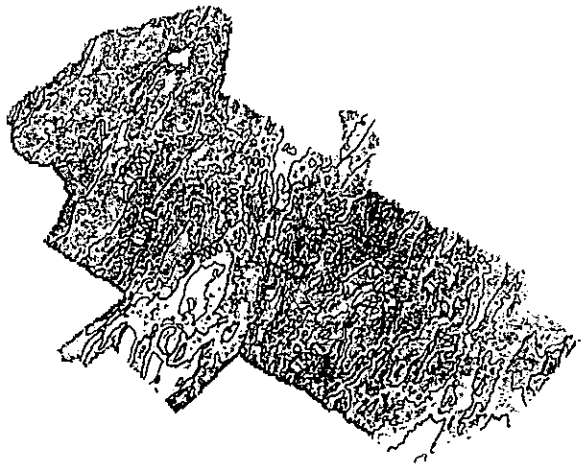

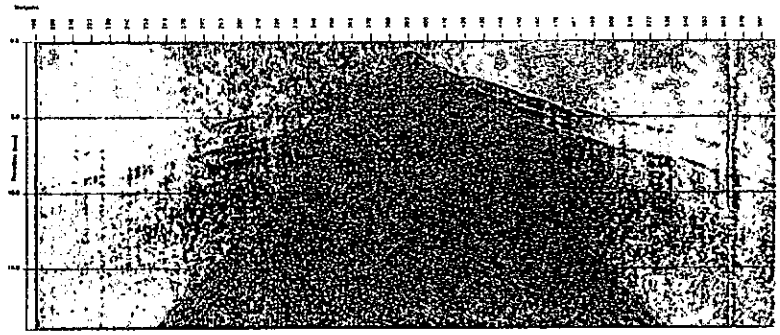

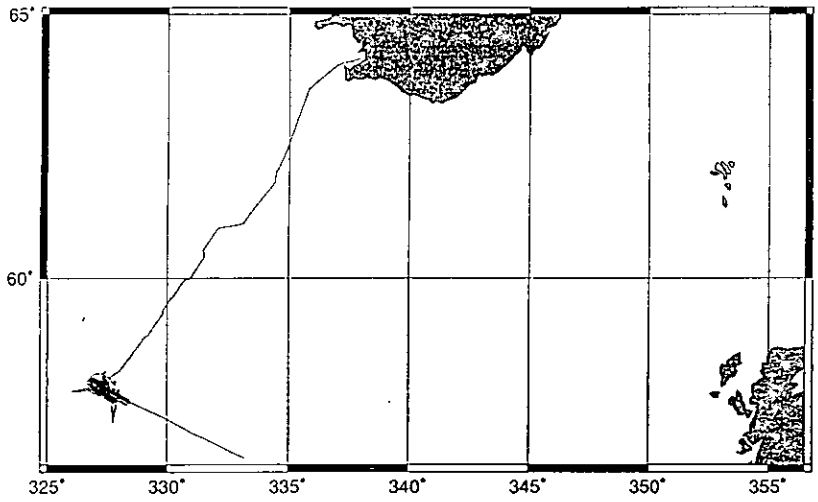

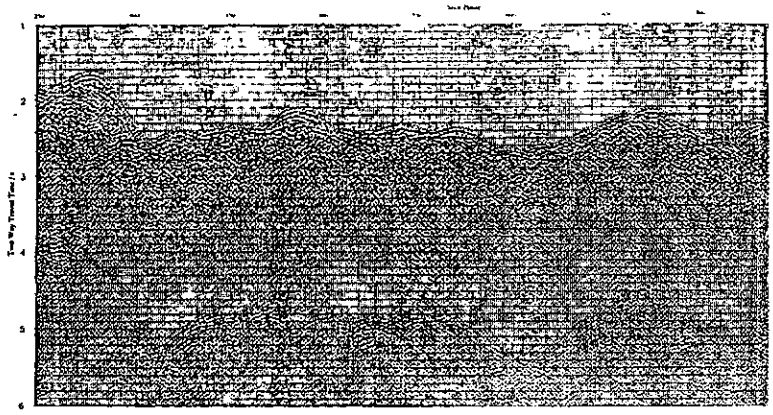

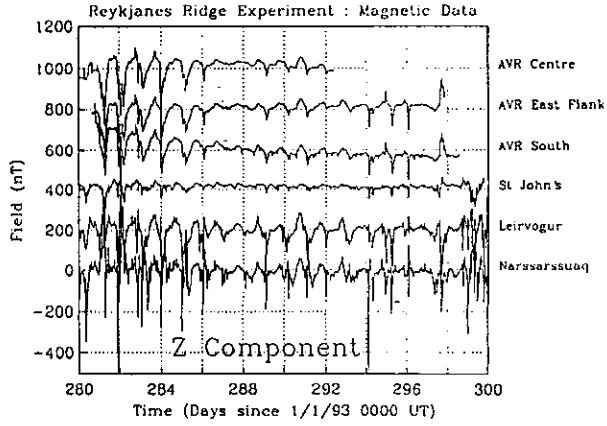

RRS Charles Darwin 81
Cruise Report

An Integrated Geophysical Investigation of the Axial Volcanic Region of the Reykjanes Ridge at 57° 45'N

3rd October - 1st November 1993
Reykjavik - Barry

Martin Sinha
Bullard Laboratories
Dept. Earth Sciences
University of Cambridge
Madingley Rise
Madingley Road
Cambridge
CB3 0EZ

Christine Peirce
Dept. Geological Sciences
University of Durham
Science Laboratories
South Road
Durham
DH1 3LE

Steven Constable
IGPP
Scripps Institution of Oceanography
University of California San Diego
La Jolla
California 92093
USA

Anthony White
School of Earth Sciences
Flinders University
Bedford Park
SA 5042
Australia

May 1994

Contents

Summary

The objective of this cruise was to investigate the processes of magma formation, delivery and emplacement beneath a slow spreading but magmatically robust mid-ocean ridge, and the resulting distribution of temperature and melt content in the crust and upper mantle, by carrying out an integrated geophysical experiment using a variety of techniques. The most important techniques used were controlled source seismic — both wide-angle, using digital ocean bottom seismometers (DOBSs) and multichannel, normal incidence reflection profiling; and electromagnetic, using both controlled source electromagnetic (CSEM) and magneto-telluric (MT) soundings. Additional geophysical datasets collected consisted of gravimetry, magnetometry and swath bathymetry. The target chosen for this study was an axial volcanic ridge (AVR) segment of the Reykjanes Ridge, centred on 57° 45' N, 32° 35' W. The AVR is approximately 40 km long, and is aligned approximately in a N-S direction. It was chosen as being the most magmatically active of the many AVRs that have been identified along the Reykjanes Ridge by recent sea floor imaging and sampling studies.

During the cruise we successfully carried out the first ever integrated geophysical experiment on a mid-ocean ridge to combine seismic and electromagnetic methods. During the seismic experiment, we deployed 11 DOBSs from Durham and Cambridge. These recorded 107 explosive shots and a large number of airgun shots from a tuned array of 12 guns, on two wide-angle profiles - one 30 km profile along the axis of the AVR, and one 90 km profile across the AVR. In addition we recorded 8-channel digital seismic reflection data along these and two other profiles across the axis. One Cambridge DOBS was lost.

For the EM experiment we deployed an array of 18 sea bottom instruments from Scripps, Flinders and Cambridge which variously recorded controlled source and/or natural source signals. The natural source instruments, from Flinders and Scripps, constituted a magneto-telluric sounding experiment, designed to investigate electrical conductivity in the mantle beneath the ridge to depths of the order of 100 km. The controlled source experiment made use of the Cambridge DASI deep-towed transmitter and sea bottom receivers from Scripps and Cambridge to investigate the crustal and uppermost mantle electrical conductivity structure beneath the AVR. We experienced a number of problems with the DASI system which, combined with bad weather, resulted in the loss of part of the planned transmission time for the controlled source work. However, we were able to complete the most important of the DASI tow lines successfully. Three instruments — one LEMUR from Cambridge, and one OBM and one OBEM from Flinders — were lost during the EM experiment. Subsidiary gravity, magnetics and 100% swath bathymetric datasets covered an area of some 12,000 km^2 surrounding the AVR. A complete track chart of CD81 is shown in Figure 1.

Very preliminary observations from the seismic data include evidence from the DOBS record sections for a seismic shadow zone associated with the AVR axis. This is consistent with a zone of low velocities and/or high attenuation at mid-crustal level, as would be expected in the presence of a mid-crustal melt reservoir beneath the AVR. The natural source EM data provide estimates of magneto-telluric and geomagnetic depth sounding responses at periods between 100 and 100,000 seconds, and indicate unusually low apparent resistivities, even by the standards of other ridge experiments — though we have yet to take account of the effects of topography and source field on these data. Two NERC funded PhD students (D.A. Navin, Durham; L.M. MacGregor, Cambridge) are working on the seismic and CSEM datasets, respectively; the MT data are being worked on at Flinders and Scripps; and the swath bathymetry/side-scan sonar, gravity and magnetic data are being made available to the wider BRIDGE community and via InterRidge to researchers in Iceland.

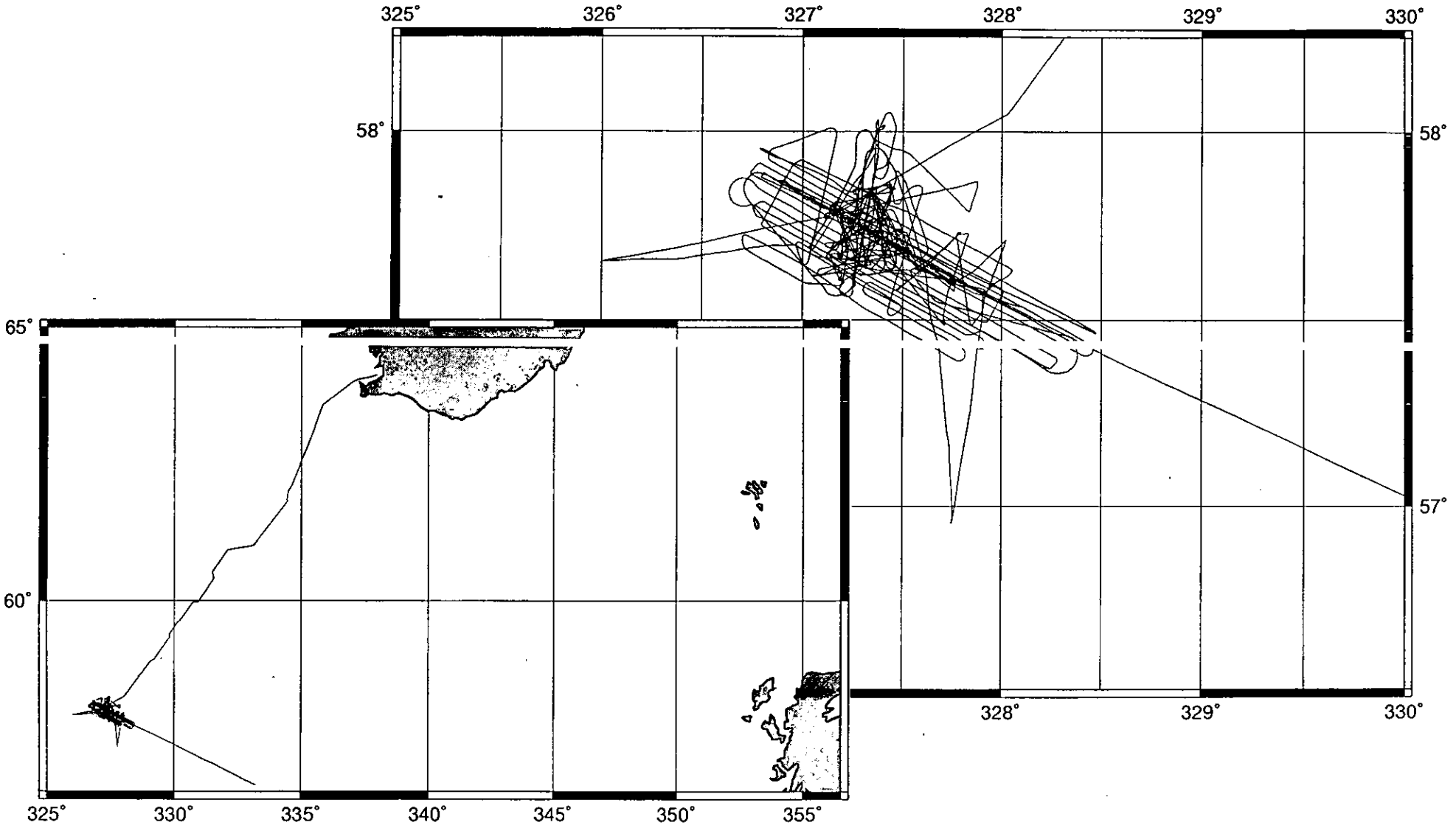

Figure 1. Summary track chart of cruise CD81.

1. Introduction and Cruise Objectives

1.1 Introduction

The Reykjanes Ridge is a section of the slow-spreading Mid-Atlantic Ridge whose structure, morphology and axial depth are profoundly affected by the influence of the Iceland hot spot, centred a short distance to the north. This influence has led to the ridge axis taking the form of a series of *en echelon* axial volcanic ridges (AVRs), separated by non-transform, overlapping, small offsets. Each AVR is aligned approximately perpendicular to the spreading direction, although the overall trend of the ridge is oblique to it. The objective of cruise CD81 was to investigate the processes of crustal accretion at a magmatically active AVR segment by carrying out a combined seismic and electromagnetic experiment, using the combined resources of Cambridge and Durham Universities, U.K.; Scripps Institution of Oceanography, U.S.A.; and Flinders University, Australia. Specifically, we planned to:

(1) use controlled source electromagnetic sounding (CSEM) profiles along and across the axis of the AVR to determine the crustal electrical conductivity structure;

(2) use two wide-angle seismic profiles along and across the AVR, coincident with the CSEM profiles, to determine the crustal seismic velocity structure using digital ocean bottom seismometers (DOBSs) and airgun and explosive shots;

(3) collect a grid of multichannel seismic reflection profiles, augmented by disposable sonobuoys to provide crustal velocity control, along and across the AVR; and

(4) simultaneously with (1), use an array of sea bottom magnetometers and electric field instruments to determine the deeper conductivity structure in the lower crust and upper mantle beneath the ridge axis, using both controlled and natural sources.

A large number of sub-sea-bottom geophysical experiments, chiefly seismic, have been carried out on the mid-ocean ridge system over the last decade to investigate the dynamics of crustal accretion, the structure of spreading centres, and the evolution of oceanic crustal structure. A number of recent, detailed seismic experiments on fast and intermediate spreading ridges (Harding *et al.*, 1989; Detrick *et al.*, 1987; Vera *et al.*, 1990; Kent *et al.*, 1990; Toomey *et al.*, 1990; Burnett *et al.*, 1989; Collier & Sinha, 1990, 1992a,b) have shown dramatically more detail of the structure of the spreading centre than has been achievable before. Features detected include fine structure of the uppermost crust, seismic low velocity zones and seismic reflections due to a region of partial melt in the middle and lower crust at the ridge axis. Some of these studies have been able to relate structures within the crust to the various scales of morphological and petrological segmentation evident from topographic (e.g. Macdonald *et al.*, 1984) and sampling (e.g. Langmuir *et al.*, 1986) studies. This work has therefore begun to provide some important constraints on the dimensions, physical state and geometry of the crustal melt reservoir and the development of oceanic crustal structure. Recent U.S. work has extended these studies to the southern East Pacific Rise, at 14° to 18°S (Detrick *et al.*, 1993).

The northern East Pacific Rise was the site of the first ever, and to date the only, controlled source electromagnetic sounding study of a mid-ocean ridge axis (Evans *et al.*, 1991; 1993). This experiment was carried out jointly by Sinha's group at Cambridge and Cox & Constable's group at Scripps in 1989, directly over the site of one of the U.S. two-ship seismic experiments. It demonstrated for the first time, the feasibility of using the CSEM technique right on a ridge axis. Electrical methods are

particularly sensitive to the presenc e of interconnected fluid phases in the lithosphere, whether they are hydrothermal flui ls or partial melt systems, and to the temperature (both above and below solidus) (f mafic and ultramafic rocks. They can provide constraints on porosity in the hydro hermal regime; on temperature in the hot, dry rock regime; and on the degree of parti il melting or re-crystallisation in zones of magma migration, accumulation and empl acement. Studies of electrical structure therefore provide information that is differen from, and complementary to, the higher resolution structural information that can be ol tained from seismic techniques.

In contrast, numerous seism c studies of the slow spreading Mid-Atlantic Ridge (MAR) show little or no evidence f or a significant crustal melt body. Indeed Detrick *et al.* (1990) show that were a melt b ody reflector comparable to that beneath the EPR present under the MAR at 23°N, it would have been imaged — and was not. Thermal modelling considerations (*e.g.* Slee p, 1975; Kusznir & Bott, 1976) have shown that any large, steady-state magma body beneath a slow spreading ridge is unlikely. Clearly MAR accretion processes are very lifferent from, and at least as complex as, those on the EPR. Due to the slow spreadin rate, the fierce topography associated with the rift valley and large scale normal faultir g, and the probably ephemeral nature of even small bodies of partial melt, progress tow ards understanding the intra-crustal and uppermost mantle processes here including th ir spatial and temporal variability is in many ways being made more slowly than for fa t and medium spreading ridge systems.

A further complication in t ie diversity of ridge processes is the presence of mantle hot spot plumes located c ose to or beneath a ridge. The largest of these features is the Iceland hot spot, lea ing to sub-aerial lithospheric spreading on Iceland, anomalous spreading, shallow ridge crest depths and unusual ridge morphology, from the Jan Mayen fracture zone at 72° N all the way to the Charlie-Gibbs fracture zone at 52°N. The Reykjanes Ridge is the p art of the MAR between the south coast of Iceland and the Charlie-Gibbs fracture zo e. It is characterised by slow spreading; shallow ridge crest depths; much smoother topography than other slow spreading ridges; the absence or poor development of a nedian or rift valley; and the absence of transform offsets between 57°N and the Reyk anes Peninsula at 63.5°N — a distance of 800 km. Throughout this region the ridge a pears to consist of elongated axial volcanic ridges with dimensions up to a few tens f kilometres long, arranged en echelon so that in general they overlap each other. Th e individual ridges trend approximately normal to the spreading direction; but since th offsets are all right-lateral, the overall trend of the ridge is oblique to the spreading dir ction. The Reykjanes Ridge is thus a section of the Mid-Atlantic Ridge where crustal a ccretion processes are profoundly affected by the thermal and geochemical anomal surrounding the Iceland hot spot; where the influence of the anomaly declines with increasing distance from Iceland; and where processes appear to share some of the features of both slow and intermediate to fast spreading ridges (Parson *et al.*, 199.; Murton & Parson, 1993).

In addition the Reykjanes Ridge offers a number of practical advantages for carrying out detailed studies of a slo w spreading ridge. These include:

(i) The relatively subdued topogra hy, compared to the steep and very high scarps associated with the median valley nd neovolcanic zone of the MAR further south, makes it an easier place to carry ou detailed geophysical work, especially with respect to the use of a deep-towed transmi ter for CSEM work. Combined with the relatively

shallow water depths, this makes it a logical site purely on logistic grounds in which to attempt the first crustal CSEM experiment on a slow spreading ridge axis.
(ii) The vesicular nature of the basalts erupted on the Reykjanes Ridge allowed relatively rapid drilling of basement during DSDP leg 49. This and the shallow water make it an attractive site for possible future hard rock drilling of the Atlantic spreading centre by ODP.
(iii) It is readily accessible from a UK port.

These and other considerations have led to the Reykjanes Ridge being selected as one of a small number of sites for detailed investigation by the BRIDGE programme.

The experience of work on other spreading centres has underlined the importance of applying a diversity of methodologies to studies of ridge processes, in order to understand the complex interactions between magmatic, tectonic and hydrothermal processes that dominate their geology. Our work on the Reykjanes Ridge combined seismic techniques, which have the finest spatial resolution of any sub-surface geophysical method, with electromagnetic sounding. EM sounding lacks the resolving power of seismic methods, but is uniquely sensitive both to temperature structure and to the presence of interconnected fluid phases — either hydrothermal or magmatic. The swath bathymetry, gravity and magnetic data which we collected throughout the survey area, and which can be merged with pre-existing data, including some deep-towed side-scan sonar images, will allow us to relate our results to the regional tectonic framework of the spreading centre.

1.2. Specific Objectives

Our objective was to investigate the mechanisms of crustal accretion at the axis of the Reykjanes Ridge by using seismic and electromagnetic methods to determine the physical structure of the crust and uppermost mantle beneath a magmatically active axial volcanic ridge. We selected an AVR centred on 57°47'N on the basis of swath bathymetry, deep-towed side-scan sonar (TOBI) and gravity data collected by Searle & Parson in 1990. The selected AVR shows clear evidence of widespread, constructional volcanic activity, including hummocky topography, bright back-scattering and fresh-looking lava flows extending for distances of several kilometres. It shows none of the signs of fissuring or faulting that characterise the TOBI data from most AVRs and that appear to indicate post-magmatic, tectonic extension; and it is associated with a negative anomaly in the mantle Bouguer anomaly gravity field. It appears to be the most magmatically robust of the many well-defined AVRs imaged by the TOBI surveys, and we therefore believe that it represents a segment of the spreading centre that is in the most magmatically active phase of its life cycle.

Specific aspects of the structure that are the targets of our investigation include:
(i) how does the porosity of the upper crust — which is likely to be the source region for a hydrothermal circulation system — vary with depth and across the AVR?;
(ii) how do the electrical resistivity and seismic velocities of the middle and lower crust vary across the AVR, and given both types of data, what can we infer about the across-ridge temperature structure and the possible presence of a partially molten region?

(iii) are any intra-crustal seismic reflectors present that can be related either to magmatic or tectonic activity?
(iv) what is the nature of the Moho transition near the axis, and what are the properties of the uppermost mantle?
(v) what is the sub-Moho distributi n of electrical resistivity in the top 100 km or so of the upper mantle? and
(vi) what can we learn from all of these about the processes of melt formation, migration, accumulation and emp acement, and the construction and evolution of oceanic crust at the Reykjanes Ridg e?

2. Work Carri d Out and Data Collected

2.1 The Wide-Angle Seismic Experiment

During the first half of the cruise we deployed a total of 11 DOBSs [6 from Durham (DDOBS) and 5 from C ambridge (CDOBS) — see Table 1] along two crossing wide-angle seismic lines (l igure 2). One Cambridge instrument (CDOBS 15) was lost. Line 1 runs across the ce ntre of the AVR orthogonal to the overall trend of the Reykjanes Ridge, and extends 1 0 km off axis to the WNW and 60 km off axis to the ESE. Line 2 runs along the axis of the AVR, and is 30 km long. Airgun shots were fired with a spacing of approximate y 100 metres along both of these lines. In addition, 31 explosive shots of 25 kg were f red with a 1 km spacing along line 2; a further 61 shots of 25 kg (of which two misfi ed) were spaced at 1 km intervals along the main 60 km section of line 1, straddling t e AVR; and a further 19 shots of 50 kg (of which two misfired) were spaced at 2 km intervals along the outer 30 km of line 1, furthest east of the AVR. The airgun sou ce was an array of 12 guns in four sub-arrays, totalling 74.8 litres (4,566 in^3) (F igure 3) and towed at depths varying between 13 and 15 metres.

Each of the Durham DOBSs was fitted with a 3-component geophone package, in addition to a hydrophone, in ord r to maximise the chances of making high quality recordings of S-waves. The Camb idge DOBSs were fitted with hydrophones only. While the airgun shots provide clc sely spaced traces which maximise trace-to-trace coherence, allowing recognition o late arriving and low amplitude P-phases and detailed travel-time and amplitude r odelling of P-wave velocity structure, it was also an objective of this experiment to s udy S-wave structure. Obtaining recordings of S-waves with sufficient signal-to-noi e ratio to allow both travel-time and amplitude modelling was our main motive for sing explosive shots in addition to closely spaced airgun shots. The S-wave velocity s tructure and, equally importantly, any evidence of S-wave shadowing due to high atte nuation will provide important constraints on the physical state of crustal rocks. The nsedimented seabed near the ridge axis results in significant conversion of P- to S-w ve energy at the water-rock interface. However, reliable recognition of S-wave arri als requires particle motion analysis of the wave field at the receiving instrument. Th e explosive shots, although more coarsely spaced than the airgun shots, have a highe signal-to-noise ratio at moderate to long ranges. Good signal-to-noise ratio is essenti l for particle motion analysis. The combination of closely spaced airgun shots and m re widely spaced but higher amplitude explosive

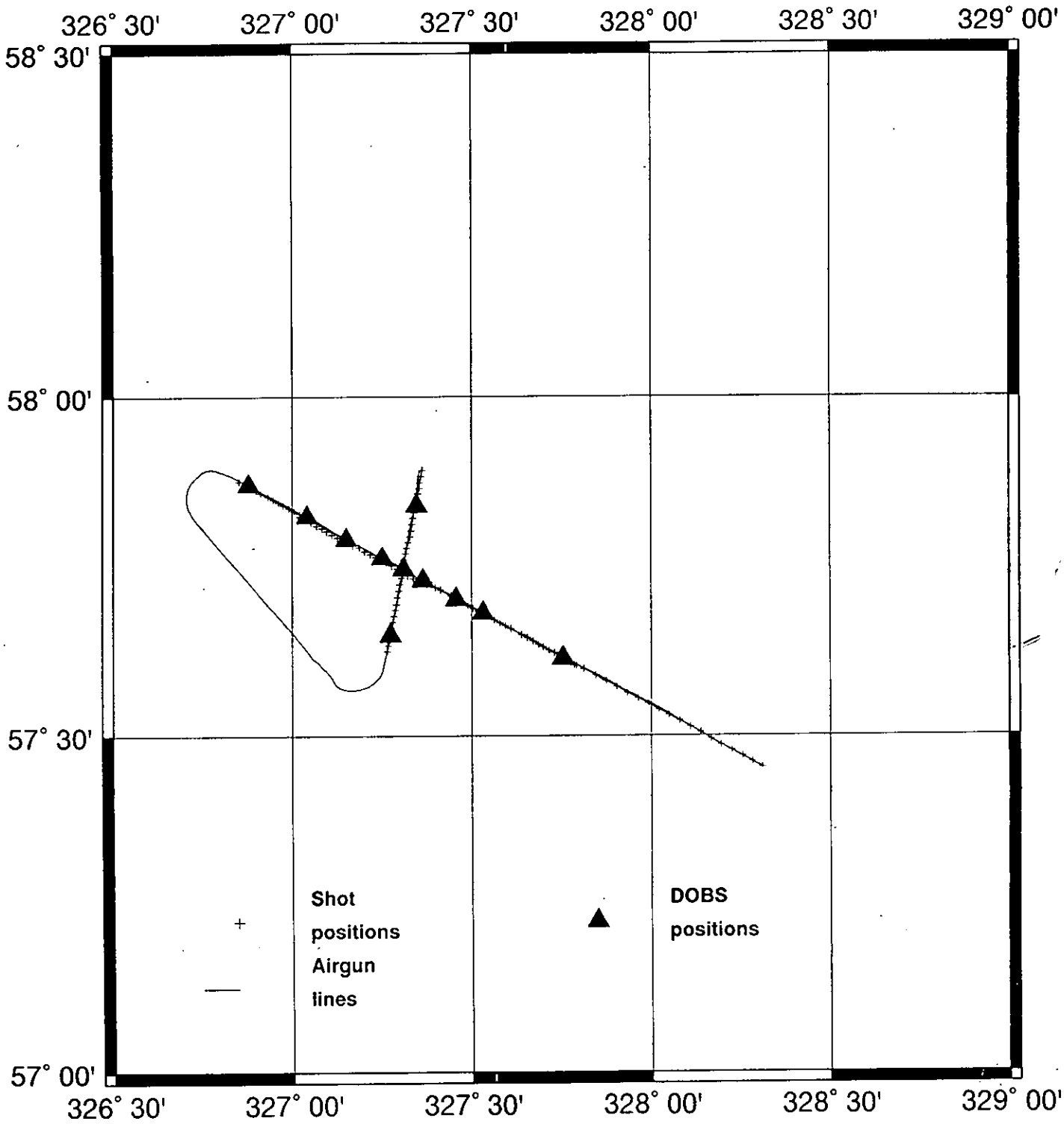

Figure 2. Shot and instrument positions for the wide-angle seismic experiment.

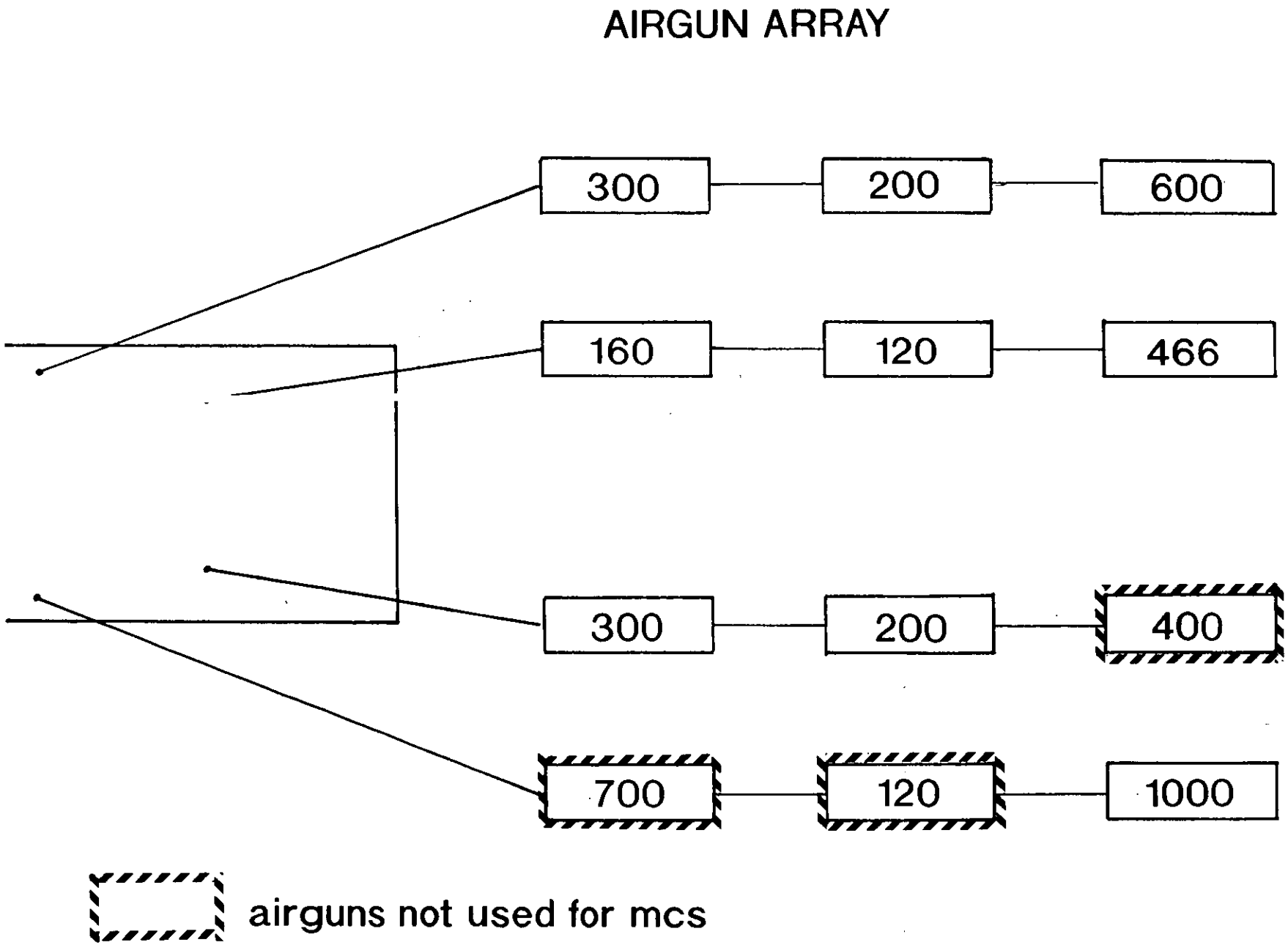

Figure 3. Airgun array.

shots, provides the best possible combination for allowing detailed P- and S-wave analyses.

Each DOBSs was programmed to record all of the explosive shots. In addition, the single channel CDOBS were programmed to record continuously during airgun shot firing. The DDOBS were programmed to record at an 80 s interval (i.e. alternate shots) in a windowed mode, mainly to enable collection of four channel data at an equivalent sampling rate to the CDOBS. The resulting wide-angle airgun trace spacings are ~100 m for the CDOBSs and ~200 m for the DDOBSs, at an average surveying speed of 4.9 knots. The DOBSs also recorded shots fired while transiting between the ends of lines 1 and 2, providing a small amount of 3-D ray coverage of the AVR. The experiment resulted in 1475 seismograms per CDOBS and 3260 seismograms per DDOBS, including the explosive shot windows.

Data quality is extremely high and some interesting features can be noted on the first final seismic sections to be constructed. These features include shadow zones and microearthquakes (Figure 4), which have been recorded by multiple instruments, and good S-waves arrivals (Figure 5). In excess of 500 Mbytes of data were recorded, some 21,679 individual seismograms (Table 2). The wide-angle seismic data are being processed at Durham and will be interpreted, using both 1-D reflectivity and 2-D ray-theoretical synthetic seismogram techniques, by NERC funded PhD student Debbie Navin.

With all remote seabed seismometers, shot timing is an extremely important factor in constructing final wide-angle record sections. All DOBS internal clocks were synchronised to and checked for drift against the Cambridge "Lucky 7" clock, which was also used as the time standard for the EM experiment. The difference between this clock and the RVS DMW shipboard clock was measured and recorded using a Siemens jet pen oscillograph. As all airgun shots were fired using, and all explosive charges logged against, the DMW clock, the relative difference between the two time bases needs to be corrected for and so had to be continually measured and recorded. All shipboard navigation, gravity, magnetic and bathymetry data was logged with respect to the DMW clock. The airgun shots were controlled by the Reftek gun synchronisation unit, using 20 s pulses from the DMW clock. An additional delay of 0.050 sec (software adjustable) was incorporated into the system by the Reftek to allow proper synchronisation of the airgun array. Over the shooting period the difference between the two clocks was ~0.076 sec ("Lucky 7" behind DMW). Hence, with respect to the "Lucky 7" clock, shots occurred at

nominal shot instant - 0.026 s

where *nominal shot instant* is the time of the shot to the nearest whole second.

Explosive detonation times relative to the "Lucky 7" clock were measured using a hydrophone towed ~75 m behind the ship, a hull geophone clamped firmly against the ship's stern plates and the SIMRAD precision echo sounder fish transducer. The signals output from each of these sensors were digitised and recorded using the spare PDAS-100 data logger (see Figure 6) and a backup copy on paper made using the Siemens jet pen. Post-cruise analysis of these records resulted in the determinations of shot instants and detonation depths shown in Table 3.

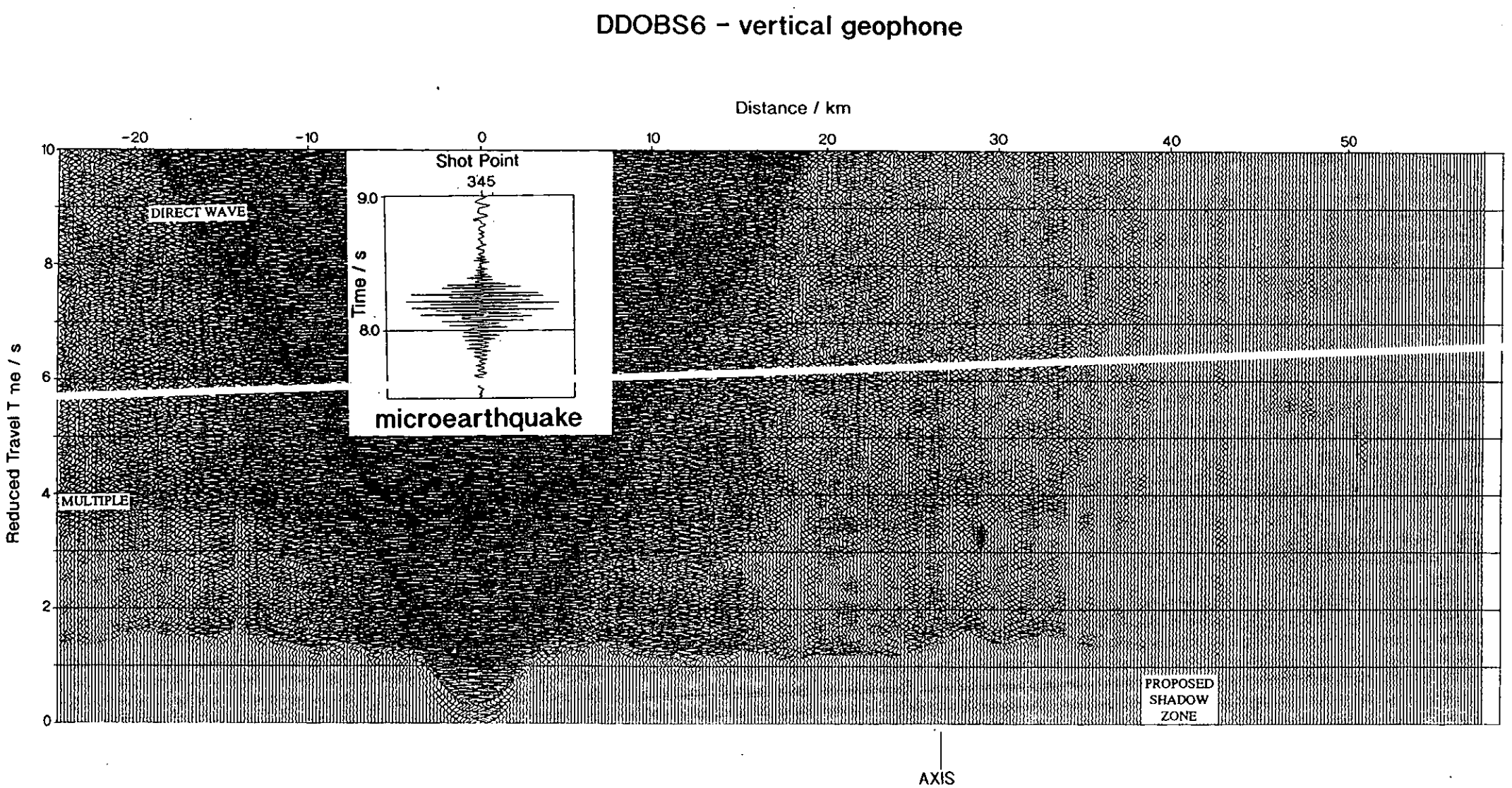

Figure 4. Seismic record section.

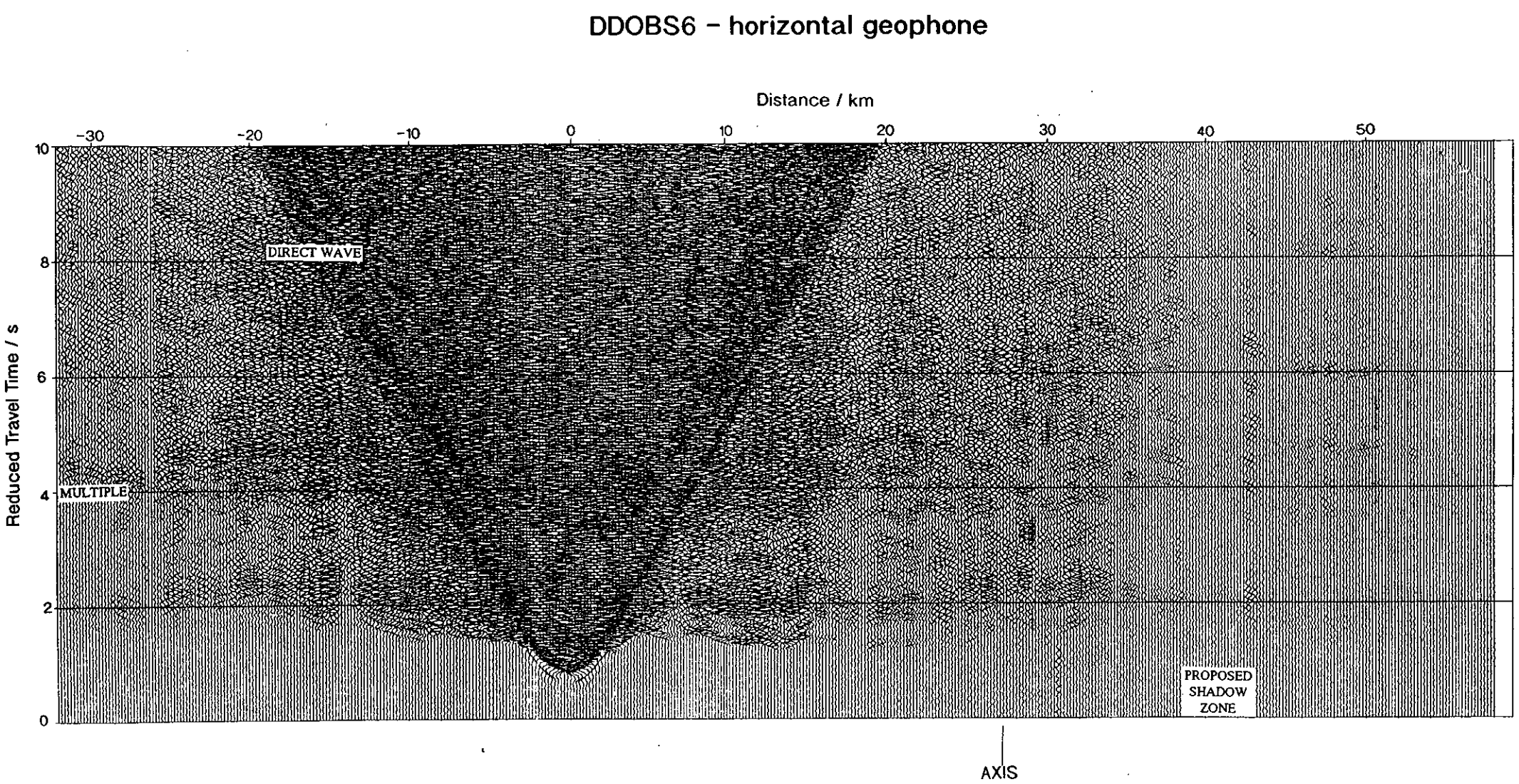

Figure 5. Seismic record section.

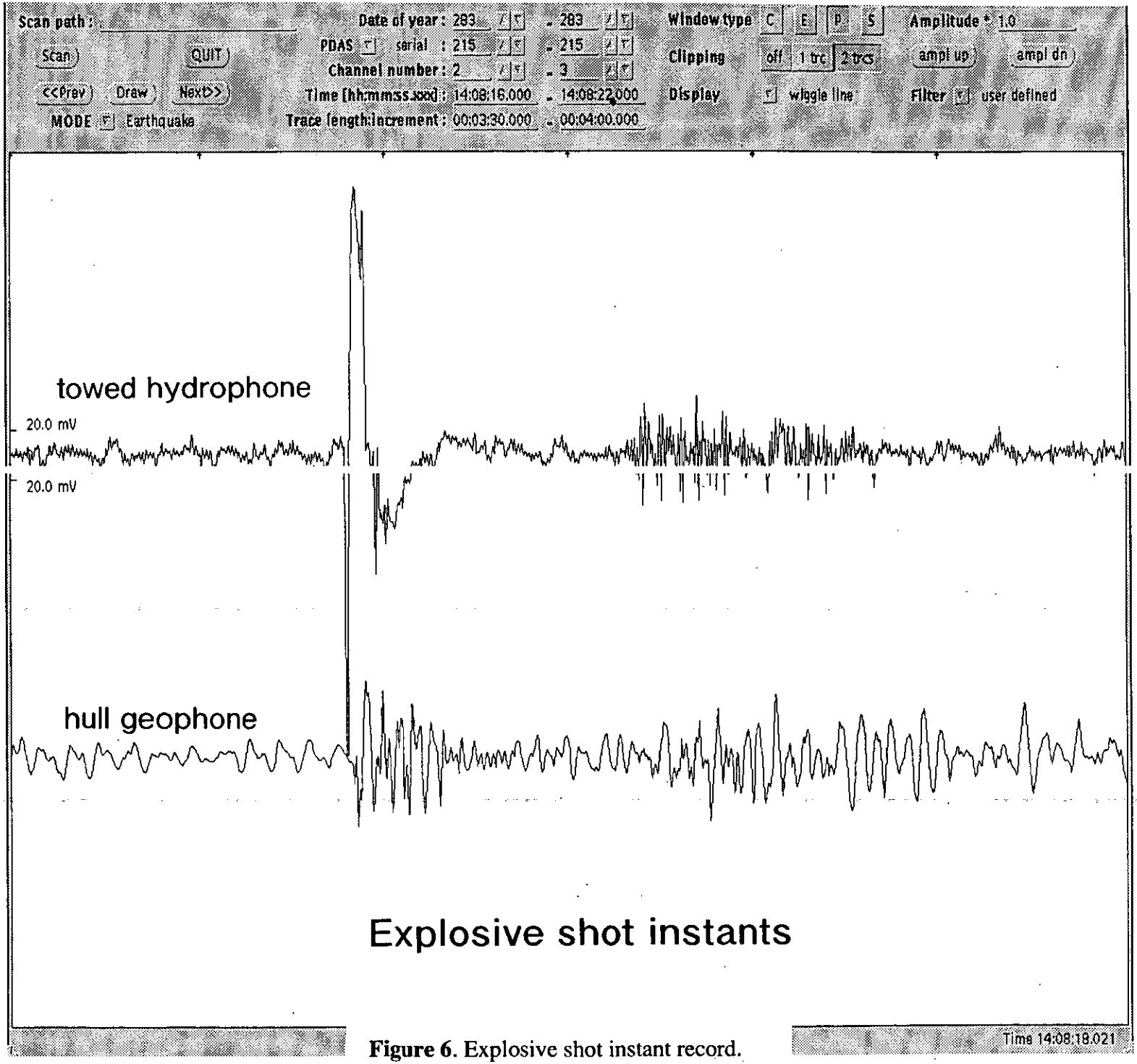

Figure 6. Explosive shot instant record.

2.2 The Seismic Reflection Experiment

The seismic reflection data were recorded using the SAQ digital acquisition system and an 8-channel Geomechanique hydrophone streamer made up of alternating, 50 metre active and passive sections. The streamer depth was maintained at 11 metres by 5 Ashbrook depth controller birds — one at the front of the array, and one behind every other active section. Data were collected along lines 1 and 2, during wide-angle shooting, with the full airgun array and 100 metre shot (40 s) spacing, to give 4-fold coverage at 50 metre CMP spacing. Two subsequent lines (3 and 4, Figure 7) were shot using a subset of the airgun array, totalling 54.8 litres (3346 in^3) (see Figure 3), and a shot spacing of 50 metres (20 s) resulting in 8-fold CMP coverage. A total of six lines were planned, but only four were shot before weather conditions (and forecasts) worsened to such an extent that we were obliged to recover the airguns and streamer, in order to avoid the possibility of progressively deteriorating weather preventing us from safely recovering the DOBSs. The reflection data will be processed at Durham University using the ProMax seismic processing package. An example of the raw seismic data collected across the ridge can be seen in Figure 8.

Four disposable sonobuoys were deployed during the reflection experiment to provide supplementary velocity data. Only two of these sonobuoys provided useful data, the other two failing before clearing the airgun array and streamer. Two were Dowty Marine type SSQ906A(D) and two were of an older type. One of each type failed. Successful sonobuoy deployment locations are shown in Table 4.

The sonobuoys were deployed from the port bridge wing. Sonobuoy signals were received using an aerial on the main mast and an ICOM receiver (ICR 7000) located in the main lab. The signals were amplified using a broad band RF pre-amplifier located as close as possible to the aerial output — in this instance at the top of the main mast. Receiver output was digitised and recorded using the spare PDAS-100 data logger (identical to those used inside the DDOBSs). Paper playouts were also made using an EPC graphic recorder.

2.3 The Controlled Source Electromagnetic Experiment

The controlled source electromagnetic (CSEM) sounding method has been described by Chave & Cox (1982), Cox *et al.* (1986), and Webb *et al.* (1985); while the equipment that has been developed at Cambridge to make use of the technique is described by Sinha *et al.* (1990). For this experiment we used the Cambridge deep-towed controlled source (DASI); 4 Cambridge and 6 Scripps sea bottom electric field recorders, each equipped with an orthogonal pair of 12 m horizontal electric dipole antennas (LEMURs and ELFs); and 4 Scripps long-wire electric field recorders, each equipped with a single, 300 m horizontal electric dipole antenna (LEMs). One of the LEMURs was lost and one of the ELFs failed to record; however the other 12 instruments were recovered with data.

The geometry of the experiment is shown in Figure 9. The receivers were deployed along two profiles, coincident with wide-angle seismic lines 1 and 2. Three short-arm instruments were laid along the axis of the AVR (coincident with seismic line 2). The remaining short arm instruments were laid along an approximately orthogonal profile, coincident with seismic line 1, extending from 4 km WNW to 15 km ESE of the axis. The four LEMS were laid further out along line 1, at distances from 21 to 40 km off axis.

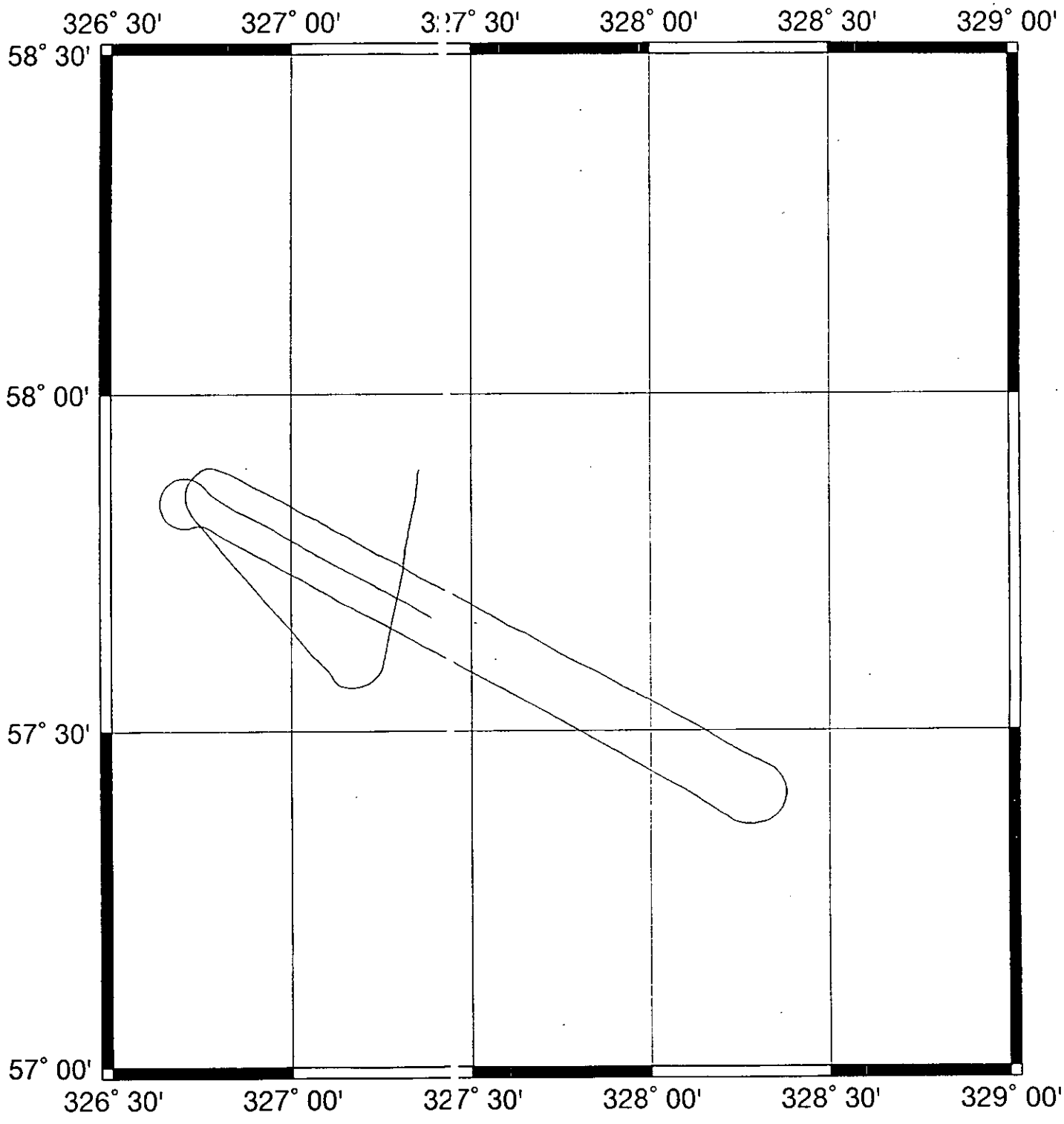

Figure 7. Seismic reflection profiles and wide-angle airgun shooting tracks.

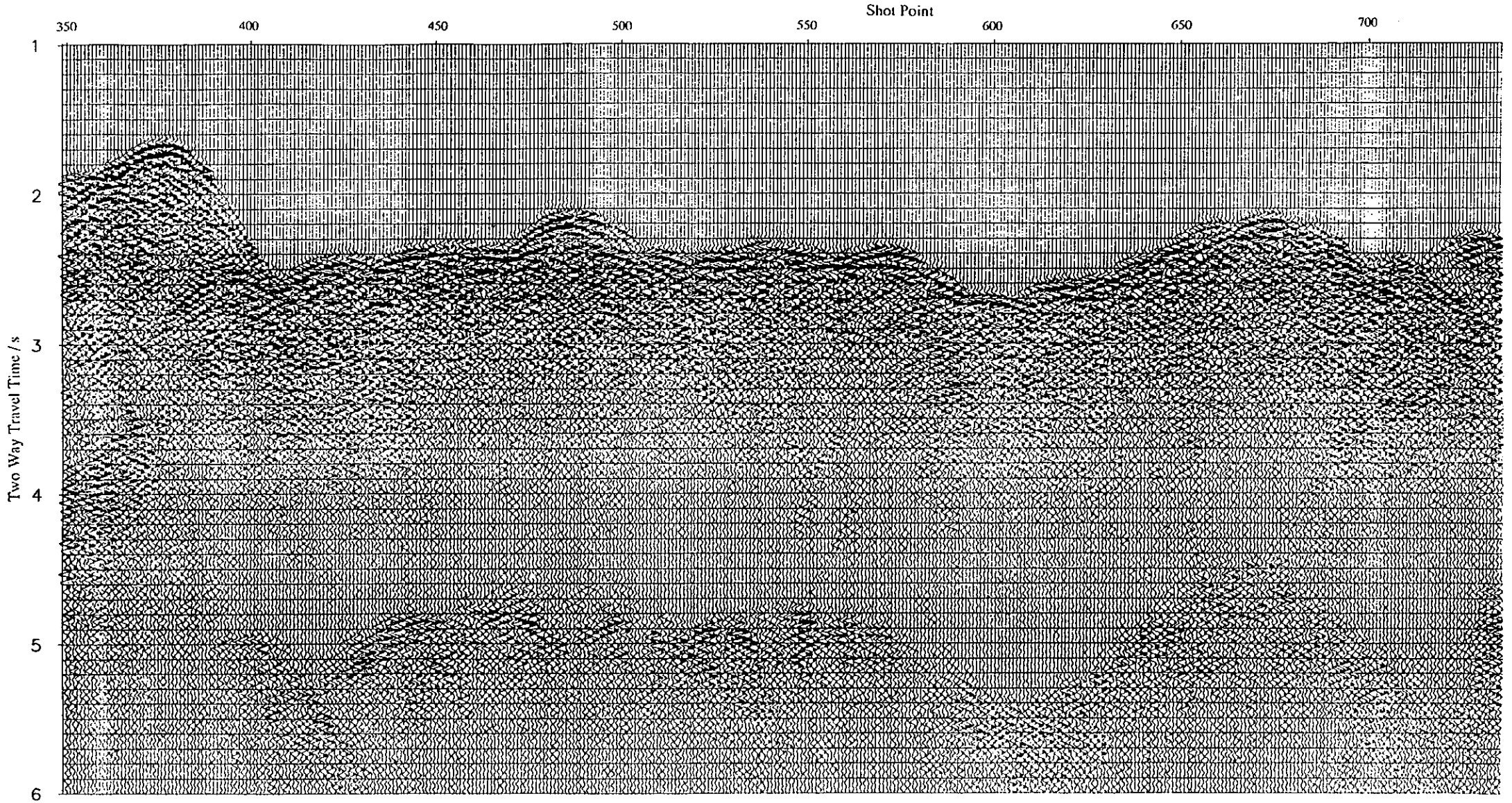

Figure 8. Sesimic reflection data.

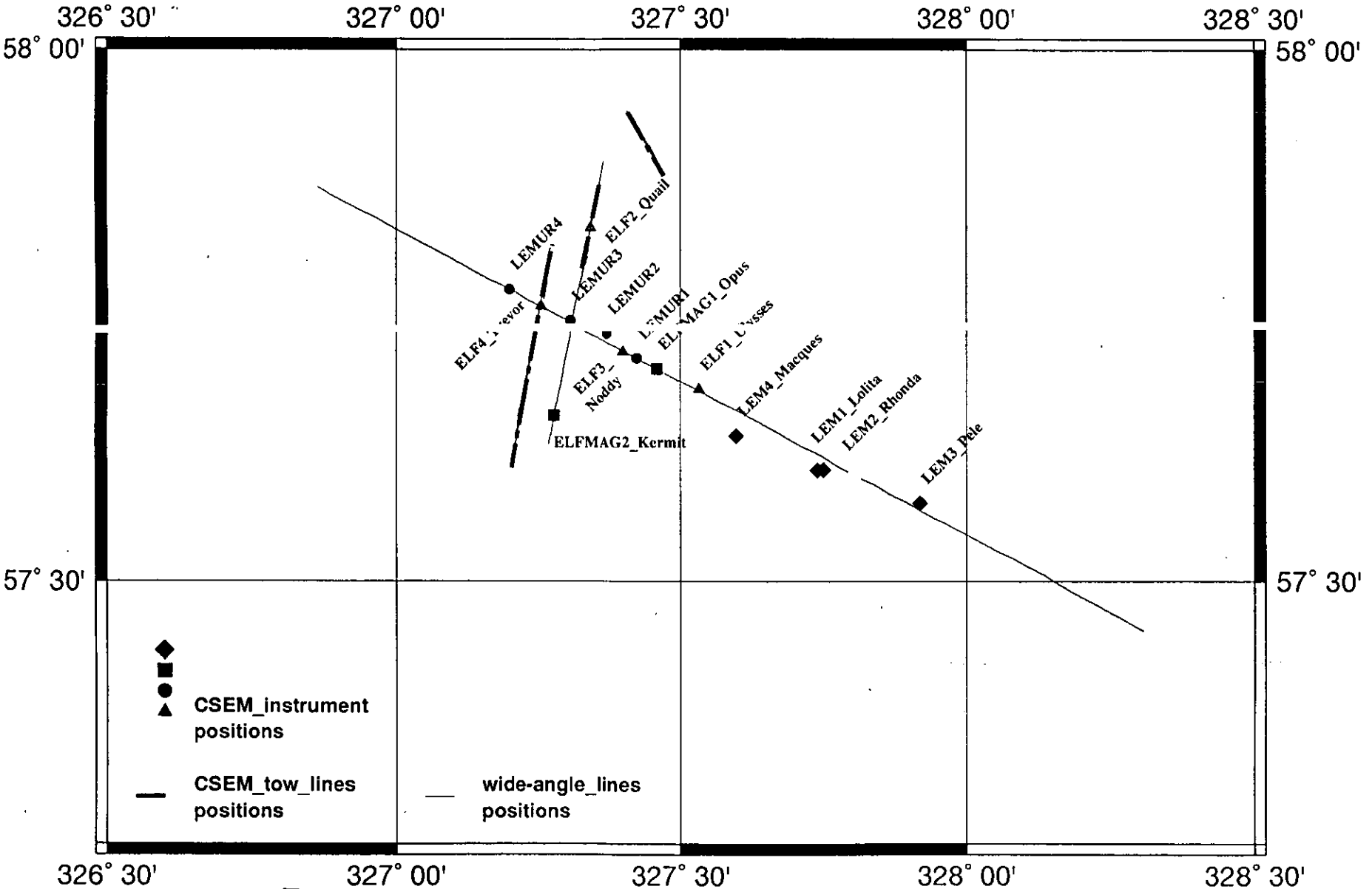

Figure 9. Controlled source EM experiment — transmitter tracks and receiver locations.

The first tow of the DASI transmitter was along a track down the axis of the AVR, coincident with seismic line 2. The tow started 16 km north of the crossing point of the two lines; and continued past ELF 2 to within 4 km of the crossing point. At this point, DASI suffered a total electrical failure, and the tow was discontinued. After a pause for repairs to the deeptow and for a further delay imposed by bad weather, a second tow line was carried out along a profile 4 km west of the AVR axis, which passed through the position of the westernmost receiver (ELF 4). This tow line was our highest priority, since it provided across-axis transmissions with a ridge-parallel transmitter E-field polarisation - the optimum experimental geometry for investigating sub-ridge crustal structure, according to 2.5 D forward modelling carried out by Unsworth (1991). After the completion of tow line 2, a combination of bad weather and damage to DASI's dipole antenna streamer prevented us from carrying out any further CSEM work.

Of the four LEMURs, one (LEMUR 4) was lost. The other three had all recorded good data. The LEMURs recorded 13-bit data with gain ranging, at a sampling rate of 64 Hz, from two orthogonal horizontal electric field channels. Analogue filters were set to 16 Hz low pass (anti-alias) and 0.125 Hz high pass (to offset the 'red' noise spectrum). To lengthen the recording time available within the small recording capacity of the LEMURs, synchronous stacking was used. The stack fold was six (resulting in sixteen bit stacked data), and the stacking period was 128 seconds, resulting in a total stack frame of 12 minutes 48 seconds. A new stack frame was started on each quarter hour. Data were written to tape at the end of each stack frame (Figure 10).

The four LEMs all recorded unstacked, fixed gain, 16-bit, continuous data on four channels — two a.c. channels for the controlled source data, and two d.c. channels for MT data. The two channels were two parallel pairs of electrodes making up a single, 300 m antenna — the second electrode pair and recording channel being provided for data redundancy. The sampling rate was 1 Hz for most of the deployment, but was increased to 64 Hz for the duration of the CSEM experiment. ELF 1 and ELF 3 both recorded continuous, unstacked, 64 Hz sampling rate, 16 bit, fixed gain data on two a.c. channels (orthogonal horizontal 12 m electrode antennas). ELF 4 recorded with the same parameters as ELFs 1 and 3, but due to a fault on a power supply board it stopped recording before DASI transmissions began. ELF 2 was also initially deployed with the same recording parameters as the other ELFs. However during the experiment it popped up prematurely (see cruise narrative), was recovered, and was re-deployed after being fitted with d.c. recording channels as well as a.c. channels. For its second deployment, it recorded both horizontal electric field components as both a.c. and d.c. channels. The four channels were again recorded as fixed gain, 16 bit, unstacked, continuous data. The sampling rate was 1 Hz for part of the second deployment, but was increased to 64 Hz during CSEM transmissions.

ELFMAG 1 failed to record any electric field data - although the magnetometer worked well (see section 2.4). ELFMAG 2 recorded the two electric field components as both a.c. and d.c. channels, with a sampling rate of 1 Hz for most of its deployment, but 32 Hz during the CSEM experiment. In common with the other Scripps instruments, data were recorded as fixed gain, 16 bit, unstacked, continuous time series.

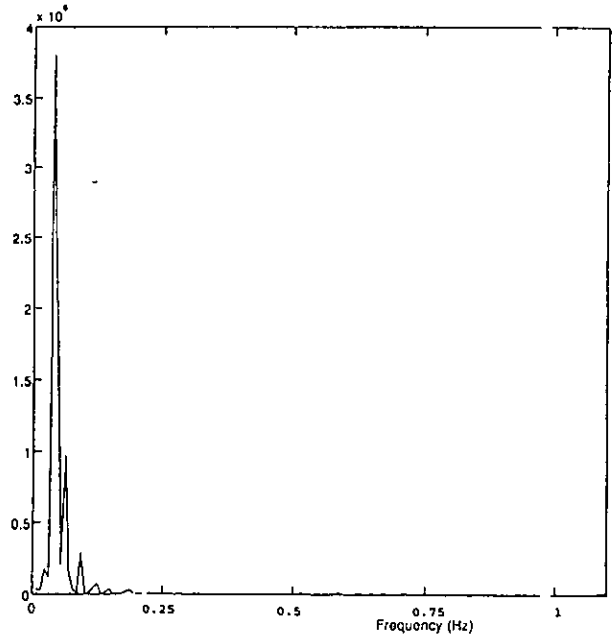

Lemur 1:
Noise spectrum.
Ridge parallel component.
Amplitude scale arbitrary.

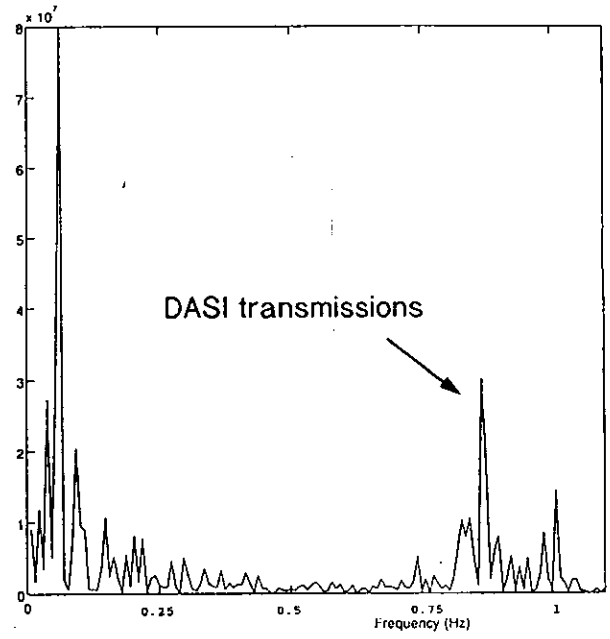

Lemur1:
Ridge parallel component.
Source-receiver offset ~12 km.
Transmission frequency ~0.75 Hz.
Recorded at 18:10 GMT, 23rd October, 1993.
Amplitude scale arbitrary.

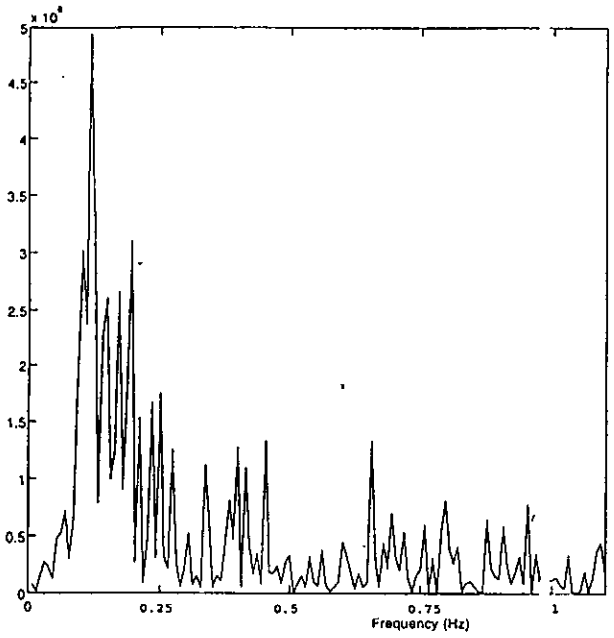

Lemur 2:
Noise spectrum.
Ridge parallel component.
Amplitude scale arbitrary.

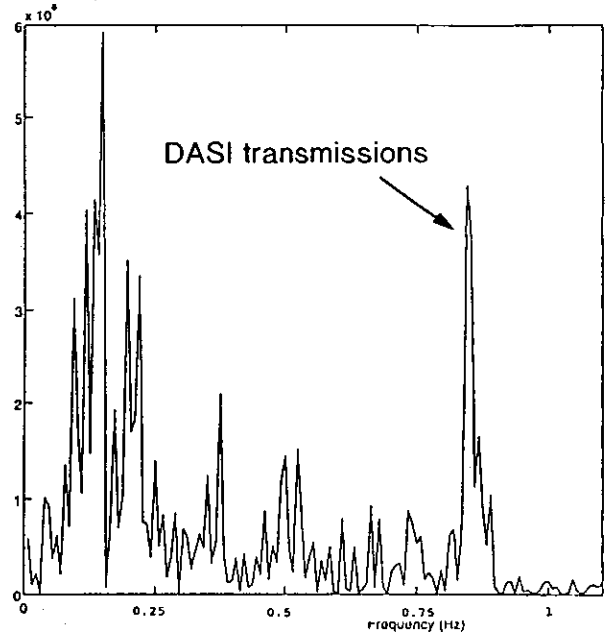

Lemur2:
Ridge parallel component.
Source-receiver offset ~9 km.
Transmission frequency ~0.75 Hz.
Recorded at 18:10 GMT, 23rd October, 1993.
Amplitude scale arbitrary.

Figure 10. Amplitude spectra of LEMUR data, showing noise records and DASI signals.

On both tow lines we experienced some problems with the DASI transmitter system. This consisted of mis-triggering of the zero-crossing detector circuit, which controls the outgoing wave form. As a result, neither the frequency nor the phase of the outgoing signal were steady, as had been planned. During DASI tow 1, transmissions were at frequencies of approximately 0.3 and 10.7 Hz; during DASI tow 2, transmission frequencies were approximately 0.8 and 23 Hz. The transmission amplitude was unaffected by this problem - on both deployments the dipole current was 100 A rms, constituting a dipole moment of 10^4 Am. We anticipate being able to use appropriate signal processing on the recorded data to eliminate the variations in the controlled source output, by determining amplitude and phase differences between different receivers.

A modification that was made to DASI before this cruise was to add a data logger system to monitor the antenna transmissions directly. This consisted of an array of electrodes positioned along the transmitting antenna, coupled to a modified CDOBS recording system. The capacity of the recording system was insufficient to allow the logger to collect data continuously. However, samples of the outgoing wave form were digitised and logged periodically in digital form; and samples of the wave form were also periodically recorded in analogue form, to preserve the highest frequency components (which consists of rectified and switched half-wave forms of the 256 Hz sinusoidal power supply frequency). The data from this logging system will be particularly useful in view of the frequency and phase problems experienced with DASI; and will also allow a more precise determination of the source dipole moment than has been possible previously.

We shall interpret the EM data from both tow lines and all receivers using a combination of 1-D inversions and 1-D and 2-D forward modelling. We shall use the seismic data from the wide-angle and reflection lines to locate boundaries or regions of steep gradients in physical properties of the crust, and to identify other regions where physical properties change more slowly. We shall use this information to constrain the interpretation of the CSEM data. The 1-D forward modelling and 1-D smooth inversion methods have been successfully applied in previous ocean bottom CSEM studies, including the 1989 EPR experiment. However this experiment is specifically intended to investigate structures that vary across the ridge axis. 2-D forward modelling using the finite element code of Unsworth, Chave & Travis (1993) will therefore be an essential component of the data analysis and interpretation. The finite element code is capable of solving the full 2.5 D problem (that is, a 3-dimensional point dipole source embedded in a two-dimensional conductivity structure), and can compute the response for any horizontal orientation of transmitter and any separation either along or across strike of source and receiver. The CSEM data are being processed at Cambridge and Scripps, and modelling and interpretation will be carried out by NERC funded PhD student Lucy MacGregor (Cambridge).

2.4 The Magneto-Telluric Experiment

For the natural source electromagnetic experiment we deployed a total of 11 sea bottom instruments, some of which were common to both the magneto-telluric (MT) and CSEM experiments. The instruments were: two Flinders 3-component ocean bottom magnetometers (OBMs 1 & 2); two Flinders combined magnetometers and electrometers (OBEMs 1 & 2); two Scripps short arm electric field instruments,

recording separate d.c. (for MT) as well as high frequency (for CSEM) data channels, which were also fitted with Flinder 3-component magnetometers (ELFMAGs 1 & 2); and 5 instruments which recorded only electric fields: the second deployment of ELF 2 and the four Scripps long-wire electric field instruments (LEMs 1 to 4), which in common with the ELFMAGs recorded d.c. electric field data in addition to the high frequency CSEM data channels. The instrument locations are shown in Figure 11. Out of these instruments, OBM 2 and OBEM 1 were lost. OBM 1 was recovered but had not recorded any data. OBEM 2, located on the axis of the AVR at the crossing point of the two wide-angle seismic profiles, recorded 3-component magnetic field plus orthogonal horizontal component electric field data, using water chopper sensors for the electric fields. All four LEMs successfully recorded d.c. electric field data. Both ELFMAGs recorded 3-component magnetic field data; and ELFMAG 2 and ELF 2 also recorded d.c. electric field data, but from short arm antennas without water choppers.

Water chopper devices have traditionally been used to collect electric field data for sea floor MT studies, but the long antennas of the LEMs can provide data of comparable quality in the frequency band of interest. Results from the EMRIDGE experiment on the Juan de Fuca ridge indicate that short antenna instruments can be useful for MT sounding as well. The electric field is distorted by three dimensional topography and shallow resistivity structure much more severely than the magnetic field, so having the spatial redundancy of the controlled source electric field array will be of great benefit to the MT sounding. Since the quality of the natural source data depends very much on the length of time over which it has been collected, we deployed the MT instruments first on arriving at the site, and as far as possible recovered them last before leaving, resulting in time series for the MT instruments of between 13 and 18 days.

Despite some obvious disappointments in the number of instruments recovered and the consequent loss of data, this experiment still represents one of the largest MT deployments across a ridge. Furthermore, the relatively fast sample rate (10 s or faster) with high precision instruments and significant ionospheric source field activity give better MT frequency coverage than has been achieved before. In addition to the seafloor MT data, three sets of Magnetic Observatory data have been generously supplied from St John's in Canada, Nassarssuaq in southern Greenland and Leirvogur in Iceland (Figures 12, 13 & 14) We are waiting for similar data from the three Magnetic Observatories in the UK from the British Geological Survey.

A review of the data collected by the Flinders instruments follows. The Flinders instruments all sampled at 10 s intervals. The magnetometers have a sensitivity of 0.1 nT per bit; and the electrometer, 0.05 mV m^{-1} per bit.

ELFMAG 2 (magnetometer 73) : Approximately 18 days of data were collected from this instrument. A large number of irregular spikes in the data occur in the middle part of the record. The cause of the spikes is unknown at present, and they were removed by an automatic method. The tilt meters show that the instrument was steady for the duration of the deployment. Battery and temperature records are normal. Clock drift over the entire experiment was only -3 s. The full fields recorded in each component differ from those predicted by the IGRF model, with H too large and Z too small by about 10000 nT. This suggests that the magnetometer was tilted by tens of degrees,

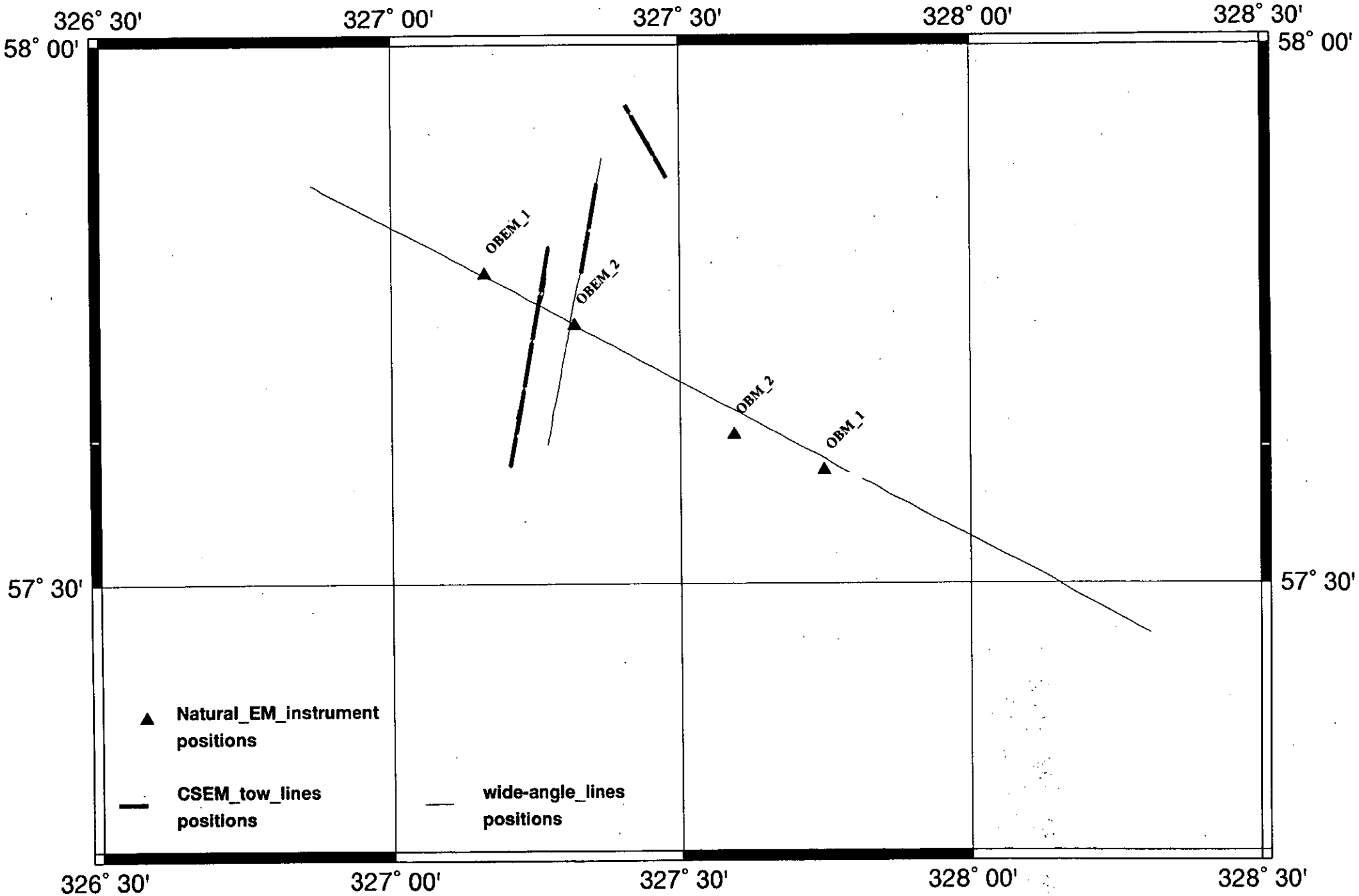

Figure 11. Natural source electromagnetic experiment — instrument locations.

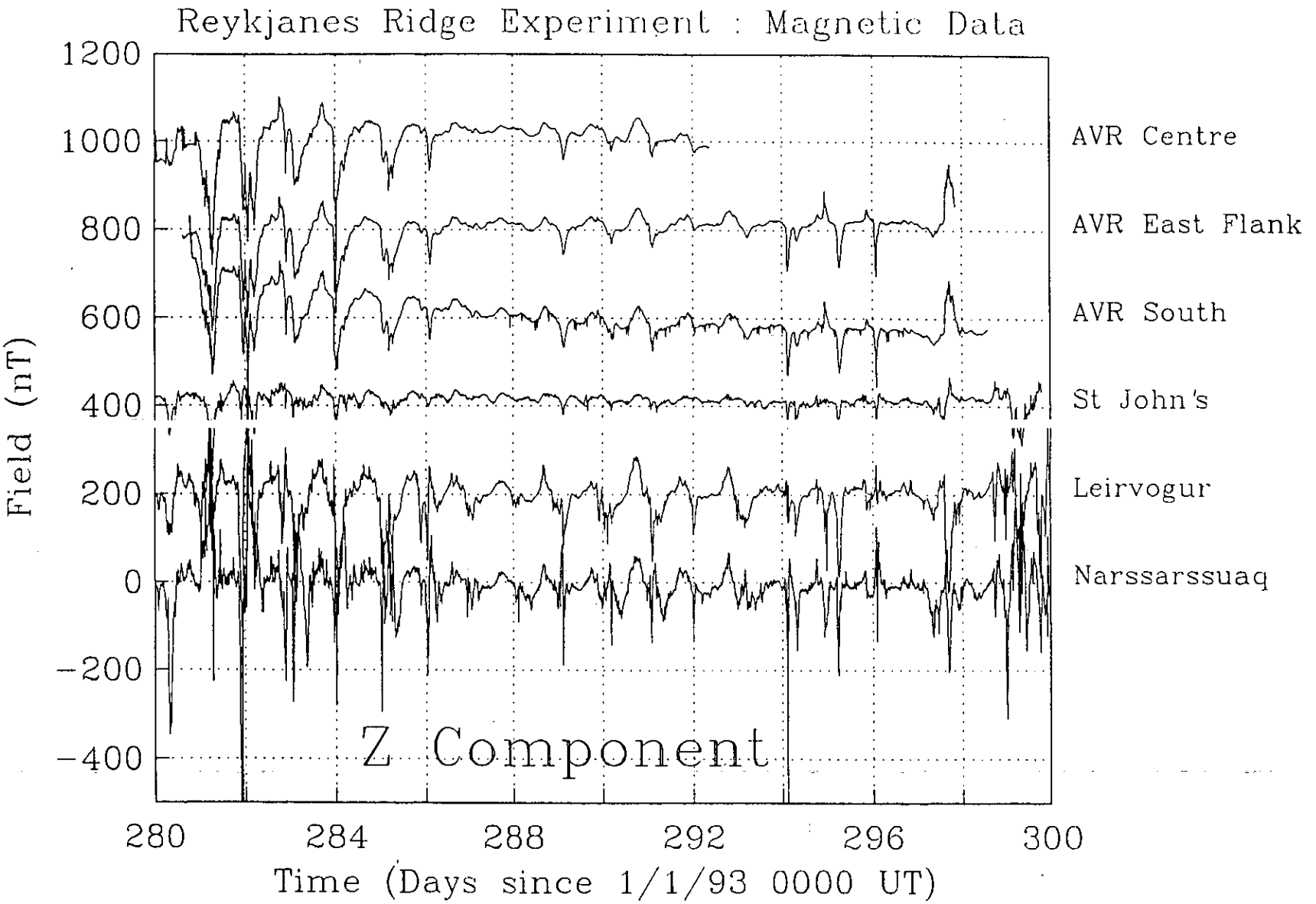

Figure 12. Z-component magnetic field data for the 3 seafloor magnetometer sites and 3 land observatories, days 280 to 300.

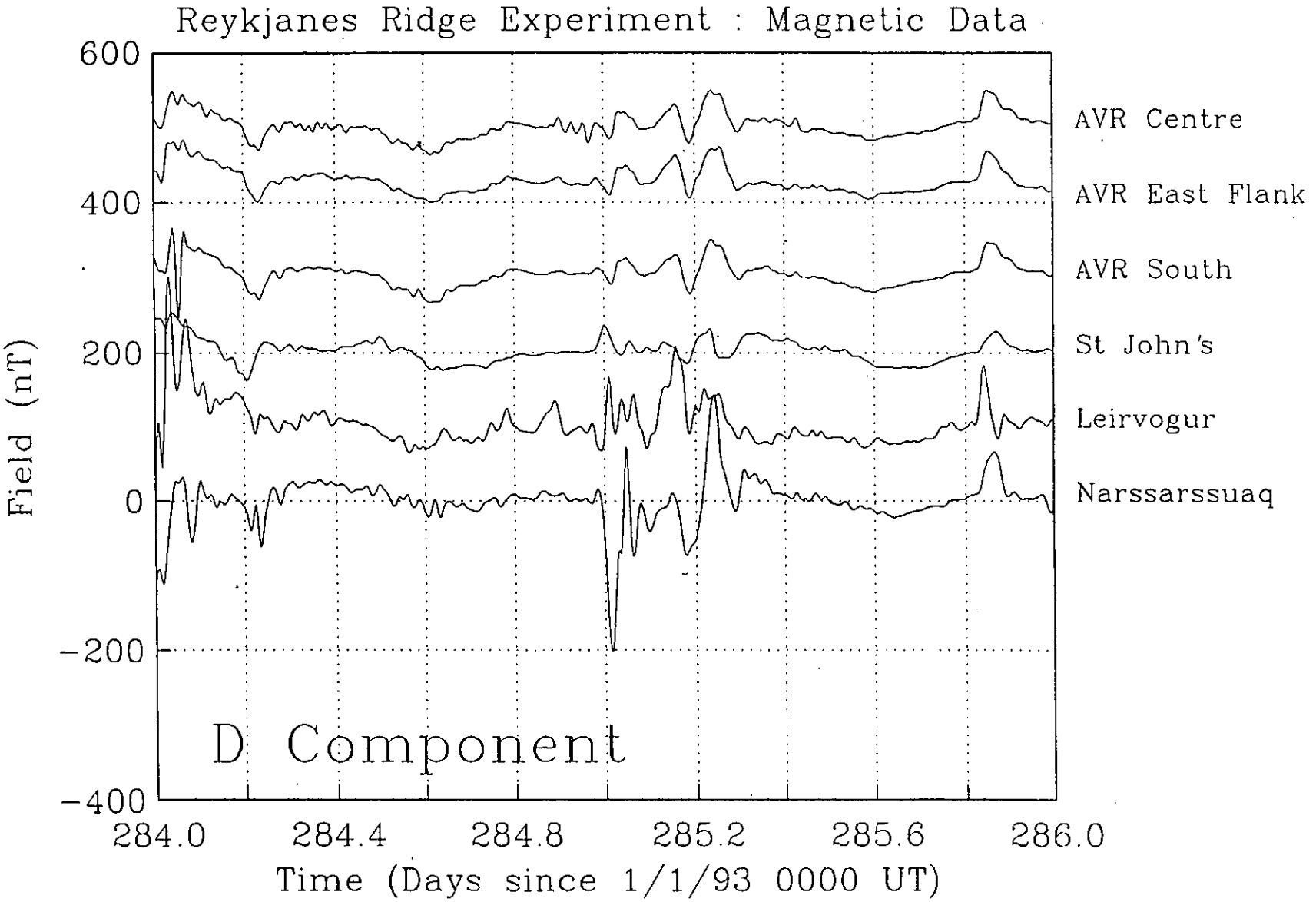

Figure 13. D-component magnetic field data for the 3 seafloor magnetometer sites and 3 land observatories, days 284 to 286.

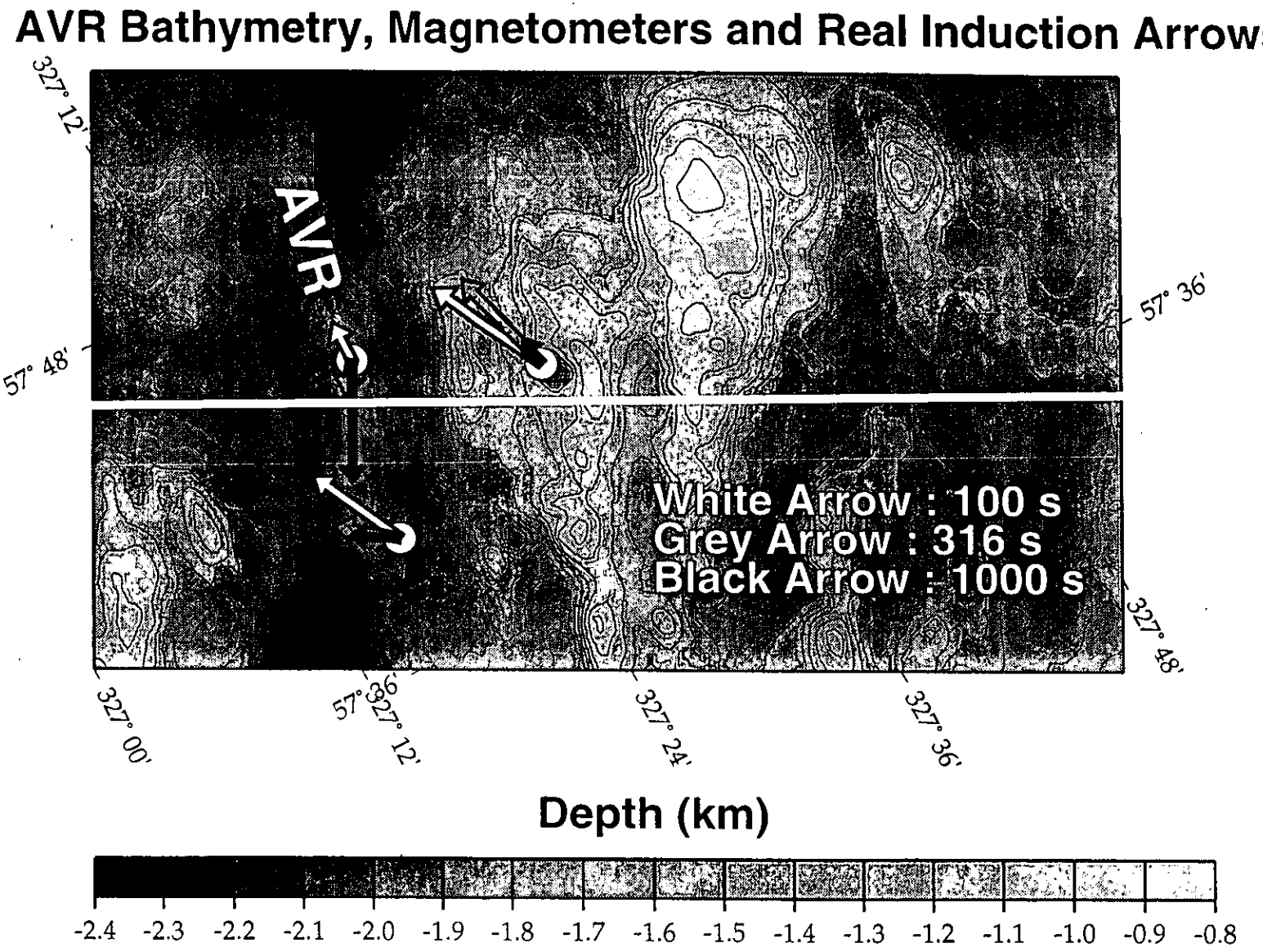

Figure 14. Real component induction arrows for the 3 seafloor magnetometer sites, at 3 frequencies (100 s, 316 s and 1000 s periods). The sites south and east exhibit very different responses.

although the tilt meters suggest a much smaller tilt. An explanation for this difference has not been determined and will have to wait for later calibration of the tilt meters and sensors. The raw XYZ data were rotated through 83 degrees (in a clockwise direction) to the horizontal components of HDZ.

ELFMAG 1 (magnetometer 74): Approximately 18 days of data were collected and data quality was good throughout. The tilt meter records show some progressive tilting in the X direction, and some small tidal variations. Battery and temperature records were normal. Clock drift was +37 s over the experiment. The full fields recorded were close to those predicted from the IGRF model (note that the tilt meter readings for magnetometer 74 were of the same order as those for magnetometer 73). The raw XYZ data were rotated 135 degrees to the horizontal components of HDZ.

OBEM 2 (magnetometer 75): Approximately 13 days of data were collected and data quality were good throughout. The tilt meter records shows that the instrument was steady throughout the deployment. Battery and temperature records show that the battery discharged at a faster rate than is normal, and the batteries should be replaced before the next deployment. Clock drift was -10 s over the experiment. The full fields recorded were close to those predicted from the IGRF model, although the horizontal fields were a little too small. The raw XYZ data were rotated -140 degrees to the horizontal components of HDZ.

OBEM 2 (electrometer 79): Approximately 18 days of data were collected and data quality were good. A large long-period drift due to electrode potential change is seen in the raw data, with high frequency ionospheric signals. The battery and temperature records were normal. Clock drift was +95 s for the deployment. A least-squares degree 6 polynomial was fitted to the data and used to remove the electrode drift from the X and Y sensors. The data were rotated from XY to EhEd, as the orientation of the electrometer relative to the attached magnetometer 75 was known.

Preliminary estimates of MT and geomagnetic depth sounding (GDS) responses have been made for the Flinders data. Electric field data from electrometer 79 was combined with the magnetic field data from the three seafloor sites to give the MT dataset. GDS estimates were obtained at each site. All the data were used in this instance, despite the fact that the source field during the first 6 days was highly disturbed by auroral activity. Consequently, these estimates are a first pass, and are not intended to be definitive. MT data using electrometer 79 and magnetometer 74 gave estimates at periods between 100 and 100,000 s (Figure 15), and were inverted using Occam's inversion (Figure 16). There is a high degree of anisotropy with the major axis of apparent resistivity being aligned along geographic north-south. Inversion shows a conductive structure becoming slightly more resistive with depth. Not surprisingly, they are not 1-D!

During future work, the electric field data from the Scripps instruments will be incorporated into this dataset to extend the scale of the survey. All of the Flinders instruments will need to be checked for sensor calibration, and the tilt-meters will need to be extensively tested to re-assess their calibration. At present no correction for tilting of the instruments has been attempted. A full MT and GDS analysis will be

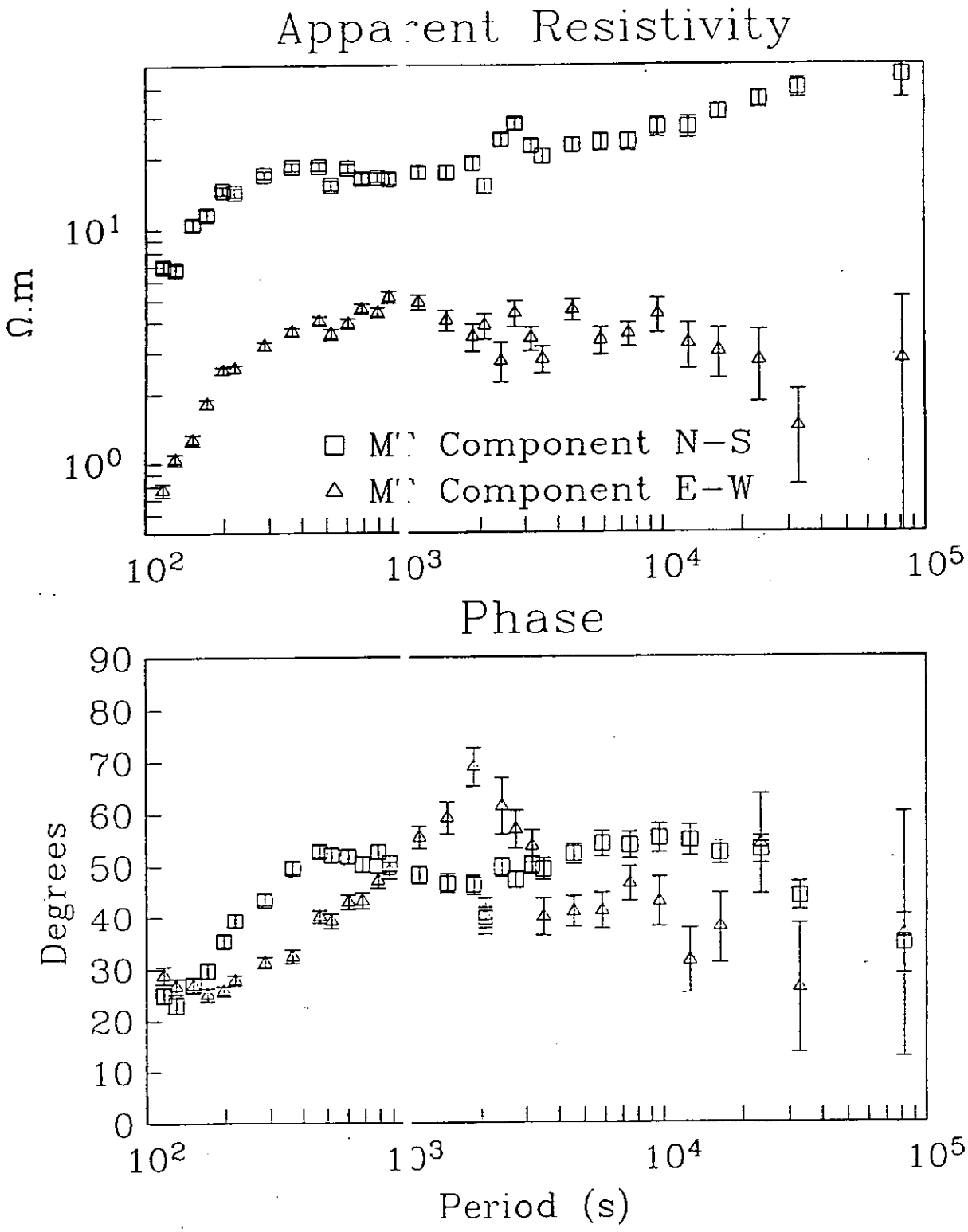

Figure 15. Magnetotelluric respo se at the AVR axis plotted as apparent resistivity and phase vs. period, derived using magnetic fields from ELFMAG 1 and electric fields from OBEM 2. Because of the length of the data, errors are small and the plot shows the MT response from 100 to 100,000 s periods.

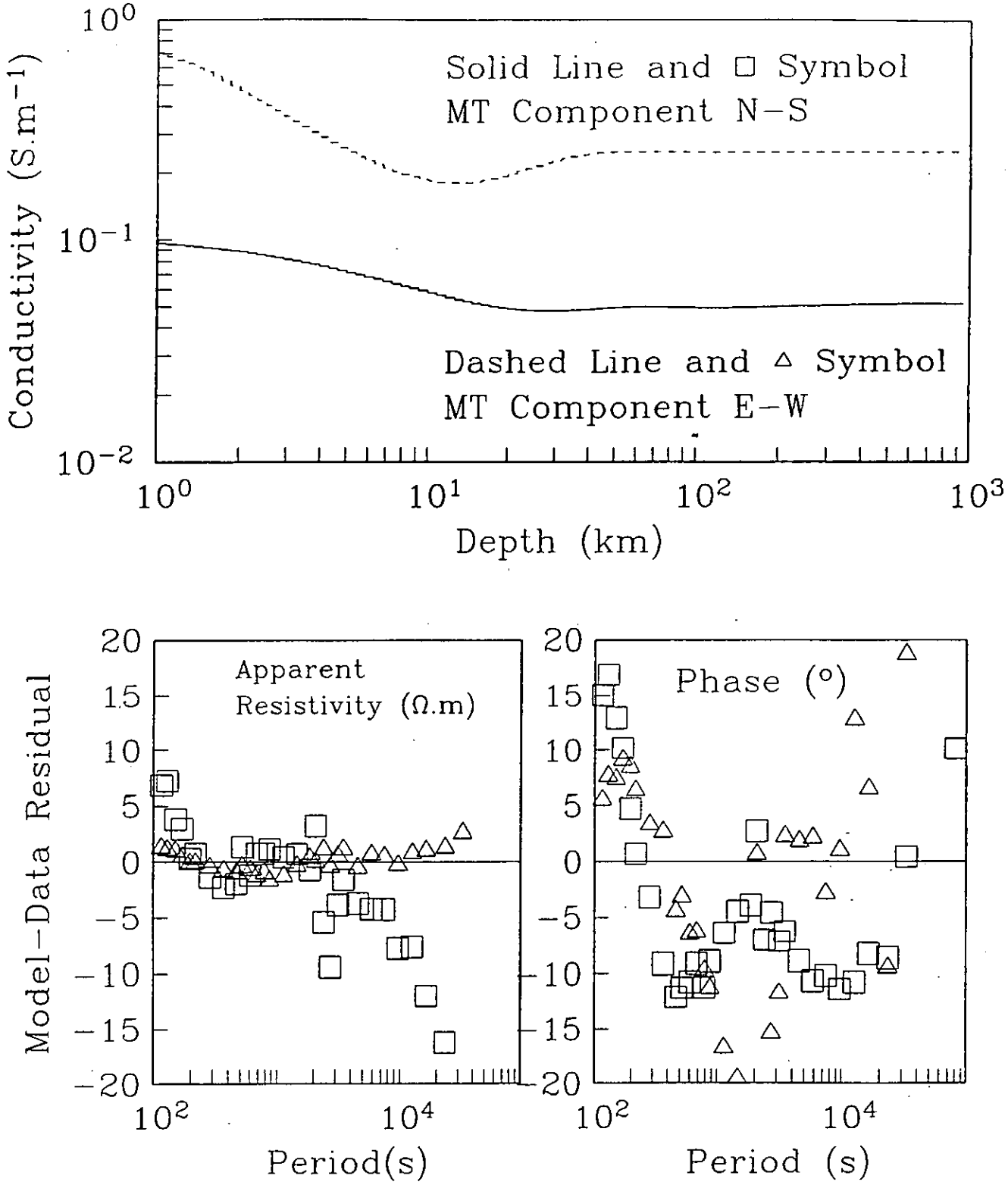

Figure 16. 1-D smooth (Occam) inversion of the MT data shown in Figure 15. Also shown are the apparent resistivity and phase residuals.

undertaken when all of the instrum nt corrections have been made. Data from the UK observatories will be very useful fo simulating fields over the entire north Atlantic. At this stage advanced modelling of tl e data, including the effects of coast lines and sea floor topography, will be undert ken to examine both the seafloor conductivity structure and auroral zone physics.

2.5 Additional Datasets

The primary objective of the cruise was to carry out the seismic and electromagnetic experiments outlin d above. However in the course of the cruise we were also able to collect significar amounts of swath bathymetry data. High quality bathymetry data will be important for the interpretation of both the seismic and the electromagnetic data — since both eismic and EM responses are substantially affected by sea floor topography. A summa y track chart showing ship tracks for which swath bathymetry data were logged anc subsequently processed and gridded during the cruise is shown in Figure 17. The t acks provide greater than 100% coverage over an area of approximately 12,000 km². The area covered overlaps with the southern boundary of Area C of Parson *et al.* (1993). A plot of the merged CD81 and AreaC datasets can be seen in Figure 18. Gravity data were collected throughout the cruise, and total field magnetic data were c ollected along all of the tracks shown in Figure 19. The track spacing used for the b thymetry/gravity/magnetics survey is denser than required for 100% swath coverage with the EM12 system, but was chosen to avoid the possibility of spatial aliasing of gi avity and magnetic fields in this water depth. In addition we collected swath bathy metry, gravity and magnetics data for most of the transit from Reykjavik to the wor area, following a track along or parallel to the Reykjanes Ridge axis and approx mately half a swath width outside the existing, narrow band of continuous axial c overage, so as to widen that band by one swath width. The Simrad EM12 multibeam system also recorded side-scan sonar images over the entire survey area. The gravity, swath bathymetry, side-scan sonar and magnetics data will be made available to I elandic and BRIDGE scientists for inclusion in regional studies of the Reykjanes Ri ige.

At the start of the experime nt we conducted a sound velocity meter dip using the AML sound velocity profiler at 57° 47.2' N, 32° 50.46' W (Figure 20). Accurate knowledge of the water column so nd velocity structure is essential for many aspects of the work carried out during this cruise; including long base line acoustic navigation of the research vessel or deep-towe package; accurate acoustic positioning of DOBSs and EM instruments on the seafl or; determination of source receiver ranges and explosive shot instants and detonati n depths; and corrections to the swath bathymetry data for travel times and ray bendin .

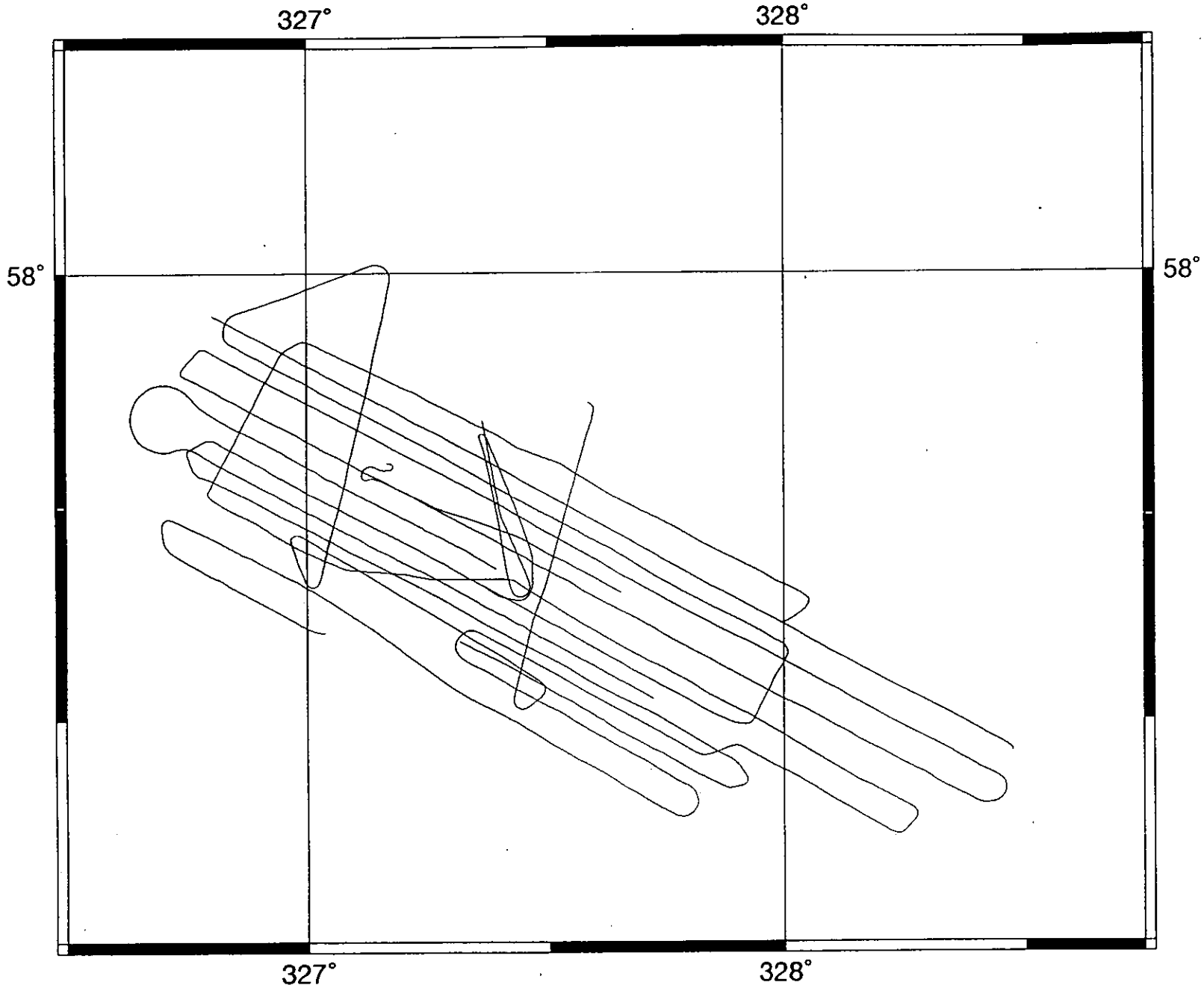

Figure 17. Swath bathymetry tracks.

Figure 18. Merged EM12 (CD81) and Hydrosweep (AreaC) datasets for 57-58°N.

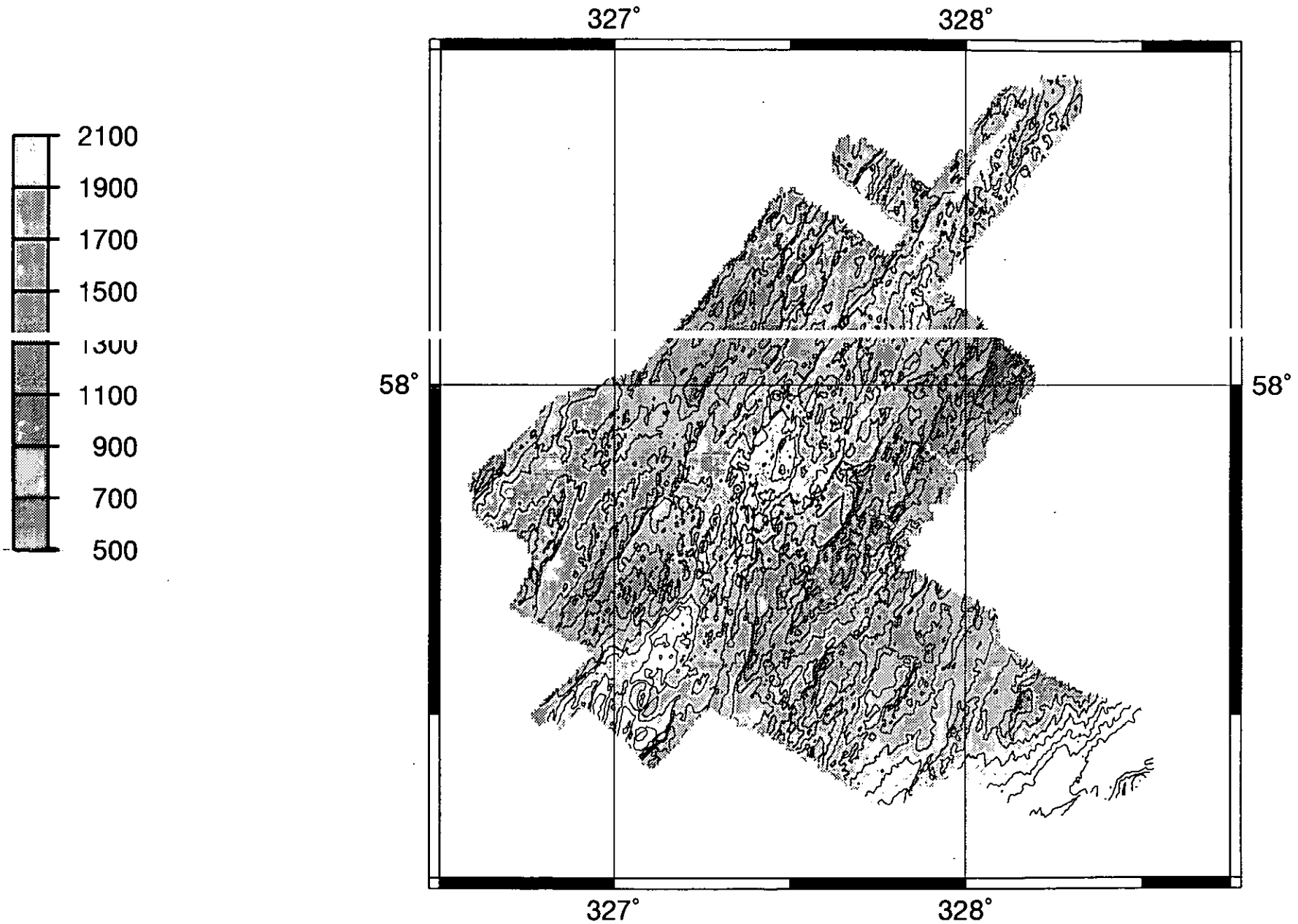

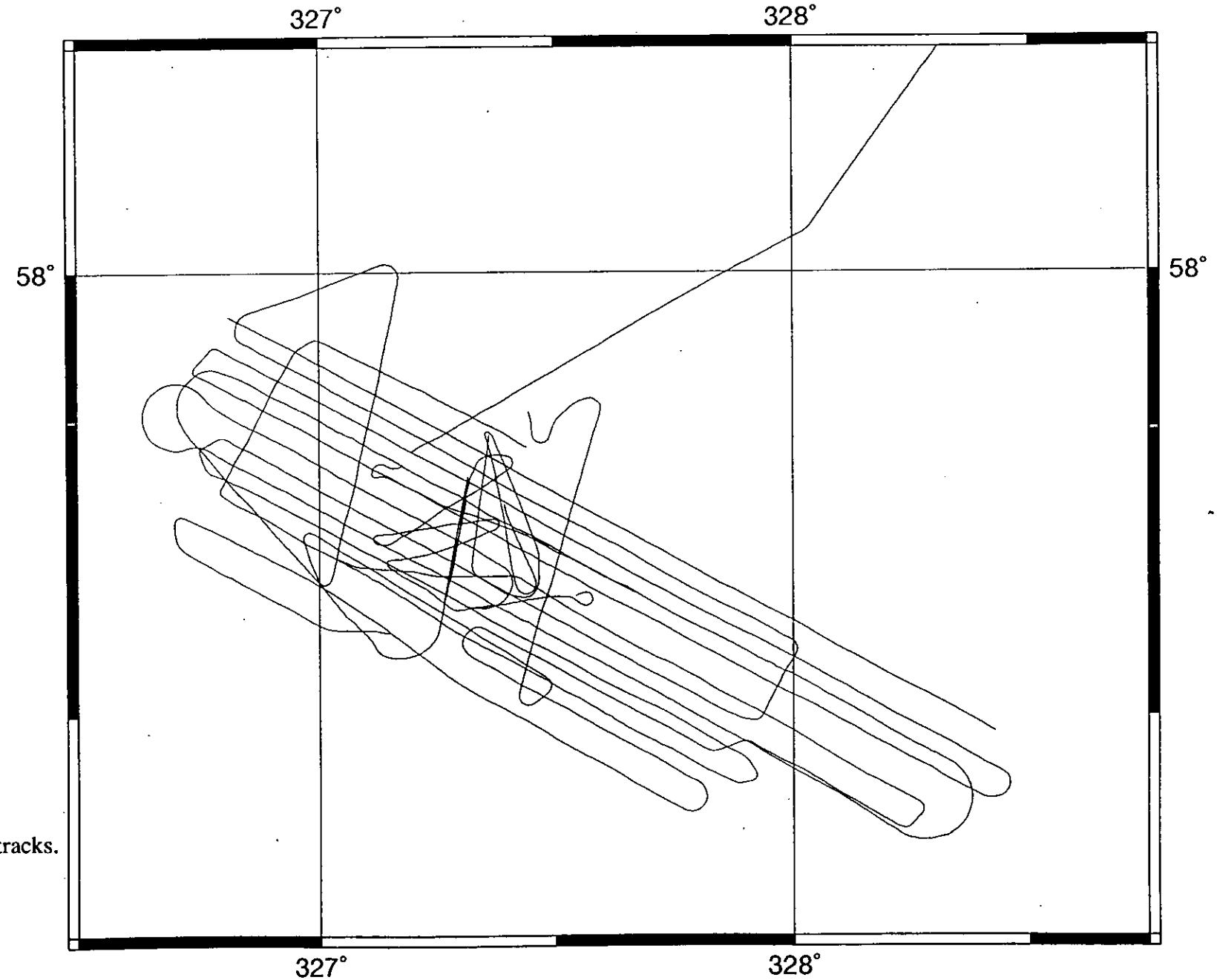

Figure 19. Magnetometry tracks.

SV DIP

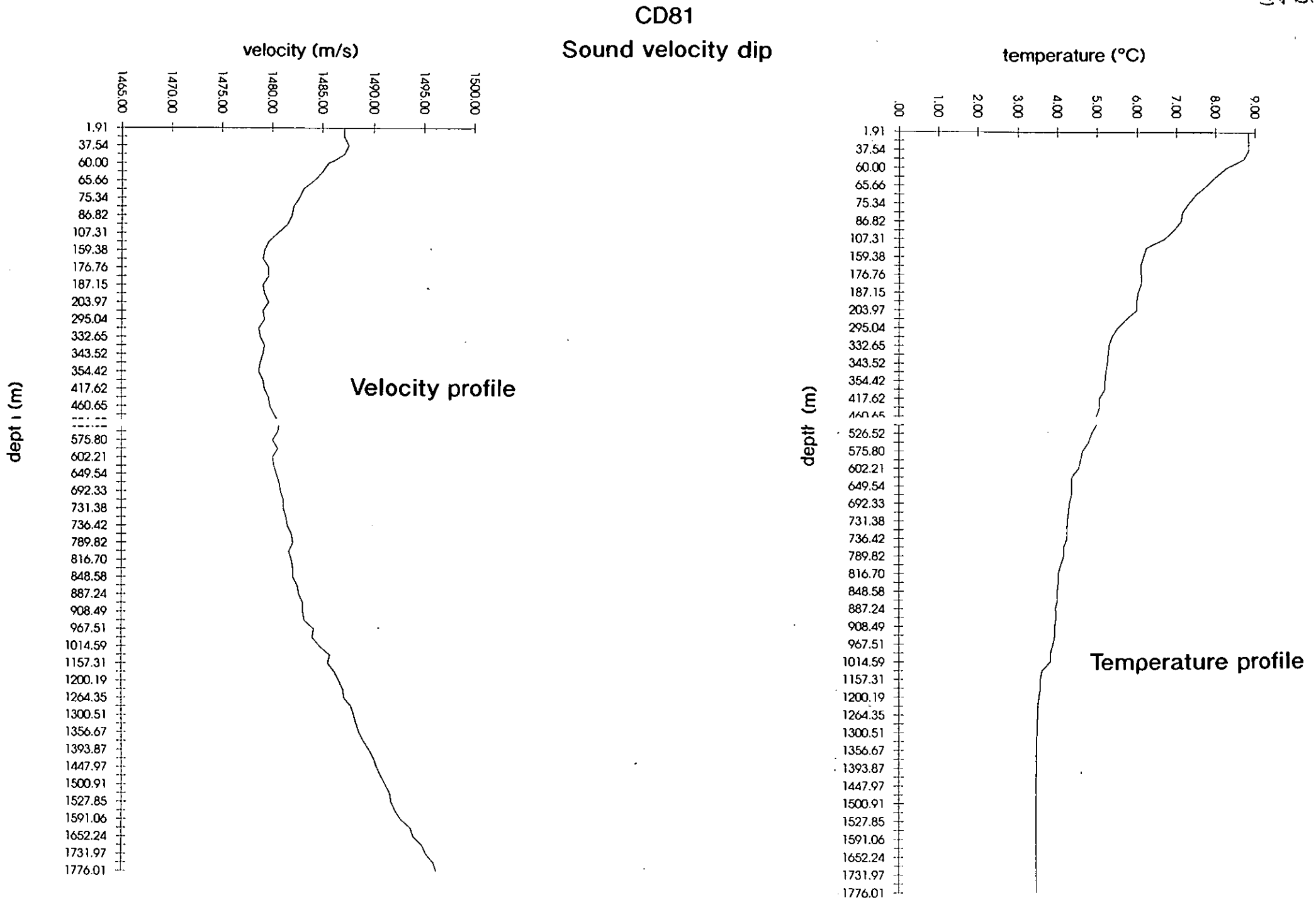

Figure 20. Sound velocity and temperature profiles in the water column.

3. Cruise Narrative

The duration of the cruise was 29 days 3 hours. Of this, 2 days were spent on passage from Reykjavik to the work area (although for much of this time we were opportunistically collecting geophysical data along the Reykjanes Ridge axis); and 4 days 5 hours were spent at the end of the cruise on passage back to Barry — leaving a total of 22 days 22 hours on station in the work area. Of this, 51 hours were lost through bad weather, leaving a total of 20 days 19 hours available for scientific work in the study area (In our ship time application submitted to NERC in November 1991 we had requested a minimum of 25 days ship time on station, to complete the highest priority components of the project.) A summary of the events that took place appears below. All times are in GMT.

3 Oct.	16:00	Sailed from Reykjavik. Commenced passage to work area.
4 Oct.	09:00	Streamed magnetometer and PES fish. Began collecting swath bathymetry, gravity and magnetics data along the axis of the Reykjanes Ridge while on passage.
5 Oct.	13:21	Reached northern boundary of Parson *et al.* Area C. Stopped logging swath bathymetry data.
	16:06	Arrived in work area at position for deploying first instrument. Recovered magnetometer fish. Wanting to start sound velocimeter dip, but delayed by problems with spooling gear on CTD winch which require hundreds of metres of wire to be run off the winch then respooled.
	19:45	Winch repaired - began sound velocimeter dip
	21:50	Sound velocity dip completed. On recovery, wire tested a Cambridge DOBS.
	23:41	Deployed Flinders magnetometer/electrometer OBEM 1.
6 Oct.	00:03	Left OBEM 1 position. Streamed magnetometer. Began swath bathymetry/gravity/ magnetics survey of the main across axis profile for the seismic experiment.
	13:39	Completed initial survey. Recovered magnetometer then headed for deployment position for LEM 1.
	16:30	Began deployment of LEM 1.
	18:35	LEM 1 in the water and being towed/lowered towards the bottom.
	21:52	LEM 1 released. Wire out = 2917 metres.
	22:45	Deep tow cable recovered.
7 Oct.	0037	Began deployment of LEM 2, orthogonal to LEM 1.
	01:18	LEM 2 in the water and being towed/lowered towards the bottom.
	04:01	LEM 2 released. Wire out = 2981 metres.
	05:23	Deep tow cable recovered. Headed towards deployment position for OBEM 2.
	07:51	Deployed OBEM 2.
	08:15	Headed towards deployment position for OBM 1.
	10:06	OBM 1 deployed. Began acoustic survey of LEM 1 and LEM 2 instrument packages and tail-end transponders; following this, recovered tail end transponders from LEM 1 and LEM 2.
	15:50	Began deployment of LEM 3.
	17:17	LEM 3 in the water and being towed/lowered towards the bottom.
	20:07	LEM 3 released. Wire out = 3063 metres.
	21:30	Deep tow cable recovered.
	23:10	Began deployment of LEM 4.
8 Oct.	00:01	LEM 4 in the water and being towed/lowered to the bottom.
	03:08	LEM 4 released. Wire out = 2993 metres.
	04:15	Deep tow cable recovered. Began acoustic survey of LEM 4 instrument package and tail end transpond
	06:20	Deployed OBM 2.
	08:07	Recovered LEM 4 tail end transponder, then returned to LEM 3.

	10:30	Recovered LEM 3 tail e ıd transponder.
	11:15	Began deployment of D)BSs and ELFMAGs, heading from WSW to ENE, in order: DDOBS 6, CDOBS 15,)DOBS 5, ELFMAG 1,CDOBS 14, DDOBS 4, ELFMAG 2, CDOBS 13, DDOBS 3, :DOBS 12, DDOBS 5, CDOBS 11, DDOBS 6.
9 Oct.	01:38	DOBS and ELFMAG d(ployments completed. Headed for start position of next stage of swath survey.
	07:57	Streamed magnetometei and started swath bathymetry/gravity/magnetics survey.
	13:19	End of swath bathymetr survey. Recovered magnetometer. Headed for deployment position of first acoustic transponder.
	15:30	Streamed Oceano acous ic navigation fish.
	15:45	Began deploying acoust : navigation beacons in order: A, B, C, D, E, F, G, H, I.
10 Oct.	02:22	Last transponder deploy d. Recovered OCEANO fish.
	06:15	Began bringing explosiv :s on deck for first shot firing run.
	07:48	Began shot firing along ine 1. Programme consisted of 2 test/scare charges followed by 61 x 25 kg shots at 4 mi ıute intervals. Two were misfires, others had flight times of approximately 2 minute 30 seconds. Shot firing run ended at 12:07.
	13:42	Continued shot firing al(ng Line 1 - 2 x test/scare charges followed by 19 x 50 kg shots, at 8 minute intervals. T\ o were misfires. Flight times again approximately 2 minutes 30 seconds. Shot firing (nded at 16:23.
	19:15	Streamed OCEANO fisl and magnetometer, then began running a network of tracks at slow speed through the : coustic navigation transponder net for calibration/GPS registration purposes. U(fortunately this procedure proved to be ineffective, since the combination of OCEAN) ship board units and Scripps sea bottom transponder units was unable to produce u :able ranges at slant ranges greater than about 3 to 4 km.
11 Oct.	06:23	End of acoustic navigati ın calibration tracks. Recovered magnetometer and OCEANO fish, then brought remai ıing explosives on deck ready for shot firing run.
	07:45	Began shot firing run al(ng Line 2 - 2 x test/scare charges followed by 31 x 25 kg shots at 4 minute intervals. N(misfires, all flight times approximately 2 minutes 30 seconds.
	10:05	End of shot firing progr: mme. Headed to position 15 nm to leeward of start point for air gunning line, then be gan deploying hydrophone streamer and air gun array.
	22:30	Reached start position a' northern end of Line 2, airguns and hydrophone streamed but experiencing problems v ith airguns and compressors.
	23:12	Airguns finally synchroı ised and firing. Continued air-gunning with full (12-gun) array along Line 2, then swun ; round to the WNW end of Line 1, then airgunned with full source array along Line .
12 Oct.	19:53	Reached the end of Line 1. Started turn onto multi-channel seismic Line 3. Weather up until now excellent.
	20:37	Switched to firing reduc(d airgun array every 20 seconds to give 8-fold CMP coverage.
	22:05	Started MCS line 3.
13 Oct.	02:03	Launched disposable soı obuoy no. 1. This failed at 02:25.
	03:04	Launched disposable soı obuoy no. 2. This also failed to work.
	08:45	End of MCS line 3. Star :d turn onto MCS line 4. Weather moderate but worsening, wind now 25 kts from th : NE.
	11:45	Start of MCS line 4. Lau ıched disposable sonobuoy no. 3.
	13:08	Launched disposable sor)buoy no. 4.
	17:17	End of multichannel sei: nics. We had received weather reports indicating a deep depression with winds ir excess of 40 knots moving into our work area in the next 24 hours; so took a decision to truncate the seismic experiment early, abandoning some of the grid of multi-channe' seismic lines that we had planned to collect, and recover as many DOBSs as possibl(before the weather made operations impossible.
	20:22	Finished recovery of air uns and hydrophone streamer, then headed for position of nearest DOBS (DDOBS 1).
	21:04	Began recovering DOBS :, in order DDOBS 4, DDOBS 6, DDOBS 5, DDOBS 3, DDOBS 2, DDOBS 1, CDOBS 11, (:DOBS 12, CDOBS 13, CDOBS 14. The OCEANO fish was streamed at 09:10/14th f(r recovery of the CDOBSs.
14 Oct.	12:49	CDOBS 14 recovered.

	13:36	Sent release signal to CDOBS 15. The instrument acknowledged receipt of the command, but failed to release from the seabed. Continued trying, unsuccessfully, to release it until 14:45. Then began deploying ELF receivers for CSEM experiment.
	15:47	Deployed ELF 1, followed by ELF 2.
	22:00	Began a second attempt to calibrate the seà bottom acoustic navigation transponder net, after making adjustments to the ship board OCEANO equipment.
15 Oct.	12:41	Finished second attempt to calibrate the acoustic navigation net. The OCEANO system had logged ranges from receivers throughout this exercise; but careful scrutiny of the ranges subsequently showed that such a high proportion of them were spurious that this survey too was useless.
	13:45	Commenced further efforts to recover CDOBS 15, and/or determine the nature of the problem.
	14:36	Abandoned efforts on CDOBS 15. Recovered OCEANO fish.
	15:19	Started deploying remaining sea bottom receivers for CSEM experiment, in the order: ELF 3, ELF 4, LEMUR 4, LEMUR 3, LEMUR 2, LEMUR 1. Only 4 LEMURs could be deployed following the loss of CDOBS 15, since the Cambridge DOBSs and LEMURs share much common hardware. During deployment of these instruments on the rugged near-axis terrain, short bathymetric surveys were carried out before each deployment to locate relatively flat landing areas for the instruments.
16 Oct.	03:06	Finished deploying ELFs and LEMURs. After this we made one more pass over CDOBS 15 to see if it had moved - it hadn't - then carried out a final acoustic survey of the positions on the sea bed of LEM 4 followed by LEM 3, while transiting out to the WSW edge of the survey area to start more swath bathymetry surveying.
	07:47	Completed the acoustic survey and started the swath bathymetry survey.
	10:57	Streamed the magnetometer and began logging magnetics as well as gravity and swath bathymetry.
17 Oct.	08:36	Finished swath/gravity/magnetics survey. Recovered magnetometer. Since by now it was clear that the acoustic transponders in the navigation net were not going to work, we decided to start recovering them now, in order to save time later in the cruise. Meanwhile, we were having some problems with the preparation of the DASI CSEM transmitter, so using ship time to recover unnecessary bottom packages at this stage, to allow more time for working on DASI, made good use of ship time.
	10:00	Began recovering acoustic navigation transponders in the order: F, G, H, I, C, D. Transponders A, B and E were left in position since they were in useful locations for ranging from DASI to provide CSEM source-receiver offsets. Even a limited number of ranges from these transponders at short ranges would provide useful constraints on the CSEM experiment geometry.
	17:47	Finished transponder recoveries; then began a detailed acoustic survey of the final sea bottom positions of ELF 1, ELFMAG 1, LEMUR 1, ELF 3, LEMUR 2, LEMUR 3, ELF 4, LEMUR 4, ELFMAG 2, transponder E, transponder B, ELF 2 and finally transponder A.
18 Oct.	11:40	Completed acoustic surveying; then headed to the deployment position for the start of DASI tow line 1.
	13:00	Arrived at deployment position; streamed OCEANO and 3.5 kHz fish; began final deck preparation and deployment of DASI.
	22:30	DASI antenna array streamed, and DASI ready for final tests and deployment. At this point a fault appeared on the DASI ship-board power supply system. Began manoeuvring the ship in a wide circle to bring us back towards the DASI launch position, while tracking down the power supply problem.
19 Oct.	08:15	The problem with the DASI power supply system was traced to the emergency stop circuits, and rectified. Final deck tests of DASI were carried out.
	11:00	DASI finally entered the water; the OCEANO acoustic relay transponder was attached to the deep tow cable 200 metres above it; and we began lowering the instrument towards the sea bed.
	13:45	Commenced DASI transmissions on Tow Line 1.
	17:40	DASI went dead. Turned power off, pulled DASI up to 200 m clear of the sea bed, and started investigating the problem.

	18:11	It was clear that the prol lem was at the deep tow end, not the ship board end, of the system; so began recove ing DASI for repairs.
20 Oct.	01:15	Having returned at slow speed, towing the DASI streamer from the stern, to the site of CDOBS 15, confirme l that it was still in the same position on the sea bed. Meanwhile, stripping dc vn DASI and searching for the fault.
	11:00	Still working on DASI. Meanwhile the weather was deteriorating, causing strain on the DASI streamer and ham ering steerage at slow speeds. We therefore recovered the DASI streamer.
	11:30	Having recovered the st eamer, we decided to make use of the ship time while DASI was being repaired by recov ring the remaining Scripps acoustic navigation transponders.
	17:05	Completed recovery of t maining transponders, E, A and B. However while recovering the last transponder (B) ve spotted another instrument floating on the surface near by. It turned out to be ELF , which had lost one of its bottom weights and returned to the surface prematurely. We recovered it safely.
	17:53	Streamed magnetometer then began the last stage of the swath bathymetry/gravity/mag etics survey.
21 Oct.	11:20	Suspended the swath ba ymetry/gravity/magnetics survey; recovered magnetometer.
	12:12	Re-deployed ELF 2 in it original position, having backed up the data it had recorded on its first deployment. For its second deployment, we programmed it to record DC/low frequency data for MT s ounding in addition to CSEM data, to make the best use of its recording capacity.
	13:55	Started an acoustic surv y around ELF 2 to determine its position after re-deployment.
	14:36	Streamed magnetometer and resumed swath bathymetry/gravity/magnetics survey.
	15:50	Realised that we had lef the acoustics on ELF 2 enabled, so turned round to head back to it to disable it.
	17:07	ELF 2 acoustics disable . Turned round to resume swath bathymetry/gravity/mag etics survey. Overnight, the weather worsened progressively, building up to Force 7 t 8 from the west.
22 Oct.	05:00	Bad weather forced us t heave to and terminate surveying. Wind now 35 kts from the west. Meanwhile, the fa lt on DASI had been traced to a blown capacitor on the HT side of the communications c ircuit, which was shorting the HT at the deep tow. DASI was now repaired and ready or deployment, but deployment was impossible in the prevailing weather cond tions.
	08:00	Recovered the magneto eter at first light, then spent the remainder of the day hove to in Force 8 winds, waitin for the weather to improve.
23 Oct.	07:00	Weather moderated slig tly - wind now SSW, 25 to 30 kts. Decided to try to deploy DASI and carry out our highest priority DASI track, parallel to the AVR axis and offset from the axis by 4 km t the west (tow line 2). Headed for a position 15 km downwind from start point of the t w line.
	09:32	Began DASI deploymer .
	15:15	DASI in the water and b ing lowered towards the sea bed.
	16:30	Began DASI transmissi ns along DASI tow line 2.
	23:40	End of DASI tow line 2 Began hauling in cable to lift DASI well above sea floor, and started slow turn to hea for start position of next DASI tow.
24 Oct.		Overnight and into the morning of the 24th, the weather steadily deteriorated again, making the prospect of carrying out further DASI work increasingly unlikely.
	08:30	Wind now 40 kts from t e ESE. There was no possibility of towing DASI along the desired track in this wea her. Lowered DASI towards the bottom while heading into the wind at low speed, in th hope of restarting DASI transmissions on an unplanned track in the only direction we could go in the prevailing weather conditions.
	10:45	It became clear that DA SI was no longer outputting any significant current, the most likely reason being dam ge to the antenna streamer. We turned down the power and began heaving DASI in o a short tow, to await recovery when the weather improved. While doing this, large waves breaking over the stern resulted in sea water flooding through the hatch cover drains into the scientific hold, where the DASI power supply system was located. Thi forced the final abandonment of any further efforts to get

		DASI operational again. The power supply was shut down, DASI was pulled up to 500 m below the surface, and we hove to await an improvement in the weather that would allow DASI to be recovered.
25 Oct.	08:52	Weather moderated slightly; began recovery of DASI.
	10:30	DASI recovered safely, though showing many signs of having taken a considerable battering during the bad weather. Recovered Oceano and 3.5 kHz fish.
	13:41	Began recovery of sea floor em instruments, in the order: LEM 3, LEM 1, LEM 2, LEM 4, ELF 1, ELFMAG 1, LEMUR 1, LEMUR 2, LEMUR 3.
26 Oct.	02:04	LEMUR 3 recovered. Released OBEM 2 from the sea bed. By this time, the weather was worsening dramatically - barometer dropping fast, and wind speed increasing.
	04:26	Recovered OBEM 2 in lively weather through the starboard A frame - wind now 40 kts from the west. Suspended operations until 10:00, when OBM 1 was due to arrive at the surface after releasing from the sea bed by timer.
	10:30	OBM 1 recovered. The weather had moderated again by this time. This was followed by recovery of ELF 3 (which surfaced with a dead, bright orange, brittle star curled up in one end of the pressure case housing); and ELFMAG 2.
	16:23	OBEM 1 released from the sea bed, but started to ascend only extremely slowly. Instead of waiting for it to surface, we attempted to release LEMUR 4 while it was on the way up.
	18:08	LEMUR 4 acknowledged release code, but did not leave the sea bed. After trying for an hour to release it, we returned to OBEM 1 - only to find that it was still in mid water and ascending extremely slowly.
	22:15	After further attempts to release LEMUR 4 and to track OBEM 1's extremely slow ascent, we started recovery of ELF 4. By now the weather was deteriorating again, and ELF 4 was finally recovered through the starboard A frame in winds in excess of 40 kts. After this we made further efforts to track OBEM 1, which had virtually stopped ascending at about 350 metres below the sea surface.
27 Oct.	05:00	Left OBEM 1, and headed ESE at the best speed we could make into a 35 kt wind, in order to be on station when OBM 2 surfaced on a timed release.
	10:40	OBM 2 due on the surface; vessel on station 0.5 nm to leeward of its position.
	12:00	Having seen no signs whatever, either visually or by radio, of OBM 2, abandoned the search for it and returned to OBEM 1.
	14:06	Found that OBEM 1 had finally stopped ascending at a depth of 250 m below the surface. We decided to try to fish for it, by constructing a rig equipped with a cross beam, wires and grapnels, and using the Scripps down-wire acoustic system on the deep tow cable to provide direct ranges from the OBEM to the fishing rig. While assembling the rig, we made a final attempt to recover LEMUR 4. This was unsuccessful, so we disabled its acoustics and abandoned it.
	20:18	Fishing gear ready - headed back to fish for the neutrally buoyant OBEM.
	22:02	Streamed the fishing gear and began fishing for the OBEM.
28 Oct.	11:30	Our fishing efforts were unsuccessful, despite several times getting the fishing gear to within 25 metres of the OBEM. Fishing for an instrument drifting at speeds of around half a knot, 250 m below the ship, had proved harder than we had expected. We recovered the fishing gear, then headed to the position of CDOBS 15.
	12:50	Made a last, unsuccessful attempt to release CDOBS 15. We then left it with its acoustics disabled.
	13:05	End of science. Recovered the PES fish and headed for Barry.
1 Nov.	18:30	Arrived alongside at R.V.S., Barry.

4. Explosive Shot Firing

The 111 planned explosive shots (see Table 3) were divided into 92 x 25 kg and 19 x 50 kg charges, constructed from 25 kg boxes of ICI E700 Powergel (UN0241, class 1.1D), one 275 g x 50 mm Multiprime primer (UN0042, class 1.1D) and 2 m of 10.6 g Cordtex (UN0065, class 1.1D ART). Each charge was double fused using 4 m of Yellow Clover safety fuse (UN0030) per no. 6 plain detonator (UN0105). Yellow Clover safety fuse is no longer manufactured by ICI, and the fuse used during CD81 was imported from ICI's stockpile in Canada. Figure 21 shows the construction of the individual charges. ICI also no longer supply pre-crimped plain detonators and safety fuse. The components of the 222 fuses were therefore delivered to and crimped by the shot firers at RVS, using tools kindly borrowed from ICI. The fuses were constructed and loaded onto the *Charles Darwin* prior to her departure from Barry for CD80. The remaining 3.25 tonnes of E700 and the Multiprime primers were loaded onto the ship two days later during a 3 hour port call at Ardrossan. Loading of the explosives was conducted during the early hours of the morning, after departure of the Belfast ferry.

The 25 kg charges were detonated at 4 min intervals (~ 1.0 km spacing at ~ 8.1 knots) and the 50 kg charges at 8 min intervals (~ 2.0 km) over two days. Shot locations and detonation times are shown in Table 3 and line locations in Table 4. Of the 111 charges only 4 misfired. The shot firing was conducted in a calm and professional way by the shot firers, which not only inspired confidence, but also contributed to the high number of successful detonations. A small number of shot windows were missed due to intermittent problems with the fuse lighters, but spare windows were built into the DOBS programmes to cope with such a problem and this avoided data loss.

The only real problem encountered throughout shot firing was the extremely variable burn rate of the Yellow Clover safety fuse in water — with variations of up to 55 sec for a 3.60 m fuse (consistent burn time — 2 min 30 sec in air — see Figure 22). However, with adjustment of fuse lengths throughout shooting, these variations could be kept within acceptable limits, i.e into the DOBS recording windows. Fuse lengths were calculated prior to CD81 to ensure that shock factors of water waves against the ship's hull were below the RVS acceptable limit of 0.01 (see Table 5). No apparent damage to the vessel was reported during shot firing — an outcome resulting mainly from forward planning and relatively small charge sizes.

5. Equipment Performance

The dominant aspect of this cruise in terms of equipment was the vast amount that we had on board in order to undertake such a large scale, multidisciplinary programme. The ship was quite literally full of equipment and of people (there were no spare berths and if there had been we could easily have filled another half dozen with useful people). We had most of RVS's stock of seismic equipment on board; complete DOBS systems with all their attendant gear from both Cambridge and Durham; the Cambridge CSEM system, which by itself can fill a 20' container; 10 sea bottom

Figure 21. Construction of explosive charges.

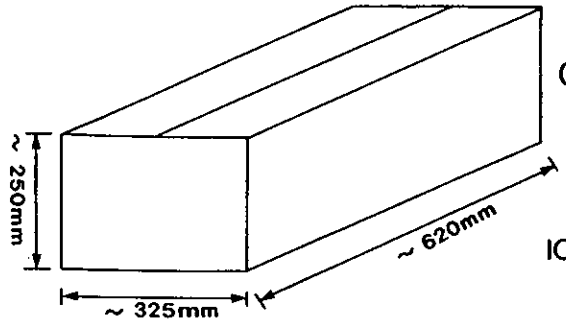

(after Barton CD 69/92)

25kg box of
ICI E-700 Powergel

Cardboard box has a flap top and contains: 5x5kg sticks
100mm in diameter

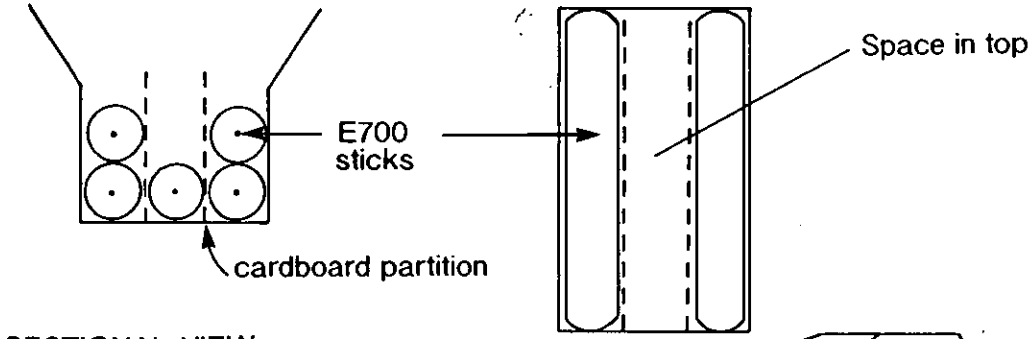

SECTIONAL VIEW

PLAN VIEW

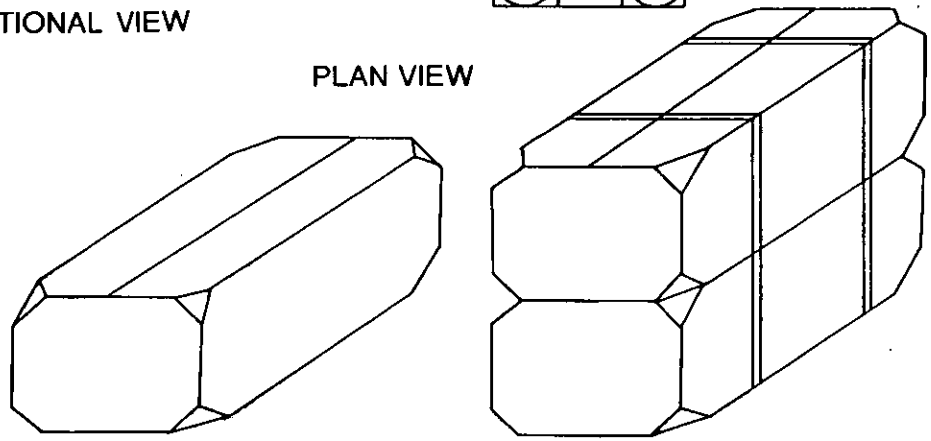

25kg charge

50kg charge

box corners removed to improve sink rate.

Detonating assembly

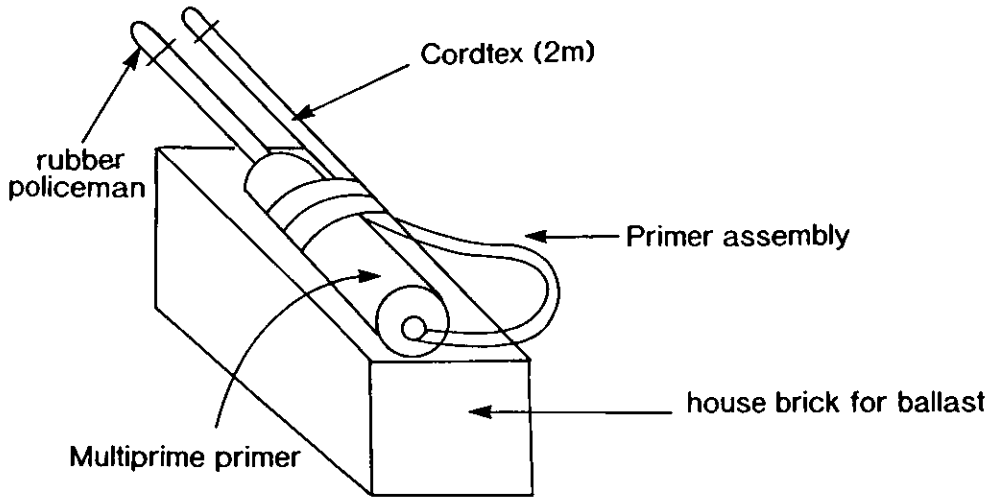

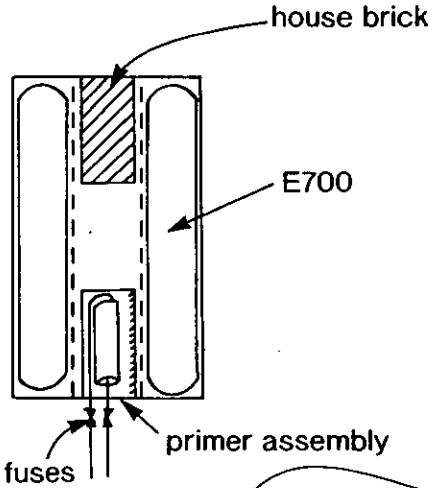

Primed box

Second box for 50kg charge
Contained two bricks only

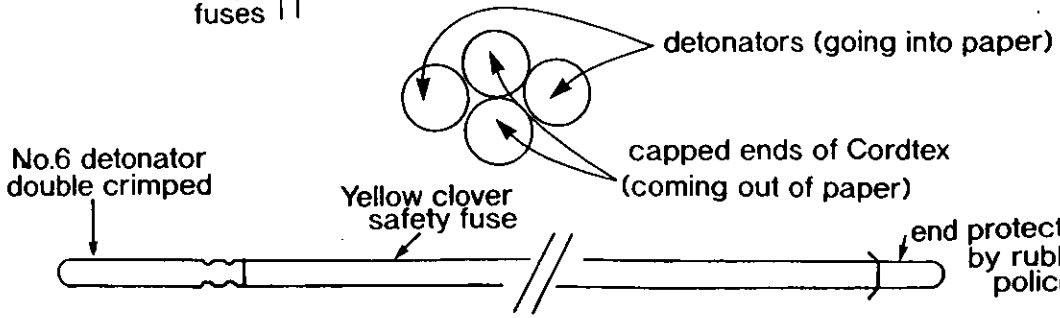

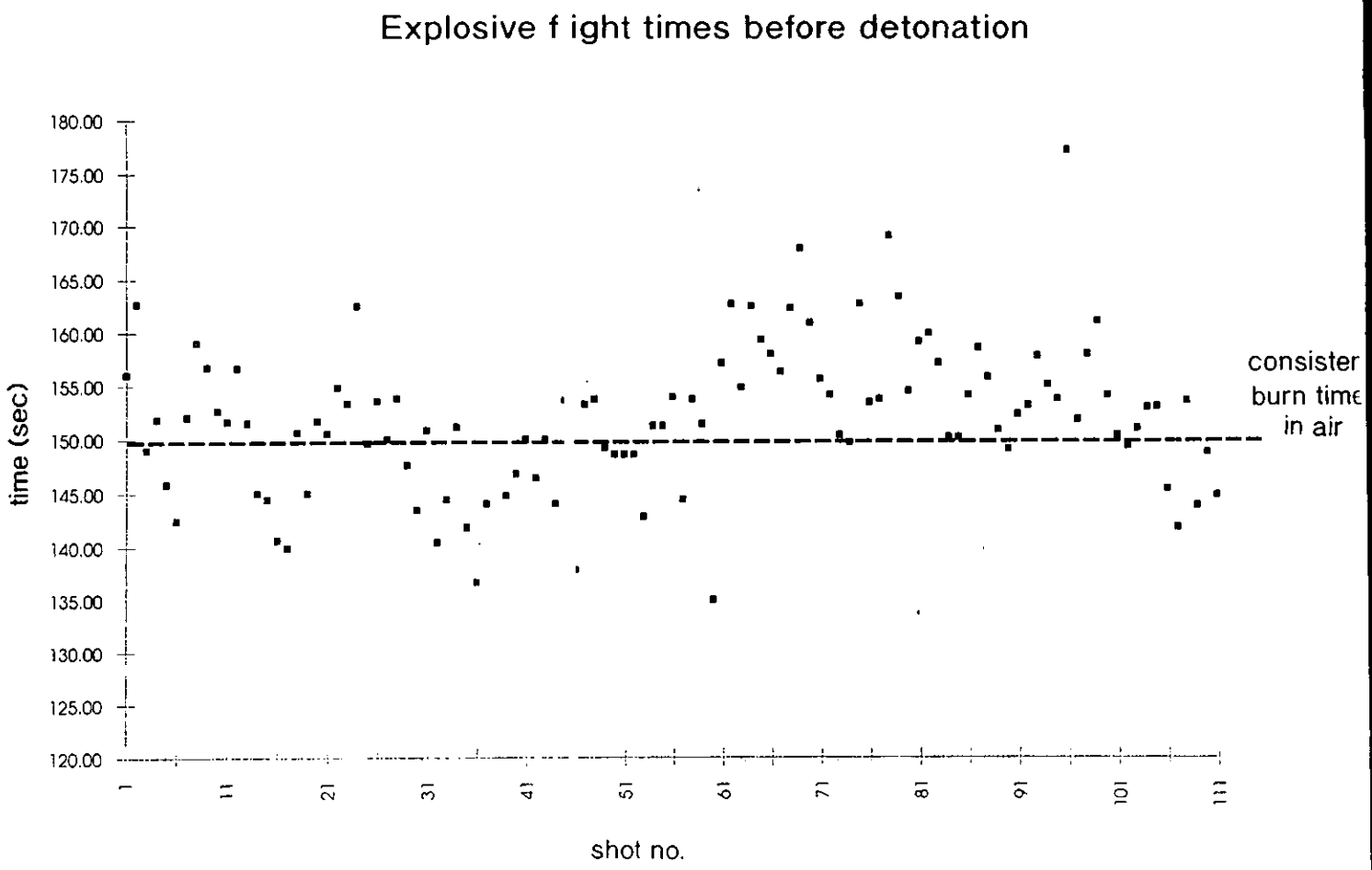

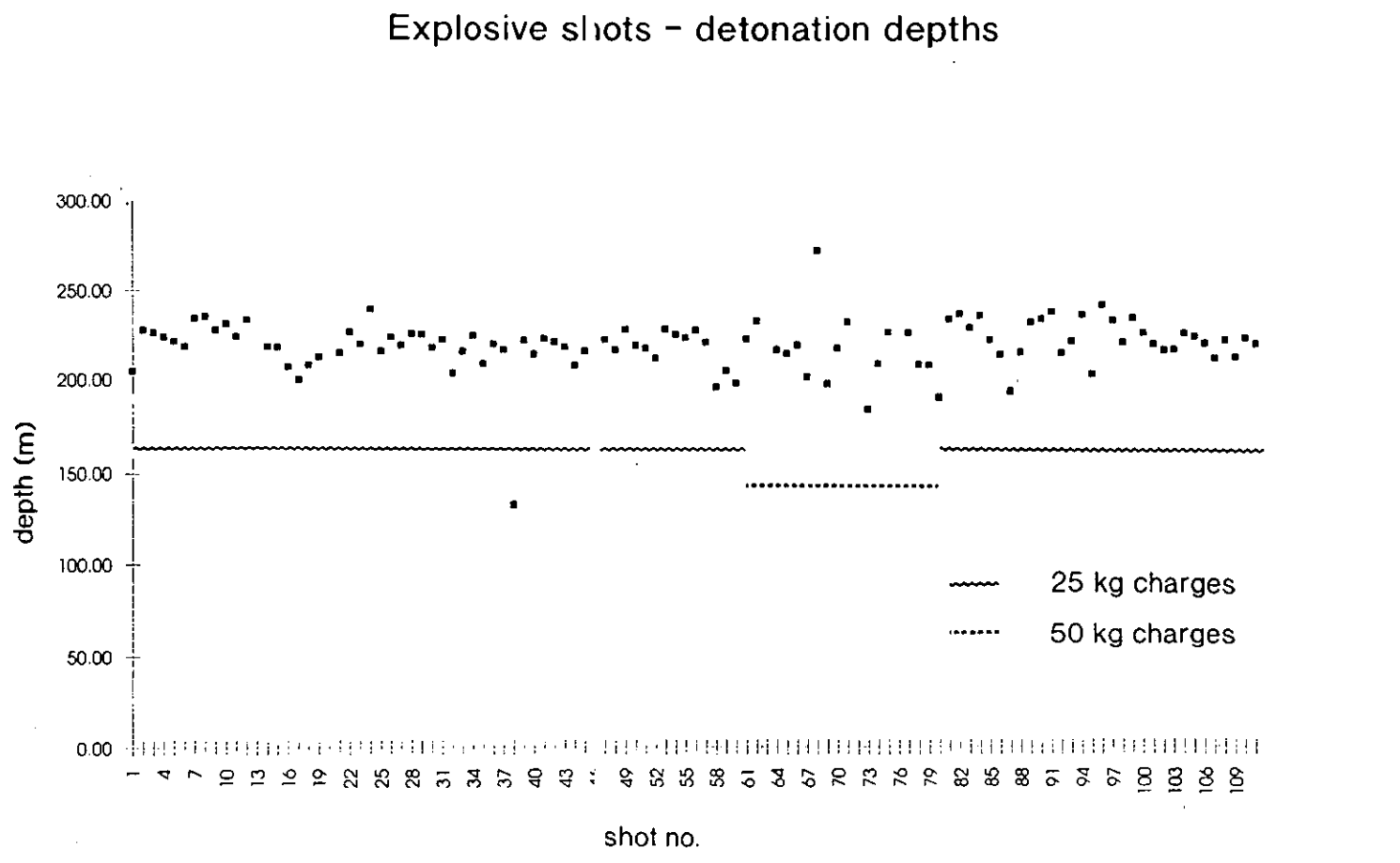

Figure 22. Explosive sl ot flight times and detonation depths.

instruments from Scripps, including antennas and a deployment winch for four long antenna electrometers; and four complete sea bottom instruments plus two additional magnetometers from Flinders. The main laboratory, wet laboratory, constant temperature laboratory and airgun annex were stuffed to overflowing with equipment, spare parts, computers and instruments. The plot too was full and heavily used — even the table tennis table was taken over for much of the cruise as a chart table. On deck we had to find room for all of the sea bottom instruments, and their bottom weights and antenna arms; a Flexotir winch with a split drum, with the seismic streamer on one side and the DASI antenna on the other; twelve airguns, four airgun beams and their umbilical winches; 3.5 kHz fish, davit and winch; explosives table; LEM antenna winch; PES fish; magnetometers; Oceano fish and winch; and the deep-tow cable termination and conducting swivel. The DASI power supply system was installed in the scientific hold, and we had 3.25 tonnes of explosives in the magazine.

On more than one occasion during mobilisation in Reykjavik, when it appeared there was not a square foot of space left on board and there were still piles of equipment and instruments on the quay side waiting to come aboard, it seemed impossible that it would all fit — let alone work. In the end we used the projecting walkway above the starboard side of the main deck (normally used for storing the gangway) as a storage area for sea bottom instruments (Scripps ELFs and LEMs at the start of the cruise and Durham DOBSs after the seismic experiment); and the boat deck aft of the funnel as an additional storage area for (among other things) the parts of a spare DASI antenna. Both container slots on the main deck had to be left empty for the airgun system. The inboard slot on the fo'c's'le deck was taken by the containerised compressors (ex *Challenger*). The outboard slot was taken by the Scripps container, which — after it had been unpacked initially — was used as extra storage space. A container flat bed was fixed on top of the compressor container, and the space this provided was also completely used.

The rest of this section should therefore be read in the context that all parts of this huge array of equipment that receive no further mention here, simply worked.

5.1 The Seismic Experiment

The seismic experiment was very successful, and on the whole the equipment worked well. The most obvious problem was the loss of a Cambridge DOBS. The mechanical arrangement of these instruments had been modified before this cruise, to convert them from tethered moorings to a new layout in which the cylindrical pressure vessels are horizontal and the instrument frame is rigidly attached to the bottom weight. This was done primarily to reduce noise arising from instrument movements when the same hardware is deployed (with different internal instrumentation) as a LEMUR. Since the Oceano release system repeatedly sent the 'acknowledge' signal, it is clear that both the acoustics and the first stage of the mechanical release system were operating correctly. Despite numerous tests of the new rig before deployment, and careful examination of the system since the cruise to try to discover some way in which the release mechanism can jam, the reason for the instrument's failure to leave the seabed is unknown.

During explosive shot firing, the main cause for concern was the uneven burn rate of the safety fuse — discussed in the preceding section. It also proved difficult initially to obtain good signals from the shot instant hydrophone towed astern of the

ship. This piece of Cambridge equipment needs some documentation and an appropriate amplifier to allow it to drive the inputs of several recording systems (e.g. jet pen, PDAS, oscilloscope). The hull geophones were installed in Barry before the ship sailed for CD80, but unfortunately the cables used (despite being labelled) were removed by a zealous RVS technician before CD81 started — so had to be installed all over again.

The airgun deployment system on the *Darwin* has now been used many times. However this was the first use of the new compressor container, which caused some problems at the start of the airgun shot firing programme and would have benefited from being more fully commissioned before the start of the cruise. Both of the containerised compressors failed to start up properly, for different reasons. One of the fixed compressors also suffered initially from a blown gasket. However, once fully operational, this containerised system will provide a significant enhancement of NERC's seismic capability. The shot instants for the airguns had to be derived from the ship's master clock through a lash-up of a system which included a home-made RVS box and 20 year old delay timers set to the wrong value to fool them into producing the right pulses. Acquiring a versatile and reliable timing system for this purpose should be a priority for RVS. The 1,000 in^3 gun on the port outer beam produced an improbably short bubble pulse, so was probably partially flooded. The 400 in^3 gun on the port inner beam appeared not to fire at all. The 120 in^3 gun on the port outer beam fired correctly, but its near field hydrophone did not work, so its timing had to be adjusted manually. Due partly to the amount of labour involved, and partly to these problems, it took 12 hours of continuous and very hard work by the RVS team to deploy the airgun array and streamer and get the guns firing with the correct timing.

This was also the first outing for four of the six Durham DOBSs. It was gratifying that they all returned safely, and had all worked flawlessly. The disks on the Durham instruments had been upgraded to larger capacity (127 Mbytes) shortly before the cruise, and problems associated with this change had caused some anxiety. In the event, the instruments worked extremely well. Data from the Durham instruments can be replayed and record sections plotted within 30 minutes of instrument retrieval. This onboard quality control is accomplished using a PC and Sun UNIX workstation network. Data down-loading is accomplished via a PC SCSI interface within about 5 minutes of removal of the logger from its pressure vessel. Data can then be transferred to the Sun for record section plotting using ftp. "First looks" at the recorded data are possible using two programmes, one written using the X11 programmers' tool kit (see Figure 23) and the other using vector plotting routines from the UNIRAS graphics package (see Figures 24 - 26).

During the seismic reflection profiling experiment, a repeated problem was the data gap resulting from tape changes on the SAQ system. This system only has one tape drive, so data are currently lost while tapes rewind before dismounting and replacement. Data tapes last for about 4.5 hours each when recording 8 channel data at 4 ms sampling rate, and recording an 8 s record every 20 s. This corresponds to about 40 km of data per tape at a profiling speed of 4.9 kts — insufficient to fit one line on a tape, in our case. This problem should be addressed urgently either by upgrading the current system to operate with two drives OR by running two systems in parallel.

Two out of four disposable sonobuoys failed to work. On one of these, the antenna could only be partially extended before it was deployed. We assume that the

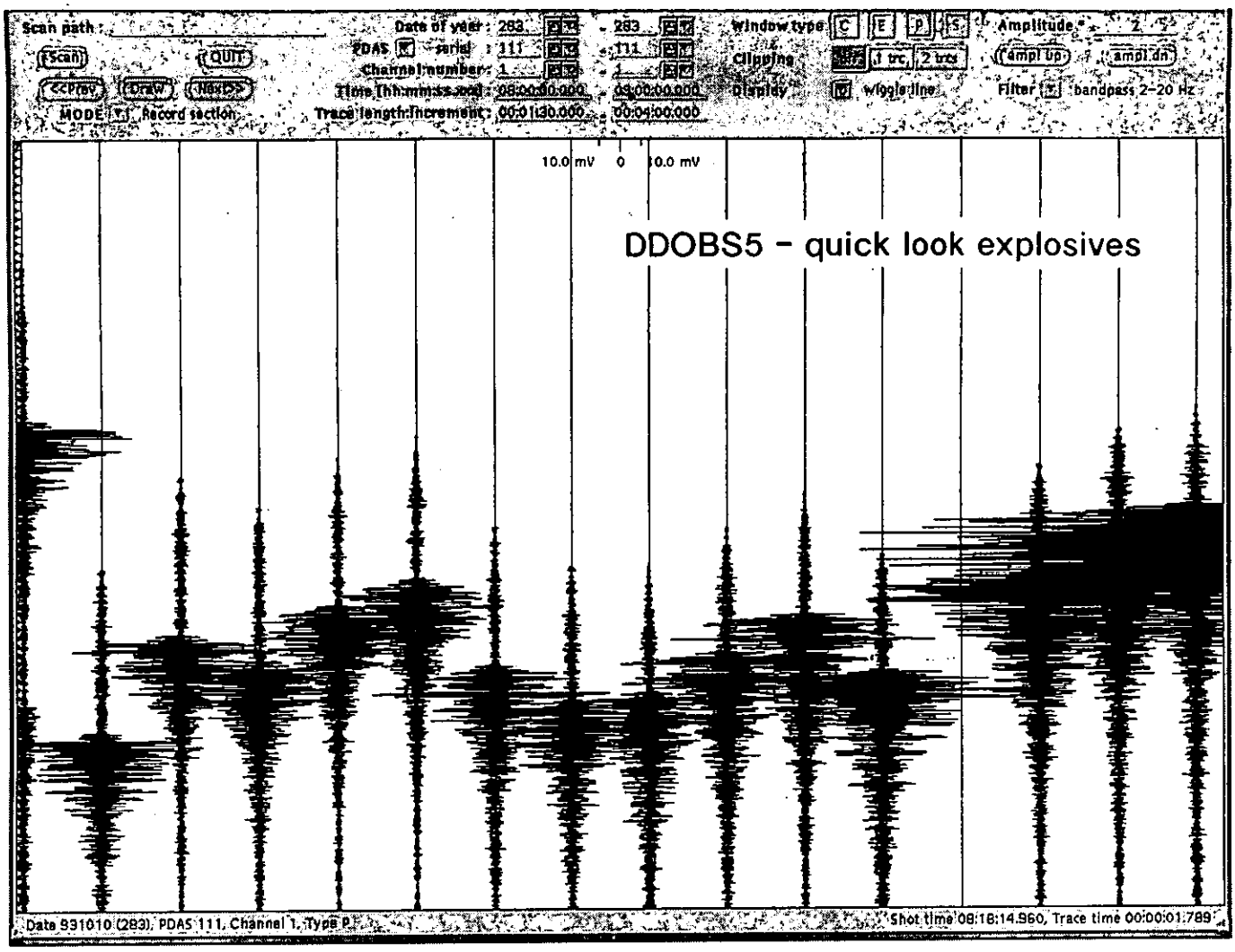

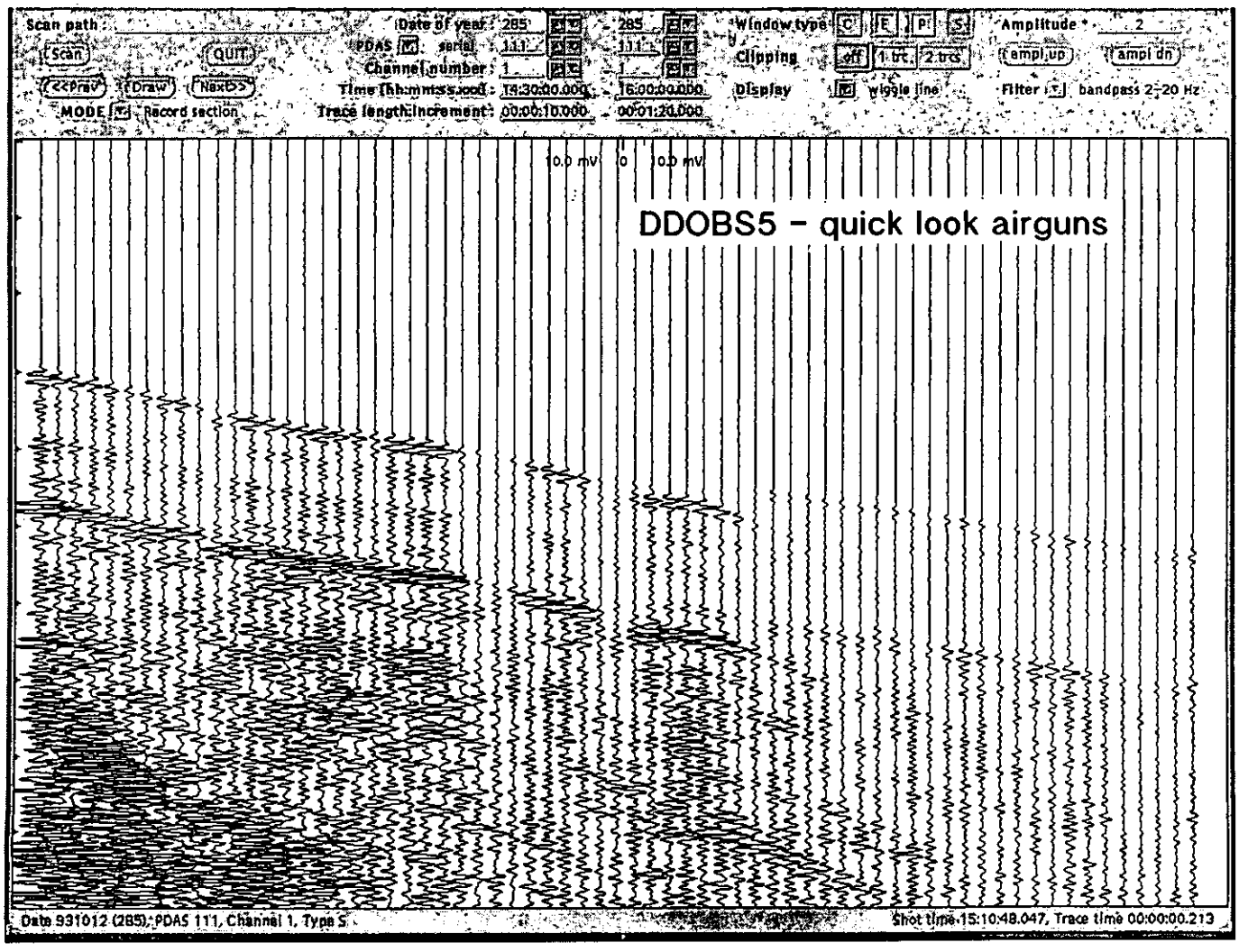

Figure 23. Wide-angle seismic record section.

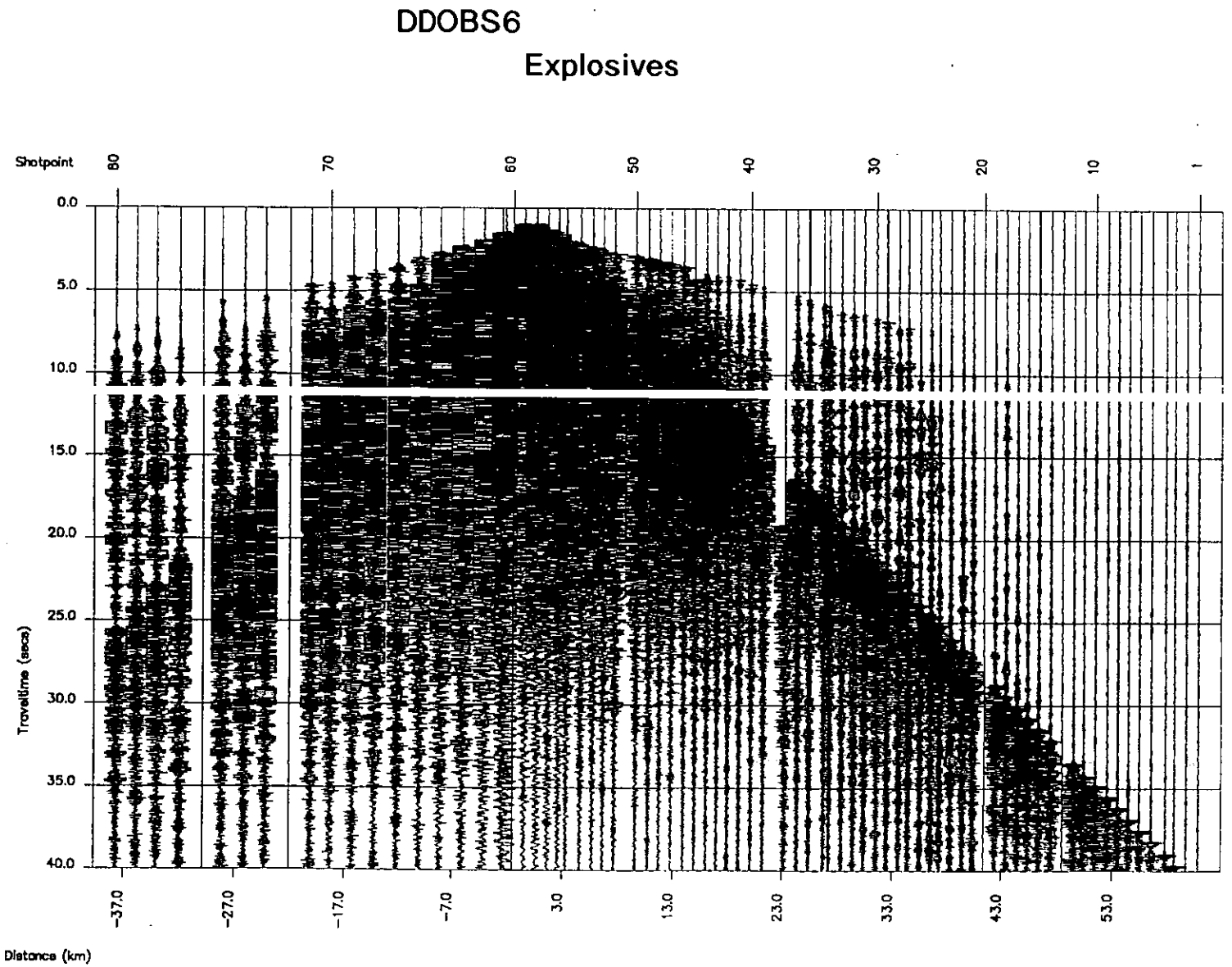

Figure 24. Wide-angle seismic record section.

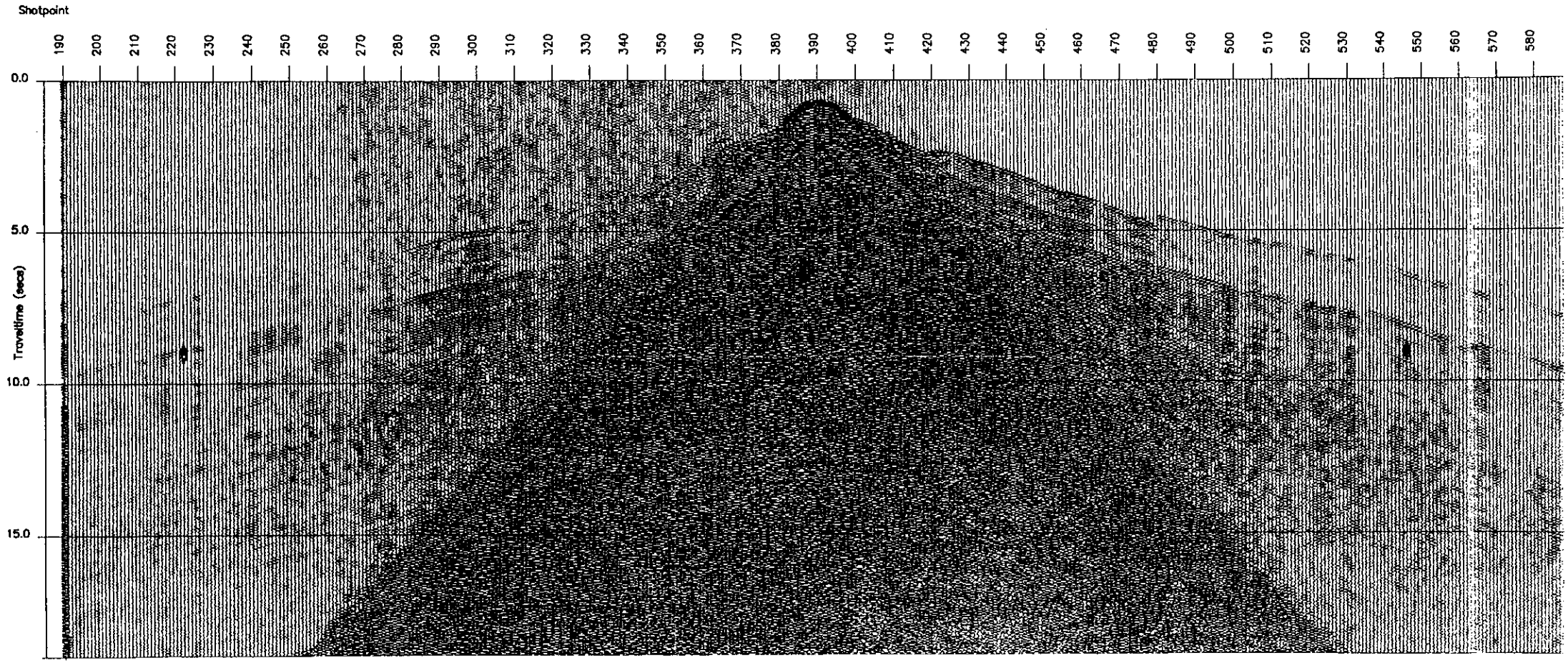

Figure 25. Wide-angle seismic record section.

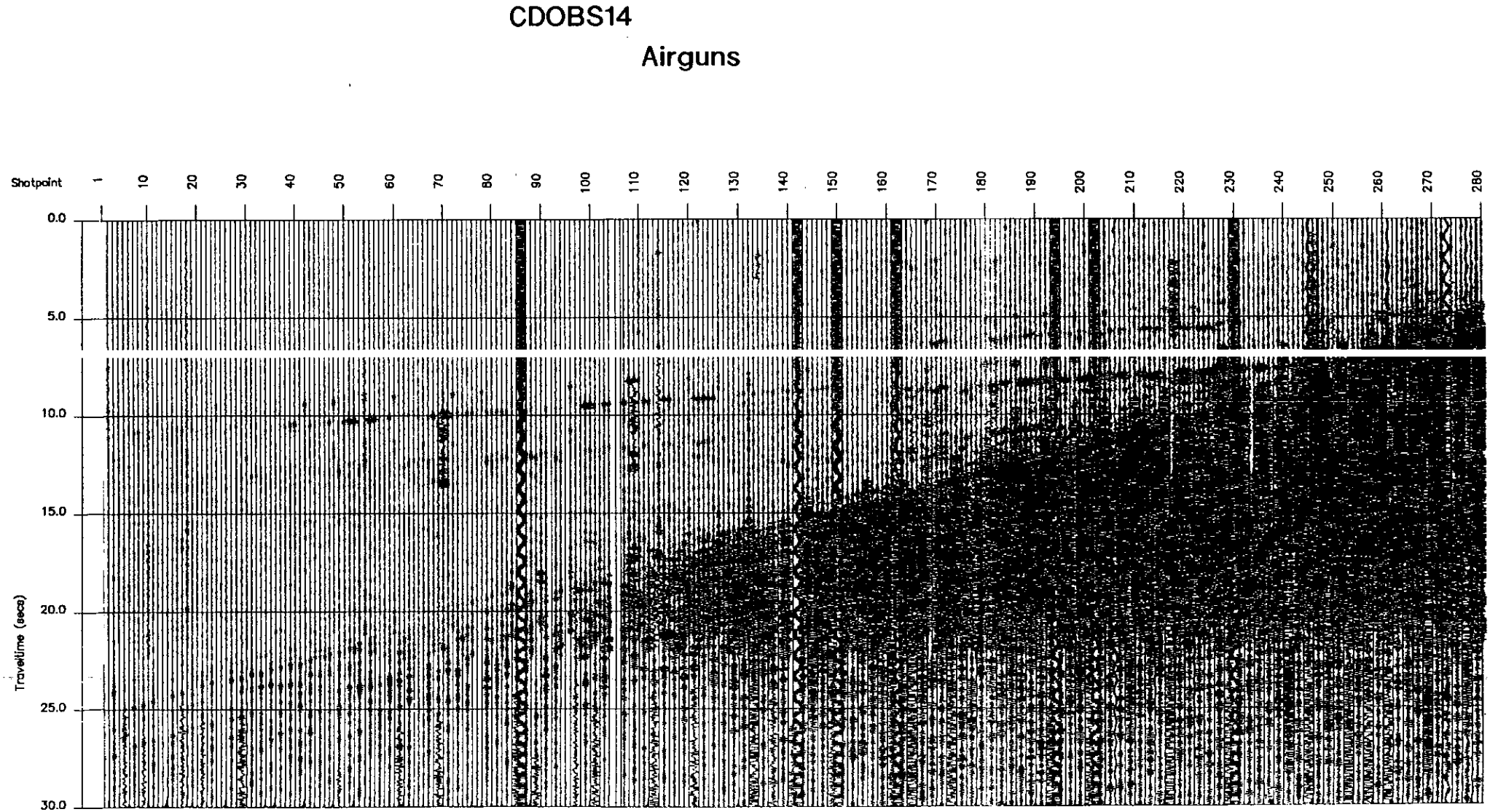

Figure 26. Wide-angle seismic record section.

other was damaged by collision with the towed reflection equipment. The two successful sonobuoys transmitted data for about 30 minutes — some 4.5 km at reflection surveying speeds. This performance was disappointing, especially after we had fitted an RF preamplifier between the antenna and the receiver in the main laboratory. In the event, the receiver in the plot with steerable antenna proved to be better at receiving the sonobuoy signals, so the PDAS logger was transferred there. An example of sonobuoy data is shown in Figure 27.

5.2 The Electromagnetic Experiment

The electromagnetic experiment was also successful, though we experienced a number of problems. The most serious of these was the loss of three instruments — a Cambridge LEMUR and two Flinders instruments (one OBM and one OBEM). The LEMUR showed exactly the same symptoms as the lost CDOBS — it responded to acoustic signals and acknowledged the release code, showing that the motor driven cam on the release unit had rotated, but it did not leave the seabed. The OBM was fitted only with a timed release system and had no acoustics, though it was fitted with a flashing light and radio beacon. Although the ship was in position to recover it at the time it was due to surface, in good visibility and full daylight, we saw no sign of it, either visually or by radio. We have no way of knowing what went wrong with it. The OBEM was unusual in that it left the seabed but we were still unable to recover it. The problem was that it had insufficient buoyancy, and so became neutrally buoyant when it reached a depth about 250 m below the sea surface. Despite our efforts to recover it using a fishing rig attached to the end of the deep tow cable, we were unable to retrieve it. It turned out to be drifting at a rate of about 0.5 kts, in a different direction to the surface current; and was not moving in a straight line. This made attempts to hook it into an almost impossible 3-dimensional problem.

The Cambridge DASI deep-towed CSEM transmitter system also caused a number of difficulties. The first arose while we were streaming its transmitting antenna, and simultaneously attaching to it the 'mini-streamer' system which allowed monitoring by separate electrodes of the outgoing wave form. A combination of mismeasurement and miscalculation meant that the mini-streamer was initially attached in the wrong position to the main streamer, leaving insufficient cable at its inboard end to reach the DASI data logger. The streamer had to be recovered, and the mini-streamer removed and reattached. The next problem arose once all the emergency cut-out switch circuits had been connected into the power supply. It turned out that the combined resistance of the wiring to all the emergency stops was large enough to prevent the power supply from switching on. The problem was not difficult to solve, but took some time to trace.

The other main problem that we experienced was concerned with the triggering of the cyclo-converter circuit that controls the outgoing wave form to the antenna. Although this part of the system had not previously caused us any problems, the result was that the outgoing wave form was not controlled as it should have been. Modifications to the triggering circuit between the first and second DASI deployments appeared to fix the problem during laboratory tests, but again during the actual deployment the problem recurred, though with somewhat different characteristics. One possible reason for these difficulties may be related to a change in the transmitting

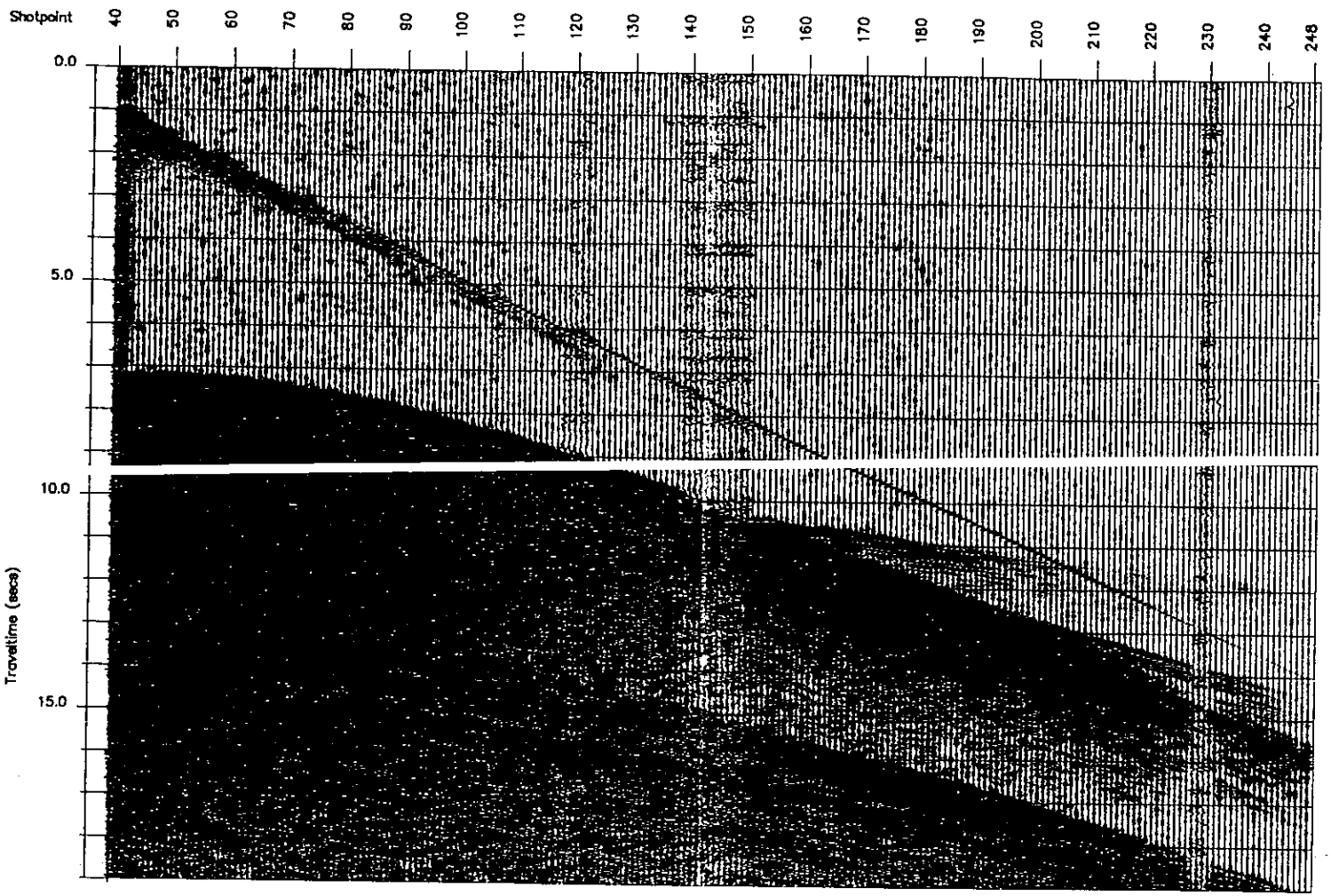

Figure 27. Disposable sonobuoy data.

electrodes since the previous uses of DASI. Modelling and analogue experiments carried out in Cambridge had shown that the electrodes we were using contributed significantly to the overall impedance of the antenna circuit. We therefore changed both the material and the size of the electrodes, in an effort to increase the amplitude of the outgoing signal. This was successful, and resulted in an antenna current of 100 A rms, but it seems probable that in so doing we increased the ratio of inductance to resistance of the antenna. The resulting phase shift between current and voltage may have caused the triggering problems.

The first DASI tow had to be abandoned when a coupling capacitor in the communications circuit blew. This component was operating considerably below its rated voltage, so should not have been expected to fail. When trying to trace this fault, we experienced some frustration in attempting to diagnose a problem inside a pressure case to which all electrical connections are transformer coupled. In the end there was no alternative but to strip down the entire instrument, including removal of the transformer package from its oil-filled pressure case — a messy, laborious and time consuming process. Again, having traced the fault it did not take long to fix it, but we then had to reassemble the stripped down instrument.

When we recovered the DASI streamer after the second tow line, we discovered that one of the two main antenna cables had parted close to the connector between it and the DASI pressure case. The far end of the antenna also showed clear signs of having touched bottom at some stage. We have no way of knowing how much of the damage to the parted cable was caused by the antenna touching bottom during the tow, and how much was caused by the time the instrument spent suspended in mid water awaiting recovery, while all operations were halted by bad weather. The mini-streamer too had suffered considerable damage near its connection to the DASI vehicle. The DASI towing fin showed signs of damage which could only have been caused by relative movements between the vehicle and the conducting swivel, with the swivel being rotated backwards until all the available movement was taken up. This shows that the effect of the bad weather, transmitted by cable heave, on the DASI vehicle was extremely violent. Under these conditions, damage to the streamer during this period would be almost inevitable.

The DASI tows were carried out at speeds of approximately 2 knots or 1 ms^{-1}. At this speed, the tail of the antenna would pass over a point on the seafloor about 3 minutes after the DASI vehicle itself — a point to be borne in mind in future when flying the system over rough topography, since lowering the vehicle immediately after crossing a topographic high is likely to land the streamer on the seabed.

The ten Scripps instruments performed impressively, especially as we had only one Scripps scientist (Constable) on board to look after them all. One instrument (ELFMAG 1) failed to record any E-field data, and one (ELF 4) stopped recording early due to a faulty power supply. ELF 2 released from the seabed early after one of its bottom weights fell off — probably due to a bad crimp on its attachment wire. We were extremely fortunate to be in the right place at the right time and looking out (for another instrument) when we spotted it on the surface. ELF 1 released only one of its bottom weights, but still reached the surface and was recovered. One of the acoustic release channels (A) did not work on LEM 1, but it was released successfully on channel B.

All the Scripps, Flinders and Durham instruments were fitted with radio transmitter beacons; however the receiver in the main laboratory proved ineffective at detecting the signals from them. The poor performance of the main laboratory radio receiver at picking up the sonobuoys was mentioned in the previous section. High quality detection of radio beacon signals would be very effective in minimising the risk of loss of instruments that surface prematurely — such as ELF 2. A programmable, scanning radio receiver with a carefully sited and good quality antenna would be extremely useful on all cruises on which sea bottom instruments fitted with radio beacons were to be deployed.

5.3 Other Equipment

One of the disappointments of the cruise was that the Scripps sea bottom transponders, which had been modified to acoustically replicate Oceano transponders, did not work with the ship-board Oceano acoustic navigation system. The amplitude and frequency of the Scripps transponders were within spec — we can only speculate that either the pulse length was too short, or that there is more to an Oceano transponder than we are aware of. The result was that we did not have long base line acoustic navigation throughout the CSEM experiment, as we had planned; and we used a lot of ship time laying, calibrating (twice) and recovering the transponder net for no real gain. The transponder releases all worked perfectly, although we were delayed for a short while during transponder recovery by a fault on the Scripps acoustic deck unit.

The Scripps 'pelican hook', used as a release for launching instruments from the ship, is a well engineered alternative to the traditional 'greasy pole'. While launching a Flinders OBEM however, the extra hooks on the pelican device became caught in the recovery lines, threatening to ruin the whole deployment. Without these extra hooks for things to snag on, the pelican hook would be a good and safe way of lifting and then releasing instruments.

The RVS towed, proton-precession magnetometer, which was used for a considerable proportion of the cruise, stopped working on a number of occasions. This is an absolutely standard piece of commercial equipment and should be more reliable — it may be that the instrument is reaching the end of its useful life.

The other instrumentation that should be singled out for mention in this section is the Simrad EM12 swath bathymetry system. This was only the second operational cruise with this equipment. It performed perfectly throughout, and provided high quality data — both bathymetry and side-scan sonar images. Clearly the RVS test and shake down cruise in summer 1993 with this equipment paid off, both in the performance of the instrumentation and in the professionalism and confidence of the RVS team in both operating the system and logging and processing the data that it produced. Also the new scientific plot, remodelled for the Simrad installation, is a great improvement. Not only is the space now being well used, but also the layout is such that the plot is a much more pleasant and comfortable place to work, even in bad weather!

5.4 Ship's Machinery and Fitted Equipment

The ship's fitted equipment and machinery, as usual, functioned efficiently and reliably throughout most of the cruise. Two minor exceptions to this were the failure of the food freezer system towards the end of the cruise, and an occasion when the bow thruster started to overheat when recovering an instrument in marginal weather conditions. From a scientific point of view neither of these was serious, though we were fortunate that the freezer did not fail earlier in the cruise.

We were however delayed by a fault on the spooling gear on the CTD winch. The spooling gear had broken down on the previous cruise, and a substantial amount of wire had been reeled onto the drum without proper spooling. Before we could carry out a sound velocity meter dip, this wire had to be run off with the vessel stationery, and the spooling gear fixed. This should clearly have been done on the previous cruise when the problem arose — it should certainly not have been left for us to deal with during our cruise. Failure or misalignment of the spooling gear on this winch is a regular occurrence — indeed it seems that at the start of every cruise, a sound velocity dip takes hours longer than it should because of winch problems. This situation is unlikely to be resolved other than by replacement of the winches.

Another problem that arose was flooding of sea water into the scientific hold through the drainage system for the hatch cover. This is particularly serious when the power supply system for the DASI instrument, operating at 2,000 V rms a.c., is located in the hold. The effects of sea water sloshing around the deck in these circumstances are potentially disastrous. This problem has occurred on at least two previous cruises — CD34 and CD39 — both cruises during which we used the DASI system. The cruise reports following both those cruises documented the need to solve this problem — nonetheless it recurred during CD81. We take this opportunity to draw the attention of NERC and RVS to this issue for a third time. We wish to underline the point that entry of sea water into the scientific hold poses a lethal threat to personnel when high voltage equipment is operating there, and also poses a serious threat to scientific equipment and the vessel's ability to carry out the scientific programme. The DASI power supply system is fitted with comprehensive earth leakage and overload protection circuits which provide as much protection as is feasible both for personnel and the equipment — but it is not reasonable to expect such equipment to have to operate in the presence of significant quantities of sea water.

6. Conclusions

This cruise was notable for the quantity and variety of equipment in use, and the complexity of the scientific programme. The outcome was a successful, integrated, geophysical investigation of the most magmatically robust AVR segment known on the Reykjanes Ridge. The data collected include comprehensive swath bathymetry, side-scan sonar, gravity and magnetic coverage over an area of 12,000 km^2; natural and controlled source electromagnetic data which we shall use to investigate the electrical resistivity structure of the crust and upper mantle beneath the AVR, from the seafloor to depths of at least 100 km; and wide-angle and normal incidence seismic data, which we shall use to determine the P- and S-wave velocity structure of the crust and uppermost mantle beneath the AVR.

The scientific work was enormously assisted by the professionalism and commitment of the ship's officers and crew, and of the RVS technicians. It was clear during the cruise that morale at RVS has reached a very low ebb — with the combination of market testing and the impending move of RVS to Southampton, confidence in the future was starkly and depressingly in short supply. Despite this, all on board made every conceivable effort to ensure the success of the programme, and our enjoyment of the cruise.

It would quite simply be impossible to undertake scientific programmes on this scale, within the resources available to university departments, without the support of an organisation such as RVS. The skills, resourcefulness, creativity, experience and dedication of the staff based in Barry make a fundamental contribution to the success of marine science in the UK. It would be nice to think that NERC, and indeed the scientific community as a whole, fully appreciate the value of the resource that they have at RVS. Unfortunately on the present evidence it is not clear, perhaps most of all to those who work at Barry, that they do.

Acknowledgements

We wish to thank the master, officers and crew of the *Charles Darwin* and the support staff and sea going technicians of NERC's Research Vessel Services for their efforts in ensuring a successful and enjoyable cruise. Ship time was funded by the U.K.'s Natural Environment Research Council, who also supported the work through research grant and research studentship awards to Cambridge and Durham Universities. Scripps and Flinders participation was funded by a research grant to Scripps Institution of Oceanography from the U.S. National Science Foundation.

Figure 28. Processed swath bathymetric map of the AVR and surrounding region.

References

Burnett, M.S., Caress, D.W. & Orcutt, J.A. (1989). Tomographic image of the East Pacific Rise at 12°50'N. *Nature*, **339**, 206-208.

Chave, A. D. & Cox, C. S., 1982. Controlled EM sources for measuring electrical conductivity beneath the oceans: I. Forward problem and model study. *J. geophys. Res.*, **87**, 5327-5338.

Collier, J. & Sinha, M. (1990). Seismic images of a magma chamber beneath the Lau Basin back-arc spreading centre. *Nature*, **346**, 646-648.

Collier, J.S. & Sinha, M.C., 1992. The Valu Fa Ridge: the pattern of volcanic activity at a back-arc spreading centre. *Marine Geology*, **104**, 243 - 263.

Collier, J.S. & Sinha, M.C., 1992. Seismic mapping of a magma chamber beneath the Valu Fa Ridge, Lau Basin. *J. Geophys. Res.*, **97**, 14,031 - 14,053.

Constable, S.C. & Duba, A. (1990). Electrical conductivity of olivine, a dunite and the mantle. *J. Geophys. Res.*, **95**, 6967-6978.

Cox, C.S., Constable, S.C., Chave, A.D. & Webb, S.C. (1986). Controlled source electromagnetic sounding of the oceanic lithosphere. *Nature*, **320**, 52-54.

Detrick, R.S., Buhl, P., Vera, E., Mutter, J., Orcutt, J., Madsen, J. & Brocher, T. (1987). Multi-channel seismic imaging of a crustal magma chamber along the East Pacific Rise. *Nature*, **326**, 35-42.

Detrick, R.S., Mutter, J.C., Buhl, P. & Kif, I.I. (1990). No evidence from multichannel reflection data for a crustal magma chamber in the MARK area on the Mid-Atlantic Ridge. *Nature*, **347**, 61-64.

Detrick, R. S., Harding, A. J., Kent, G. M., Orcutt, J. A., Mutter, J. C. and Buhl, P. (1993). Seismic structure of the southern East Pacific Rise. *Science*, **259**, 499-503.

Evans, R.L., Constable, S.C., Sinha, M.C. & Cox, C.S. (1991). Upper crustal resistivity structure of the East Pacific Rise near 13°N. *Geophys. Res. Lett.*, **18**, 1917-1920.

Evans, R. L., Sinha, M. C., Constable, S. C. & Unsworth, M. J., 1993. On the electrical nature of the axial melt zone at 13°N on the East Pacific Rise. Accepted for publication in *J. Geophys. Res.*

Harding, A.J., Orcutt, J.A., Kappus, M.E., Vera, E.E., Mutter, J.C., Buhl, P., Detrick, R.S & Brocher, T.M. (1989). The structure of young oceanic crust at 13°N on the East pacific Rise from expanding spread profuiles. *J. Geophys. Res.*, **94**, 12,163-12,196.

Kent, G.M., Harding, A.J. & Orcutt, J.A. (1990). Evidence for a smaller magma chamber beneath the East pacific Rise at 9°30'N. *Nature*, **344**, 650-653.

Kusznir, N.J. & Bott, M.H.P. (1976). A thermal study of the formation of oceanic crust. *Geophys. J. Roy. astr. Soc.*, **47**, 83-95.

Langmuir, C.H., Bender, J.F. & Batiza, R. (1986). Petrologic and tectonic segmentation of the East Pacific Rise, 5°30'N to 14°30'N. *Nature* , **322**, 422-429.

Macdonald, K.C., Sempere, J.C. & Fox, P.J. (1984). East Pacific Rise from Siqueiros to Orozco fracture zones: along strike continuity of axial neovolcanic zone and structure and evolution of overlapping spreading centres. *J. Geophys. Res.*, **89**, 6049-6069.

Murton, B. J. & Parson, L. M., 1993. Segmentation, volcanism and deformation of oblique spreading centres: a quantitative study of the Reykjanes Ridge. *Tectonophysics*, in press.

Parson, L. M. *et al.* (1993). En echelon axial volcanic ridges at the Reykjanes Ridge: a life cycle of volcanism and tectonics. Submitted to *Earth Planet. Sci. Lett.*

Sinha, M.C., Patel, P.D., Unsworth, M.J., Owen, T.R.E. & MacCormack, M.R.G. (1990). An active source electromagnetic sounding system for marine use. *Mar. Geophys. Res.*, **12**, 59-68.

Sleep, N.H. (1975). Formation of oceanic crust - some thermal constraints. *J. Geophys. Res.*, **80**, 4037-4042.

Toomey D.R., Purdy G.M., Solomon S.C. & Wilcock W.S.D. (1990). The three-dimensional seismic velocity structure of the East Pacific Rise near 9°30'N. *Nature*, **347**, 639-645.

Unsworth, M. J., Travis, B. J. & Chave, A. D., 1993. Electromagnetic induction by a finite electric dipole source over a 2-D earth. *Geophysics*, **58**, 198-214.

Vera, E.E., Mutter, J.C., Buhl, P., Orcutt, J.A., Harding, A.J., Kappus, M.E., Detrick, R.S. & Brocher, T.M. (1990). Structure of 0- to 0.2-m.y. old oceanic crust at 9°N on the East Pacific Rise from expanded spread profiles. *J. Geophys. Res.*, **95**, 15529-15556.

Webb, S.C., Constable, S.C., Cox, C.S. & Deaton, T.K., 1985. A seafloor electric field instrument. *J. Geomag. Geoelectr.*, **37**, 1115-1129.

List of Figures

List of tables

Table 1
Instrument Positions for the Seismic Experiment

Instrum. Type	Instrum. Number	Latitude (Deg.)	Latitude (Min.)	Longitude (Deg.)	Longitude (Min.)	Water Depth (m)
DDOBS	6	57	36.80	32	14.70	1650
DDOBS	5	57	42.00	32	32.60	1350
DDOBS	4	57	38.80	32	43.50	1825
DDOBS	3	57	50.30	32	39.20	1775
DDOBS	2	57	47.30	32	50.80	1760
DDOBS	1	57	52.10	33	7.25	1680
CDOBS	15	57	40.80	32	28.00	1500
CDOBS	14	57	43.60	32	38.10	1725
CDOBS	13	57	44.60	32	41.30	1675
CDOBS	12	57	45.60	32	44.80	2000
CDOBS	11	57	49.30	32	57.50	1490

Table 2
Summary of data collected by DOBSs

CD82 DOBSs locations							
DOBS no.	**Logger No.**	**Src**	**No. shots/chan**	**Total shots**	**Samp rate/duration /repeat/delay**	**Bytes/shot**	**Total Bytes per instrument**
DDOBS1	105	exp	111	444	200 / 150 / 240 + 480	120 000	53 280 000
		airg	690	2760	100 / 19 / 80	7 600	20 976 000
DDOBS2	106	exp	111	444	200 / 150 / 240 + 480	120 000	53 280 000
		airg	690	2760	100 / 19 / 80	7 600	20 976 000
DDOBS3	107	exp	111	444	200 / 150 / 240 + 480	120 000	53 280 000
		airg	-		100 / 19 / 80		
DDOBS4	108	exp	111	444	200 / 150 / 240 + 480	120 000	53 280 000
		airg	363	2760	100 / 19 / 80	7 600	20 976 000
DDOBS5	111	exp	111	444	200 / 150 / 240 + 480	120 000	53 280 000
		airg	690	2760	100 / 19 / 80	7 600	20 976 000
DDOBS6	112	exp	111	444	200 / 150 / 240 + 480	120 000	53 280 000
		airg	690	2760	100 / 19 / 80	7 600	20 976 000
CDOBS11	11	exp	109	109	256 / 30 / 240 + 480	15 360	1 674 240
		airg	345	345	256 / 30 / 40	15 360	5 299 200
CDOBS12	12	exp	109	109	256 / 30 / 240 + 480	15 360	1 674 240
		airg	1365	1365	256 / 30 / 40	15 360	20 966 400
CDOBS13	13	exp	78	78	256 / 30 / 240 + 480	15 360	1 198 080
		airg	1546	1546	256 / 30 / 40	15 360	23 746 560
CDOBS14	14	exp	110	110	256 / 30 / 240 + 480	15 360	1 689 600
		airg	1553	1553	256 / 30 / 40	15 360	23 854 080
CDOBS15	15	exp	inst lost		256 / 30 / 240 + 480		
		airg	inst lost		256 / 30 / 40		
Sonobuoy			**TOTAL**	**21 679 seismograms**		**TOTAL**	**504 662 400 Bytes**
1	215	airg	n/a		500/continuous		
2	215	airg	n/a		500/continuous		

Table 3
Explosive shots

Charles Darwin Cruise 81				Date	Day 283/284									
				SHOT INSTANTS										
Shot table 1.1														
Day		Time												
				CHARGE AWAY					CHARGE FIRED				SHOT TIME	
Shot #	Size	Fuse	Composed	Time	Lat (N)	Long (W)	Depth	Flight	Time	Lat (N)	Long (N)	Det. Depth	Hr : min	sec . msec
1	25 kg	3.50 m	1x25kg	07:57:32	57.8742	33.1468	1787.00	156.00	08:00:06	57.8713	33.1357	204.50	08:00	05.127
2	25 kg	3.50 m	1x25kg	08:01:30	57.8698	33.1301	1685.50	162.70	08:04:13	57.8666	33.1202	227.30	08:04	12.227
3	25 kg	3.50 m	1x25kg	08:05:33	57.8645	33.1152	1612.50	149.00	08:08:02	57.8622	33.1062	225.80	08:08	01.167
4	25 kg	3.50 m	1x25kg	08:09:35	57.8605	33.1000	1673.00	151.80	08:12:06	57.8573	33.0893	223.60	08:12	05.402
5	25 kg	3.60 m	1x25kg	08:13:34	57.8565	33.0869	1624.00	145.80	08:16:00	57.8530	33.0741	221.00	08:15	59.690
6	25 kg	3.60 m	1x25kg	08:17:36	57.8515	33.0674	1706.00	142.40	08:19:58	57.8489	33.0588	217.90	08:19	57.321
7	25 kg	3.60 m	1x25kg	08:21:36	57.8439	33.0531	1676.50	152.00	08:24:08	57.8446	33.0433	233.80	08:24	08.167
8	25 kg	3.60 m	1x25kg	08:25:35	57.8432	33.0379	1636.00	159.00	08:28:13	57.8406	33.0292	234.90	08:28	13.007
9	25 kg	3.60 m	1x25kg	08:29:36	57.8390	33.0244	1692.00	156.70	08:32:13	57.8359	33.0136	227.20	08:32	12.790
10	25 kg	3.60 m	1x25kg	08:33:37	57.8342	33.0080	1650.00	152.60	08:36:09	57.8315	32.9991	230.80	08:36	08.722
11	25 kg	3.60 m	1x25kg	08:37:33	57.8299	32.9942	1688.00	151.60	08:40:05	57.8278	32.9850	223.50	08:40	04.813
12	25 kg	3.60 m	1x25kg	08:41:37	57.8264	32.9793	1548.00	156.60	08:44:13	57.8231	32.9691	232.80	08:44	12.339
13	25 kg	3.60 m	1x25kg	08:45:34	57.8217	32.9793	1493.00							
14	25 kg	3.60 m	1x25kg	08:49:37	57.8172	32.9640	1400.00	145.00	08:52:02	57.8144	32.9374	217.70	08:52	02.105
15	25 kg	3.60 m	1x25kg	08:53:34	57.8130	32.9478	1453.00	144.40	08:55:58	57.8102	32.9227	217.40	08:55	58.117
16	25 kg	3.60 m	1x25kg	08:57:36	57.8084	32.9319	1399.00	140.60	08:59:56	57.8065	32.9094	206.70	08:59	55.717
17	25 kg	3.60 m	1x25kg	09:01:36	57.8046	32.9168	1328.00	139.90	09:03:56	57.8015	32.8943	199.50	09:03	55.311
18	25 kg	3.60 m	1x25kg	09:05:34	57.8000	32.9029	1840.00	150.60	09:08:04	57.7975	32.8789	207.50	09:08	03.684
19	25 kg	3.60 m	1x25kg	09:09:36	57.7957	32.8883	1787.50	145.00	09:12:01	57.7927	32.8644	211.90	09:12	00.429
20	25 kg	3.60 m	1x25kg	09:13:33	57.7911	32.8131	1907.00							
21	25 kg	3.60 m	1x25kg	09:17:34	57.7869	32.8583	1768.00	150.50	09:20:04	57.7847	32.8343	214.00	09:20	04.243
22	25 kg	3.60 m	1x25kg	09:21:35	57.7834	32.8428	1628.00	154.80	09:24:08	57.7806	32.8184	225.80	09:24	08.142
23	25 kg	3.60 m	1x25kg	09:25:32	57.7789	32.8294	1734.50	153.30	09:28:05	57.7760	32.8020	219.00	09:28	05.013
24	25 kg	3.60 m	1x25kg	09:29:32	57.7459	32.8119	1800.50	162.50	09:32:14	57.7720	32.7851	239.00	09:32	14.487
25	25 kg	3.60 m	1x25kg	09:33:35	57.7699	32.7965	1761.50	149.60	09:36:04	57.7666	32.7719	215.00	09:36	04.003
26	25 kg	3.60 m	1x25kg	09:37:32	57.7651	32.7813	1825.50	153.50	09:40:07	57.7623	32.7568	223.10	09:40	07.165
27	25 kg	3.60 m	1x25kg	09:41:35	57.7611	32.7665	1934.50	150.00	09:44:04	57.7587	32.7426	218.40	09:44	03.463
28	25 kg	3.60 m	1x25kg	09:45:34	57.7572	32.7516	2019.00	153.80	09:48:08	57.7543	32.7271	225.00	09:48	07.921
29	25 kg	3.60 m	1x25kg	09:49:35	57.7527	32.7370	1970.50	147.60	09:52:02	57.7498	32.7127	224.40	09:52	02.111
30	25 kg	3.60 m	1x25kg	09:53:34	57.7486	32.7217	1805.00	143.40	09:55:57	57.7458	32.6978	216.90	09:55	57.012
31	25 kg	3.60 m	1x25kg	09:57:36	57.7440	32.7064	1675.00	150.80	10:00:06	57.7412	32.6832	221.30	10:00	06.374
32	25 kg	3.60 m	1x25kg	10:01:33	57.7391	32.6920	1664.00	140.40	10:03:54	57.7358	32.6699	202.80	10:03	53.482
33	25 kg	3.60 m	1x25kg	10:05:35	57.7339	32.6783	1800.00	144.40	10:07:59	57.7316	32.6525	214.90	10:07	58.985
34	25 kg	3.60 m	1x25kg	10:09:35	57.7301	32.6621	2024.50	151.10	10:12:07	57.7274	32.6379	223.80	10:12	06.708
35	25 kg	3.60 m	1x25kg	10:13:34	57.7260	32.6468	1763.50	141.80	10:15:56	57.7236	32.6235	207.90	10:15	54.879

36	25 kg	3.60 m	1x25kg	10:17:34	57.2247	32.6175	1635.50	136.60	10:19:51	57.7196	32.6089	218.80	10:19	50.886
37	25 kg	3.60 m	1x25kg	10:21:34	57.7172	32.6024	1205.00	144.00	10:23:57	57.7152	32.5938	215.80	10:23	56.917
38	25 kg	3.60 m	1x25kg	10:25:36	57.7133	32.5879	1450.50	96.10	10:27:12	57.7113	32.5818	132.10	10:27	10.880
39	25 kg	3.60 m	1x25kg	10:33:32	57.7045	32.5583	1313.50	144.80	10:35:57	57.7045	32.5479	220.90	10:35	56.376
40	25 kg	3.60 m	1x25kg	10:37:38	57.7001	32.5422	1310.00	146.80	10:40:06	57.6975	32.5330	213.30	10:40	04.263
41	25 kg	3.60 m	1x25kg	10:41:40	57.6956	32.5264	1233.00	150.00	10:44:10	57.6927	32.5169	221.80	10:44	09.504
42	25 kg	3.60 m	1x25kg	10:45:35	57.6913	32.5117	1052.00	146.40	10:48:01	57.6887	32.5032	219.90	10:48	01.125
43	25 kg	3.60 m	1x25kg	10:49:37	57.6870	32.4972	1115.50	150.00	10:52:04	57.6843	32.4872	217.20	10:52	06.615
44	25 kg	3.60 m	1x25kg	10:53:35	57.6828	32.6815	1287.50	144.00	10:55:59	57.6803	32.4724	207.10	10:55	58.584
45	25 kg	3.60 m	1x25kg	10:57:36	57.6783	32.4660	1440.50	153.60	11:00:09	57.6754	32.4564	214.90	11:00	08.734
46	25 kg	3.60 m	1x25kg	11:01:36	57.6739	32.4508	1428.00	137.80	11:03:53	57.6712	32.4420	196.00	11:03	53.117
47	25 kg	3.60 m	1x25kg	11:05:36	57.6692	32.4358	1062.00	153.20	11:08:08	57.6667	32.4263	221.10	11:08	07.823
48	25 kg	3.60 m	1x25kg	11:09:35	57.6650	32.4199	1105.50	153.70	11:12:09	57.6625	32.4096	215.60	11:12	08.655
49	25 kg	3.60 m	1x25kg	11:13:36	57.6608	32.4041	1104.80	149.20	11:16:05	57.6584	32.3949	226.70	11:16	04.487
50	25 kg	3.60 m	1x25kg	11:17:39	57.6564	32.3888	1222.50	148.60	11:20:08	57.6534	32.3793	217.90	11:20	07.070
51	25 kg	3.60 m	1x25kg	11:25:33	57.6476	32.3587	1508.00	148.60	11:28:02	57.6445	32.3488	216.20	11:28	01.302
52	25 kg	3.60 m	1x25kg	11:29:35	57.6434	32.3436	1469.50	148.60	11:32:03	57.6401	32.3335	210.80	11:32	02.865
53	25 kg	3.60 m	1x25kg	11:33:34	57.6386	32.3278	1558.00	142.80	11:35:57	57.6359	32.3193	226.90	11:35	56.395
54	25 kg	3.60 m	1x25kg	11:37:36	57.6336	32.3129	1742.50	151.20	11:40:07	57.6314	32.3043	224.00	11:40	06.792
55	25 kg	3.60 m	1x25kg	11:41:33	57.6295	32.2987	1920.00	151.20	11:44:14	57.6266	32.2887	222.00	11:44	03.966
56	25 kg	3.60 m	1x25kg	11:45:34	57.6250	32.2832	1510.00	153.90	11:48:08	57.6228	32.2741	226.30	11:48	07.804
57	25 kg	3.60 m	1x25kg	11:49:32	57.6215	32.2688	1592.00	144.40	11:51:56	57.6193	32.2594	219.50	11:51	56.408
58	25 kg	3.60 m	1x25kg	11:53:34	57.6173	32.2528	1568.00	153.70	11:56:05	57.6141	32.2438	194.90	11:56	04.502
59	25 kg	3.60 m	1x25kg	11:57:33	57.6122	32.2384	1676.50	151.40	12:00:04	57.6089	32.2292	204.10	12:00	03.741
60	25 kg	3.60 m	1x25kg	12:01:34	57.6069	32.2232	1722.00	134.90	12:13:48	57.6048	32.2148	197.00	12:04	59.625
61	25 kg	3.60 m	1x25kg	12:05:36	57.6028	32.2082	1615.00	157.10	12:08:13	57.5999	32.1991	221.50	12:08	12.946
62	50 kg	3.60 m	2x25kg	13:57:33	57.6039	32.2134	1490.50	162.70	14:00:15	57.6012	32.2028	231.50	14:00	01.108
63	50 kg	3.60 m	2x25kg	14:05:33	57.5975	32.1892	1544.50							
64	50 kg	3.60 m	2x25kg	14:13:37	57.5885	32.1551	1400.00	162.50	14:16:15	57.5853	32.1465	215.40	14:16	14.893
65	50 kg	3.50 m	2x25kg	14:21:34	57.5794	32.1264	1449.50	159.30	14:24:13	57.5766	32.1158	213.10	14:24	12.866
66	50 kg	3.50 m	2x25kg	14:29:33	57.5714	32.0967	1539.50	157.90	14:32:11	57.5682	32.0869	217.90	14:32	11.033
67	50 kg	3.50 m	2x25kg	14:37:33	57.5620	32.0672	1763.50	156.30	14:40:09	57.5589	32.0565	200.60	14:40	09.191
68	50 kg	3.50 m	2x25kg	14:45:35	57.5542	32.0366	1726.00	162.30	14:48:18	57.5508	32.0258	270.80	14:48	15.950
69	50 kg	3.50 m	2x25kg	14:53:34	57.5457	32.0068	1716.50	167.90	14:56:22	57.5424	31.9968	196.60	14:56	22.087
70	50 kg	3.50 m	2x25kg	15:01:35	57.5372	31.8779	1840.50	160.90	15:04:15	57.5350	31.9678	216.00	15:04	15.379
71	50 kg	3.40 m	2x25kg	15:09:34	57.5292	31.9496	1921.00	155.60	15:12:04	57.5263	31.9396	230.80	15:12	09.132
72	50 kg	3.40 m	2x25kg	15:17:33	57.5214	31.9196	1658.50							
73	50 kg	3.40 m	2x25kg	15:25:34	57.5129	31.8897	1729.40	150.40	15:28:04	57.5106	31.8800	182.40	15:28	03.789
74	50 kg	3.40 m	2x25kg	15:33:35	57.5050	31.8609	1415.00	149.70	15:36:05	57.5018	31.8571	207.50	15:36	04.757
75	50 kg	3.40 m	2x25kg	15:41:34	57.4952	31.8317	1515.00	162.70	15:44:17	57.4921	31.8232	224.90	15:44	16.580
76	50 kg	3.40 m	2x25kg	15:49:35	57.4868	31.8044	1589.00							
77	50 kg	3.40 m	2x25kg	15:57:34	57.4784	31.7742	1740.50	153.70	16:00:08	57.4755	31.7640	224.70	16:00	07.590
78	50 kg	3.40 m	2x25kg	16:05:33	57.4697	31.7451	1996.00	169.10	16:08:22	57.4673	31.7358	207.00	16:08	21.880

79	50 kg	3.40 m	2x25kg	16:13:34	57.4614	31.7169	2221.80	163.40	16:16:17	57.4585	31.7076	206.80	16:16	16.931
80	50 kg	3.40 m	2x25kg	16:21:34	57.4536	31.6900	2215.50	154.50	16:24:09	57.4508	31.6801	189.00	16:24	08.296
81	25 kg	3.60 m	1x25kg	07:57:32	57.6226	32.7342	1766.50	159.10	08:00:10	57.6285	32.7322	232.50	08:00	10.231
82	25 kg	3.60 m	1x25kg	08:01:34	57.6319	32.7310	1796.00	159.90	08:04:14	57.6373	32.7282	235.20	08:04	13.211
83	25 kg	3.60 m	1x25kg	08:05:36	57.6401	32.7272	1845.00	157.10	08:08:13	57.6455	32.7256	227.40	08:08	12.682
84	25 kg	3.60 m	1x25kg	08:09:38	57.6488	32.7245	1824.00	150.20	08:12:08	57.6548	32.7236	234.40	08:12	07.503
85	25 kg	3.60 m	1x25kg	08:13:35	57.6578	32.7229	1925.00	150.20	08:16:05	57.6584	32.7228	220.60	08:16	05.088
86	25 kg	3.60 m	1x25kg	08:17:35	57.6772	32.7181	1852.50	154.10	08:20:09	57.6717	32.7161	212.70	08:20	09.447
87	25 kg	3.60 m	1x25kg	08:21:33	57.6748	32.7150	1809.50	158.50	08:24:11	57.6809	32.7128	192.50	08:24	11.338
88	25 kg	3.60 m	1x25kg	08:25:36	57.6839	32.7113	1838.50	155.80	08:28:11	57.6895	32.7098	213.80	08:28	11.220
89	25 kg	3.60 m	1x25kg	08:29:35	57.6928	32.7083	1757.00	150.90	08:32:05	57.6990	32.7065	230.50	08:32	04.794
90	25 kg	3.60 m	1x25kg	08:33:33	57.7027	32.7058	1746.00	149.10	08:36:02	57.7088	32.7037	232.40	08:36	01.737
91	25 kg	3.60 m	1x25kg	08:37:32	57.7123	32.7018	1705.00	152.30	08:40:04	57.7180	32.6996	236.30	08:40	04.122
92	25 kg	3.60 m	1x25kg	08:41:32	57.7213	32.6988	1701.50	153.10	08:44:05	57.7273	32.6961	213.40	08:44	04.715
93	25 kg	3.60 m	1x25kg	08:45:36	57.7306	32.6944	1599.00	157.70	08:48:13	57.7368	32.6934	219.90	08:48	12.744
94	25 kg	3.60 m	1x25kg	08:49:33	57.7398	32.6931	1584.00	155.10	08:52:08	57.7453	32.6916	234.70	08:52	07.738
95	25 kg	3.60 m	1x25kg	08:53:33	57.7487	32.6901	1649.00	153.70	08:56:07	57.7542	32.6883	202.00	08:56	06.341
96	25 kg	3.60 m	1x25kg	08:57:33	57.7573	32.6873	1657.50	177.20	09:00:30	57.7639	32.6849	240.40	09:00	29.642
97	25 kg	3.60 m	1x25kg	09:01:36	57.7666	32.6834	1601.00	151.80	09:04:07	57.7719	32.6812	231.80	09:04	06.822
98	25 kg	3.60 m	1x25kg	09:05:32	57.7756	32.6810	1687.00	157.90	09:08:11	57.7808	32.6786	219.30	09:08	10.967
99	25 kg	3.60 m	1x25kg	09:09:33	57.7840	32.6762	1640.00	161.10	09:12:13	57.7896	32.6733	232.90	09:12	13.216
100	25 kg	3.60 m	1x25kg	09:13:35	57.7926	32.6719	1744.00	154.10	09:16:08	57.7983	32.6695	224.70	09:16	08.216
101	25 kg	3.60 m	1x25kg	09:17:32	57.8014	32.6686	1727.50	150.40	09:20:02	57.8072	32.6669	218.40	09:20	01.297
102	25 kg	3.60 m	1x25kg	09:21:32	57.8102	32.6661	1698.50	149.40	09:24:02	57.8159	32.6643	215.30	09:24	01.402
103	25 kg	3.60 m	1x25kg	09:25:34	57.8196	32.6630	1862.50	151.00	09:28:05	57.8251	32.6614	215.60	09:28	04.657
104	25 kg	3.60 m	1x25kg	09:29:33	57.8283	32.6608	1762.00	152.90	09:32:06	57.8340	32.6590	224.40	09:32	05.983
105	25 kg	3.60 m	1x25kg	09:33:35	57.3738	32.6576	1778.50	153.00	09:36:08	57.8426	32.6548	222.50	09:36	07.996
106	25 kg	3.60 m	1x25kg	09:37:36	57.8458	32.6538	1799.50	145.40	09:40:01	57.8515	32.6519	218.90	09:40	00.822
107	25 kg	3.60 m	1x25kg	09:41:46	57.8557	32.6503	1921.50	141.80	09:44:07	57.8610	32.6479	210.50	09:44	06.789
108	25 kg	3.60 m	1x25kg	09:45:32	57.8635	32.6464	2006.50	153.50	09:48:05	57.8693	32.6453	220.60	09:48	05.005
109	25 kg	3.60 m	1x25kg	09:49:31	57.8723	32.6447	1959.50	143.80	09:51:54	57.8772	32.6424	211.50	09:51	53.477
110	25 kg	3.60 m	1x25kg	09:53:33	57.8812	32.6410	2012.80	148.80	09:56:01	57.8863	32.6389	221.80	09:56	00.799
111	25 kg	3.60 m	1x25kg	09:57:34	57.8898	32.6376	2037.50	144.80	09:59:58	57.8904	32.6374	218.50	09:59	57.974

Table 4
Multi-Channel Seismic Reflection Lines

CD81 seismic line locations					
	FROM		TO		
Line no.	Lat. (N)	Long. (W)	Lat. (N)	Long. (W)	Length (km)
Refraction lines					
1 (expl)	57.8742	33.1468	57.4536	31.6900	96.5
2 (expl)	57.6226	32.7342	57.8898	32.6376	31.5
1 (airg)	57.8742	33.1468	57.4536	31.6900	97.5
2 (airg)	57.6226	32.7342	57.8898	32.6376	32.5
Reflection lines					
1	57.8742	33.1468	57.4536	31.6900	97.5
2	57.6226	32.7342	57.8898	32.6376	32.5
3	57.4417	32.0083	57.7917	33.2000	80.0
4	57.8358	33.1750	57.6700	32.6033	38.0
Sonobuoy					
1	57.5330	32.3060			
2	57.5720	32.4420			

Table 5
Shock factors for explosive shots

Assumptions used in calculations:

Sink rate	**1 m/s**
Ship's speed	**15 km/hr (8.1 knts)**
Firing rate	**4 mins**
	8 mins
Flight time	**2 min 30 sec**
Charge size	**25 kg**
	50 kg
Detonation depth (m)	**150m (range used 80 - 160 m)**
Actual average	**217.90 m (min 132.10 m max 270.80)**

$$S = 0.23\left[\frac{1+\sin\alpha}{R}\right]w^{1/2}$$

where

S **is the shock factor**

R **is the slant range to the shot in m**

α **is the dip angle to shot i.e. sinα = shot range behind ship / detonation depth**

w **is the charge size in kg**

Calculated shock factors for CD81

Det. Dep (m)	**80**	**100**	**120**	**140**	**160**	**130 (act min)**	**270 (act max)**	$0.23w^{1/2}$
25 kg	**0.0021**	**0.0021**	**0.0022**	**0.0022**	**0.0023**	**0.0022**	**0.0024**	**1.15**
50 kg	**0.0030**	**0.0030**	**0.0031**	**0.0031**	**0.0032**	**0.0031**	**0.0034**	**1.63**
R (m)	**623.2**	**626.0**	**629.5**	**633.7**	**638.4**	**631.5**	**674.4**	
$\frac{1+\sin\alpha}{R}$	**0.00181**	**0.00185**	**0.00189**	**0.00193**	**0.00196**	**0.00191**	**0.00208**	

Table 6
EM instrument positions

Instrum. Type	Instrum. Number	Instrum. Name	Latitude (Deg.)	Latitude (Min.)	Longit. (Deg.)	Longit. (Min.)	Water Depth (m)
ELF	1	Ulysses	57	40.82	32	28.08	1549
ELF	2	Quail	57	50.01	32	39.54	1794
ELF	3	Noddy	57	42.98	32	36.03	1238
ELF	4	Trevor	57	45.59	32	44.76	1991
Lemur	1		57	42.61	32	34.60	1440
Lemur	2		57	44.01	32	37.74	1780
Lemur	3		57	44.76	32	41.66	1680
Lemur	4		57	46.54	32	48.09	1801
ELFMAG	1	Opus	57	42.00	32	32.50	1302
ELFMAG	2	Kermit	57	39.35	32	43.40	1814
LEM	1	Lolita	57	36.26	32	15.70	1605
LEM	2	Rhonda	57	36.27	32	15.07	1700
LEM	3	Pele	57	34.41	32	4.90	1830
LEM	4	Macques	57	38.18	32	24.19	1540
OBM	1		57	36.30	32	15.06	1607
OBM	2		57	38.28	32	24.42	1540
OBEM	1		57	47.28	32	50.46	1782
OBEM	2		57	44.46	32	41.09	1650

Table 7
Summary of instruments deployed for EM experiments, and types of data recorded by each instrument.

Instrum. Type	Instrum. No.	Instrum. Name	MT Magnetic	MT E-field	CSEM E-field	Comments
OBM	1		No	No	No	Didn't record
OBM	2		No	No	No	LOST
OBEM	1		No	No	No	LOST
OBEM	2		Yes	Yes	No	
ELFMAG	1	Opus	Yes	No	No	No E-field data
ELFMAG	2	Kermit	Yes	Yes	Yes	
LEM	1	Lolita	No	Yes	Yes	
LEM	2	Rhonda	No	Yes	Yes	
LEM	3	Pele	No	Yes	Yes	
LEM	4	Maques	No	Yes	Yes	
ELF	1	Ulysses	No	No	Yes	
ELF	2	Quail	No	Some	Yes	Deployed twice
ELF	3	Noddy	No	No	Yes	
ELF	4	Trevor	No	No	Some	
LEMUR	1		No	No	Yes	
LEMUR	2		No	No	Yes	
LEMUR	3		No	No	Yes	
LEMUR	4		No	No	No	LOST

Table 8
Positions of acoustic navigation transponders

Transponder	Name	Latitude (Deg.)	Latitude (Min.)	Longitude (Deg.)	Longitude (Min.)	Water Depth (m)
A	April	57	50.52	32	44.73	1719
B	Bertha	57	51.30	32	33.83	2051
C	Cleo	57	46.27	32	34.92	1647
D	Deidre	57	40.71	32	33.76	1304
E	Emily	57	38.85	32	41.63	1776
F	Flossie	57	36.68	32	48.95	2114
G	Guillemot	57	40.50	32	22.56	1407
H	Hilda	57	44.83	32	45.37	1734
I	Iris	57	46.27	32	43.80	1968

Table 9
Sound velocity dip data

Depth (m)	Velocity (m/s)		Depth (m)	Temp. (°C)
1.91	1487.09		1.91	8.82
32.49	1487.09		32.49	8.83
37.54	1487.51		37.54	8.83
53.42	1487.09		53.42	8.70
60.00	1485.57		60.00	8.26
63.72	1485.01		63.72	8.00
65.66	1484.18		65.66	7.77
69.80	1483.08		69.80	7.50
75.34	1482.66		75.34	7.31
85.64	1482.11		85.64	7.15
86.82	1481.97		86.82	7.11
96.65	1481.56		96.65	6.93
107.31	1480.60		107.31	6.70
155.09	1479.63		155.09	6.23
159.38	1479.22		159.38	6.15
171.51	1479.08		171.51	6.08
176.76	1479.63		176.76	6.09
181.91	1479.63		181.91	6.09
187.15	1479.08		187.15	6.01
198.64	1479.22		198.64	5.98
203.97	1479.63		203.97	5.98
246.00	1479.08		246.00	5.72
295.04	1479.22		295.04	5.51
300.10	1478.67		300.10	5.37
332.65	1478.81		332.65	5.30
338.41	1479.22		338.41	5.28
343.52	1479.08		343.52	5.26
348.96	1478.81		348.96	5.22
354.42	1478.67		354.42	5.20
359.53	1479.08		359.53	5.19
417.62	1479.22		417.62	5.05
422.95	1479.63		422.95	5.06
460.65	1479.77		460.65	4.98
465.85	1480.18		465.85	4.98
526.52	1480.73		526.52	4.86
543.11	1480.60		543.11	4.78
575.80	1480.05		575.80	4.62
596.56	1480.60		596.56	4.57
602.21	1480.05		602.21	4.52
644.25	1480.18		644.25	4.35
649.54	1480.46		649.54	4.35
654.84	1480.73		654.84	4.34
692.33	1480.87		692.33	4.29
697.82	1481.15		697.82	4.27

731.38	1481.15		731.38	4.24
733.69	1481.42		733.69	4.23
736.42	1481.56		736.42	4.23
784.36	1481.97		784.36	4.15
789.82	1482.11		789.82	4.15
795.31	1481.70		795.31	4.08
816.70	1481.97		816.70	4.02
822.07	1482.11		822.07	4.02
848.58	1482.11		848.58	3.99
852.14	1482.53		852.14	4.00
887.24	1482.66		887.24	3.95
892.55	1483.08		892.55	3.96
908.49	1483.08		908.49	3.93
914.24	1483.22		914.24	3.93
967.51	1484.18		967.51	3.89
1009.44	1484.05		1009.44	3.82
1014.59	1484.74		1014.59	3.82
1126.74	1485.71		1126.74	3.61
1157.31	1485.57		1157.31	3.57
1162.73	1486.12		1162.73	3.57
1200.19	1486.54		1200.19	3.53
1237.26	1486.96		1237.26	3.50
1264.35	1487.09		1264.35	3.50
1298.01	1487.79		1298.01	3.48
1300.51	1488.07		1300.51	3.48
1329.37	1488.35		1329.37	3.47
1356.67	1488.62		1356.67	3.47
1361.86	1489.04		1361.86	3.46
1393.87	1489.60		1393.87	3.47
1420.27	1490.02		1420.27	3.46
1447.97	1490.30		1447.97	3.45
1473.88	1490.71		1473.88	3.46
1500.91	1491.13		1500.91	3.45
1511.74	1491.55		1511.74	3.45
1527.85	1491.69		1527.85	3.45
1564.21	1492.11		1564.21	3.45
1591.06	1492.67		1591.06	3.45
1646.83	1493.65		1646.83	3.45
1652.24	1493.93		1652.24	3.45
1705.06	1494.77		1705.06	3.45
1731.97	1495.19		1731.97	3.45
1770.21	1495.90		1770.21	3.45
1776.01	1496.18		1776.01	3.45

Table 10
Scientific Party

M. Sinha	Cambridge
C. Peirce	Durham
S. Constable	Scripps
A. White	Flinders
J. Leonard	Cambridge
P. Patel	Cambridge
L. MacGregor	Cambridge
M. MacCormack	Cambridge
G. Heinson	Flinders
D. Navin	Durham
D. White	IOSDL
A. Cumming	R.V.S.
C. Paulson	R.V.S.
K. Smith	R.V.S.
A. Taylor	R.V.S.
M. Davies	R.V.S.
D. Booth	R.V.S.
G. Knight	R.V.S.